INTRODUCTION

The U.S. Department of Energy's (DOE) Office of Advanced Automotive Technologies conducts research and development on advanced rechargeable batteries for application in electric vehicles (EVs) and hybrid electric vehicle (HEV) systems. Problems impeding the development of high-energy batteries for use in EVs and high-power batteries for use in HEVs are addressed by this program. These batteries require continuing research to alleviate materials problems, provide better understanding of life-limiting and performance-limiting phenomena, improve relevant engineering science and design, and insure a high level of safety.

DOE battery R&D supports two major programs: the United States Advanced Battery Consortium (USABC), which develops advanced batteries for EVs, and the Partnership for a New Generation of Vehicles (PNGV), which seeks to develop passenger vehicles with a fuel economy equivalent to 80 mpg of gasoline. This report describes the activities of the Exploratory Technology Research (ETR) Program, managed by the Lawrence Berkeley National Laboratory[1] (LBNL). The role of the ETR Program is to perform supporting research on the advanced battery systems under development by the USABC and PNGV Programs, and to evaluate new systems with potentially superior performance, durability and/or cost characteristics. The specific goal of the ETR Program is to identify the most promising electrochemical technologies and transfer them to the USABC, battery industry and/or other Government agencies for further development and scale-up. This report summarizes the research, financial and management activities of the ETR Program in CY 1999. This is a continuing program, and reports for prior years have been published; they are listed at the end of this Program Summary.

This annual report is sub-divided into eight ETR task areas: 1) Optimized Li-ion System, 2) High-Performance Non-flammable Electrolytes, 3) Non-carbonaceous Anode Materials, 4) Novel Cathode Materials, 5) Advanced Solid Polymer Electrolytes, 6) Advanced Diagnostic Methods, 7) Improved Electrochemical Models, and 8) Novel Electrode Couples. The first five tasks cover focused areas of research, and the last three form the foundation of a sound exploratory research program.

[1] Participants in the ETR Progam include the following LBNL scientists: E. Cairns, J. Evans, J. Kerr, K. Kinoshita, F. McLarnon and J. Newman of the Environmental Energy Technologies Division; and L. De Jonghe and P. Ross of the Materials Sciences Division.

RESEARCH PROJECT SUMMARIES

OPTIMIZED LITHIUM-ION SYSTEM

Several key materials issues must be resolved, and optimization of current technology is required to develop a practical high-performance, safe, and low-cost Li-ion battery for EV and HEV applications. The objective of this task is to investigate the full realm of interactions that occur in a Li-ion battery, from surface interactions of electrodes with electrolytes, to system interactions in the case of thermal breakdown and runaway. The studies focus on the solid electrolyte interphase (SEI) layer, stability issues related to the electrolyte and binder, and the corrosion stability of current collectors for Li-ion batteries. Any advancements developed under this effort will be tested in baseline cells so that they may be evaluated on a system level as opposed to an isolated environment.

Reactivity and Safety Aspects of Carbonaceous Anodes

M. David Curtis and Gholam-Abbas Nazri
University of Michigan, Department of Chemistry, Ann Arbor MI 48109-1055
(734) 763-2132; fax: (734) 763-2307; e-mail: mdcurtis@umich.edu

Objective

- Develop a surface coating technology to minimize electrolyte decomposition and enhance Li^+-ion conduction in carbonaceous anodes for advanced Li batteries.
- Improve safety of Li^+-ion technology by incorporating ion-conducting and fire-retarding polymers in carbonaceous anodes.

Approach

- Establish a baseline for thermal behavior of carbonaceous anodes at various states of charge.
- Produce lithiated graphite by chemical intercalation and evaluate its thermal behavior with a surface coating.
- Evaluate reactivity of modified surface-coated carbon to electrolyte decomposition, gas generation, and surface film formation.

Accomplishments

- Developed a high-temperature process to prepare single-phase lithiated graphite with various Li concentrations.
- Evaluated thermal stability and reactivity of lithiated graphite.
- Improved safety and reactivity of graphite anodes by surface treatment and coating.
- Developed a Li^+-ion conducting polymer with fire-retardant properties.

Future Directions

- Improve the charge rate capability of carbonaceous anodes for high-power application.
- Optimize overall performance of high-rate, safe and low-cost graphitic anodes for high-power and high-energy applications.

A high-temperature process was developed to prepare bulk lithiated graphite anodes with controlled degrees of lithiation from LiC_{36} to LiC_6. Graphite and Li disks were stacked together, and heat treated at 250-300°C in an Ar atmosphere under 5000 Kg/cm^2 pressure for 12 hours.

X-ray diffraction (XRD) and thermal behavior of the lithiated graphite in contact with various binder materials were investigated. XRD analysis confirmed the formation of lithiated graphite at high state of charge (LiC_6). The thermal behavior of the chemically lithiated graphite is shown in Fig. 1. No thermal decomposition of pure LiC_6 occurs up to 400°C. Above 400°C, lithium carbide starts to form. In contrast, electrochemically lithiated graphites show a series of decomposition exotherms below 250°C. These exotherms are related to the decomposition of the SEI on the carbonaceous electrode. The binder used in this work is a non-fluorinated polymer that is stable to 300°C.

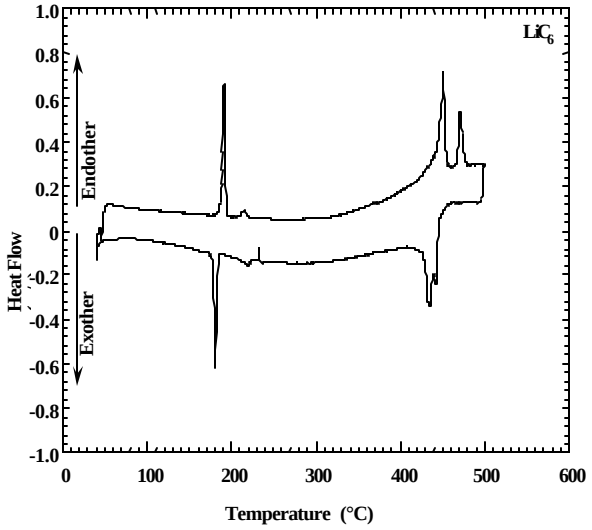

Figure 1. Thermal behavior of lithiated graphite LiC_6.

We have prepared silylated graphite anodes by reacting trimethylchlorosilane with various graphite samples. These samples were evaluated in Li/C cells, which were monitored for release of gaseous species during charge and discharge cycles. These tests indicated a significant reduction (by a factor of 1/10) in gas generation on silylated graphite compared to untreated graphite. Titration with triethylaluminum silylation showed that the silylation reaction removed surface-active groups from the carbonaceous materials. The process is highly efficient, providing close to quantitative conversion of the surface groups.

A different silylating reagent was used to both block gas formation and facilitate Li^+-ion transport across the SEI. This synthesis uses commercially available materials as shown in Scheme 1.

Scheme 1

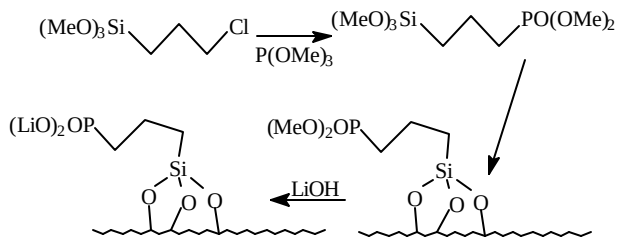

We have also synthesized a series of unique Li-phosphonates as single-ion polymer electrolytes. These materials are prepared by the reaction of the dilithium salt of ethylene glycol with phosphorous pentoxide, both are low-cost precursors. The ratio of Li_2EG to P_2O_5 can be varied to optimize the properties of the resulting polymer. One example is shown as **EG3P4** (3 Li_2EG:2 P_2O_5). In addition to the EGnPm series, other new Li-phosphonate polymers, e.g., **LiPPS**, have been prepared by the reactions of $P(OMe)_3$ with chloromethylated polystyrene. These will be characterized for Li conductivity, stability under cell conditions, and fire retardancy.

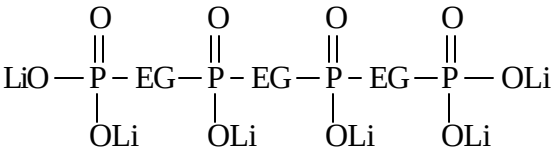

EG3P4 (EG=ethylene glycolate)

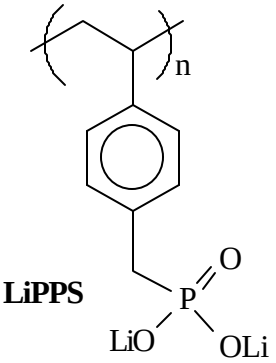

LiPPS

Optimization of Cathode Materials

Tadeusz Malinski
Oakland University, Department of Chemistry, Rochester MI 48309
(248) 370-2339; fax: (248) 370-2321; email: malinski@oakland.edu

Objective

- Develop a stable lithium nickelate cathode by systematic substitution of multiple cations that prevent phase and domain segregation in the oxide slabs.

Approach

- Develop a multicomponent substitution process with sp metals (Al, Ga, Mg and Ca) and early transition metals to partially substitute for nickel in NiO_2 slabs.
- Determine the role of substituted elements by measuring electrochemical properties, charge-discharge capacity, cycling, and catalytic properties toward electrolyte oxidation.

Accomplishments

- Identified Ti, Mg and Al as elements that effectively stabilize the structure of cathode materials.
- Successfully developed a mechano-milling process to prepare single-phase multidoped cathode materials.

Future Directions

- Study the effect of doping elements on cycle life, calendar life, reactivity and safety of cathode materials.
- Study the low-temperature and high-temperature performances of cathode materials under continuous charge/discharge cycling.
- Determine the effect of doping elements on electrode impedance.

The goal of this work is to systematically tailor the covalency of M-O bonds in metal oxides to improve their stability, kinetics, and electronic conductivity as cathode materials. As a base-line material, we prepared the well-known compositions of $LiCoO_2$ and $LiNi_{0.75}Co_{0.25}O_2$. A process was developed to fabricate electrodes from the baseline materials containing up of 80 wt% active material, 15 wt% composite conductive diluent, and 5 wt% non-fluorinated binder. The electrochemical performance and thermal stability of the oxide cathodes were examined at 70% state-of-charge (SOC), using a specially designed TGA-DSC which operates inside an argon-filled glove box.

To examine the role of elemental substitution on stability and electrochemical performance of nickelate-based cathode materials, the following compositions were prepared at 750°C with an oxygen-rich environment in a tube furnace:

1) $LiNi_{0.75}Co_{0.25}O_2$,
2) $LiNi_{0.75}Co_{0.15}Ti_{0.10}O_2$,
3) $LiNi_{0.75}Co_{0.15}Ti_{0.05}Ca_{0.05}O_2$,,
4) $LiNi_{0.75}Co_{0.15}Sc_{0.05}Mg_{0.05}O_2$,
5) $LiNi_{0.75}Co_{0.15}Ti_{0.05}Ga_0$,
6) $LiNi_{0.75}Co_{0.15}Ti_{0.05}Mg_{0.05}O_2$,
7) $LiNi_{0.75}Co_{0.10}Ti_{0.05}Mg_{0.05}Al_{0.05}O_2$.

In general, materials containing Ti, and in particular Al, require longer heat treatment at 750°C to form single-phase materials. The crystal structures of the cathode materials were determined by XRD and Rietveld refinement. In most cases, good-quality materials were obtained after 8 h of heat treatment. These results show that energetic mechano-milling of the initial precursors can significantly reduce the duration of heat treatment. The electrochemical performances of the materials synthesized in this work are shown in Fig. 2. The electrode materials had about 12 mg/cm^2 loading of active material, which was placed on a carbon-coated Al substrate

and hot calendared (at 90°C). The samples were tested in 2.5-cm diameter cells with a Li counter electrode in 0.8 M $LiPF_6$(acid-free)/ethylene carbonate-diethyl carbonate (70/30 mole ratio). The thermal properties of the samples at 70% SOC are presented in Fig. 2.

Conclusions:

- Incorporation of a larger cation in the MO_2 slabs improves the thermal stability of the sample. However, formation of high-purity metal oxide with large cations in the MO_2 slabs requires higher temperature and longer time for heat treatment.
- The results also indicate that the initial mechano-milling of the precursor can significantly reduce the processing time for formation of a single-phase cathode material.
- $LiNi_{0.75}Co_{0.10}Ti_{0.05}Mg_{0.05}Al_{0.05}$ is a practical electrode material for Li-ion batteries with an acceptable specific capacity of 178 Ah/Kg and negligible exotherm from ambient to 250°C at 70% SOC.
- Future work will focus on tailoring the rate capability of the oxide by optimizing the electrode thickness, active-material particle size, electrode impedance, and cell design.

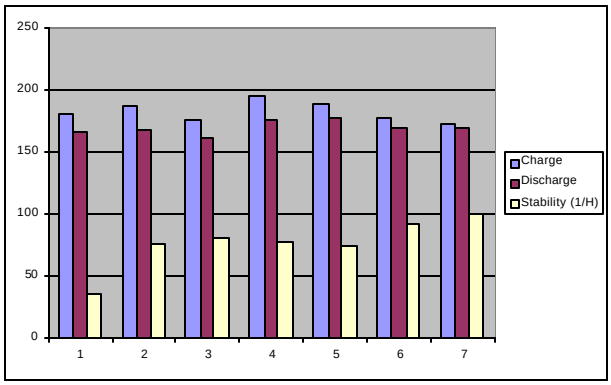

Figure 2 Specific capacity of initial charge/discharge, and normalized stability based on ΔH of reaction at (200-280°C) for 1)$LiNi_{0.75}Co_{0.25}O_2$, 2)$LiNi_{0.75}Co_{0.15}Ti_{0.10}O_2$, 3)$LiNi_{0.75}Co_{0.15}Ti_{0.05}Ca_{0.05}O_2$, 4)$LiNi_{0.75}Co_{0.15}Sc_{0.05}Mg_{0.05}O_2$ 5)$LiNi_{0.75}Co_{0.15}Ti_{0.05}Ga_{0.05}O_2$, 6)$LiNi_{0.75}Co_{0.15}Ti_{0.05}Mg_{0.05}O_2$, 7)$LiNi_{0.75}Co_{0.10}Ti_{0.05}Mg_{0.05}Al_{0.05}O_2$.

Optimized Lithium-Ion Electrolyte and Binder

Ricardo Aroca
University of Windsor, Department of Chemistry, Windsor, Ontario N9B 3P4 Canada
(519) 253-4232; fax: (519) 973-7098; e-mail: g57@uwindsor.ca

Objectives

- Develop electrolytes with improved temperature stability and ionic conductivity for high-power applications.
- Develop low-cost binders and separators for Li-ion batteries.

Approach

- Blend cyclic and linear carbonate-based solvents with different concentrations of Li salts to obtain maximum conductivity and fluidity.
- Enhance low-temperature conductivity of the electrolytes by using mixed Li salts.
- Investigate ion association in the electrolytes by vibrational spectroscopy, viscosity and conductivity measurements.

Accomplishments

- Designed a unique set-up for purification of solvents and salt for reliable and reproducible conductivity measurements.
- Achieved the highest conductivity with a 2/1 mole ratio of EC/DMC, which showed a minimum in ion-pairing and less structural ordering.

- Calculated Li^+-ion solvation energy in various electrolyte blends and observed preferential solvation.

Future Directions

- Study the thermal behavior of various multi-blend solvents and electrolytes in contact with lithiated graphite
- Develop a theoretical model to predict the usefulness of mixed Li salts for low-temperature performance.
- Develop a thermally stable and chemically compatible binder for Li-ion cells.

Linear and cyclic carbonates were purified because they contain low-molecular-weight organic molecules and residual moisture. The Li salts were vacuum dried and evaluated using thermal analysis techniques. The conductivity of electrolytes based on ethylene carbonate (EC) was improved by addition of a linear carbonate such as dimethyl carbonate (DMC). The highest conductivity was achieved with a 2/1 mole ratio of EC/DMC, which showed a minimum in ion-pairing and less structural ordering. A similar trend was observed for a 2 EC/diethyl carbonate (DEC) ratio. Addition of an asymmetric cyclic carbonate such as propylene carbonate (PC) and asymmetric, linear carbonate such as methyl ethyl carbonate (MEC) also produced electrolytes with lower ion-pairing and improved ionic conductivity and fluidity. The addition of a linear carbonate has a more pronounced effect on low-temperature conductivity than on ambient-temperature conductivity. This effect was also observed in the viscosity measurements. The EC phase separates in the electrolyte at temperatures below –15°C to form solid transparent flakes, which were examined by vibrational spectroscopy. We have also observed a strong preferential solvation of Li^+-ions by carbonate solvents using Raman spectroscopy (Fig. 3). The addition of PC significantly improved the low-temperature conductivity. No phase separation was observed when EC-PC-DMC based electrolytes were used.

Further improvement in the low-temperature ionic conductivity was observed with mixed Li salts in electrolyte with an overall Li^+-ion concentration of 1 molar (e.g., $LiPF_6$ and $LiCF_3SO_3$ mixture with 0.8/0.2 mole ratio). Ion association and the energetics of Li^+-ion solvation with various carbonate solvents were studied using *ab initio* calculations.

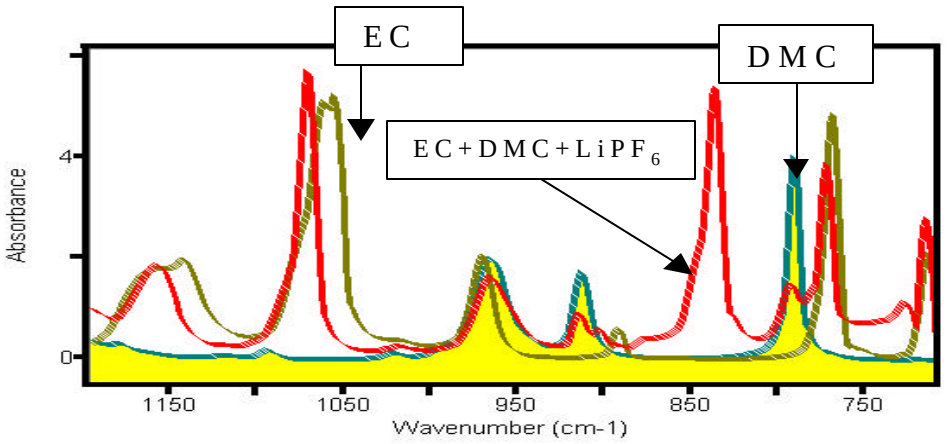

Figure 3. Raman spectra of ethylene carbonate, dimethyl carbonate, and electrolyte (EC+DMC+1M$LiPF_6$). The results indicate preferential solvation of the Li ion.

SEI Layer Formation on Carbon Anodes

Philip N. Ross, Jr.
Lawrence Berkeley National Laboratory, 2-100, Berkeley CA 94720
(510) 486-6226, fax: (510) 486-5530; e-mail: pnross@lbl.gov

Objectives

- Determine the mechanism of formation and the physical and electrochemical properties of the passive film formed on carbon anodes.
- Determine the role of electrolyte composition and surface chemistry of carbon on the mechanism of formation and the physical and electrochemical properties of the passive film.
- Develop new cell chemistries to improve the performance of Li-ion batteries.

Approach

- Apply a combination of ultra-high vacuum (UHV) surface analytical methods and *in situ* infrared vibrational spectroscopy.

Accomplishments

- Completed a study of the chemistry of Li intercalation into highly oriented pyrolytic graphite (HOPG) by evaporation and annealing in UHV. Determined the surface chemistry of UHV cleaved LiC_6(0001).
- Completed a full *ab initio* computational study of the electrochemical reduction of solvents for Li-ion batteries.

Future Directions

- Experimentally confirm *ab initio* computations of solvent reduction potentials using *in situ* infrared vibrational spectroscopy.
- Perform *ab initio* computational studies of the electrochemical reduction of candidate electrolyte additives.
- Carry out exploratory studies of pre-formed (dry process) layers on carbon/graphites.

The study of Li intercalation into graphite (HOPG) in UHV by vacuum deposition and thermal annealing was effectively completed. A thin film of lithiated graphite was formed on the basal plane of the HOPG by vapor deposition in UHV. The composition and structure of the film was characterized using angle-resolved X-ray photoelectron spectroscopy (PES). The take-off angle dependence of the Li 1s and C 1s photoelectron intensities were calculated for various models of the Li-graphite multilayer, and the results were compared with experiment. The film structure and composition was a function of the HOPG substrate temperature during deposition: metallic Li overlayer at T < ~220 K; a mixed metallic Li overlayer on intercalated graphite at ~220 K < T< ~400 K; and intercalated graphite at T > ~400 K. There was no evidence of staging in this surface intercalation process, just direct formation of Stage III layers. Thus, under the appropriate conditions of synthesis, the composition (the Li/C stoichiometry) and electronic properties of the surface layer are identical to those of a bulk LiC_6 crystal.

A more difficult problem, and one which is not fully resolved at this time, is to determine the surface termination in lithiated HOPG and/or in LiC_6(0001), i.e., which is the equilibrium surface plane, the graphene plane or the Li^+-ion plane. Again, we are attempting to make this determination using the take-off angle dependence of the Li 1s and C 1s photoelectron intensities and detailed modeling of the photoelectron emission/diffraction from the different surface terminations. The data appear to

indicate termination in the graphene plane, in agreement with chemical intuition.

The reaction of DEC with lithiated C(0001) was studied using PES, and the spectra were compared carefully against those for DEC on Li. The initial stage of reaction appears to be identical, but at higher temperatures (> ca. 300 K) the spectra were quite different. Interestingly, at 470 K all of the reaction products from DEC reduction desorb from the surface (!!) of lithiated C(0001), in contrast to the metallic Li surface, where thermally stable Li compounds are formed. With the assumption that the surface of lithiated C(0001) is terminated in the graphene plane, an interesting picture of the reaction with DEC emerges. The first step is electron transfer from the graphene sheet to the DEC molecule, which dissociates to form two anions, ethyl carbonate and ethyl carbanion. These anions are bound electrostatically to Li^+ ions beneath the intervening graphene sheet. Because the binding is relatively weak, and no direct bonding to Li^+ occurs, the anions thermally decompose and/or recombine and desorb from the surface upon heating to 470 K. The final gaseous products are postulated to be n-butane, CO and/or CO_2, and diethyl ether.

Electronic structure calculations were performed on a number of carbonate and ethereal solvent molecules and their radical anions. These calculations were then used to calculate from classical Born-Haber type thermochemical cycles the standard potentials (E^o) for electrochemical reduction of the solvent molecules at an inert electrode, e.g., such as glassy carbon or graphite. These calculations showed that E^o for reduction of the carbonates PC, EC and DEC are ca. + 1.0 V $\pm$ 0.3 V (vs. Li/Li^+) whereas for the ethers tetrahydrofuran (THF), dimethoxyethane (DME) and dioxolane the reduction potentials are all negative of 0 V (vs. Li/Li^+). For the carbonates, the major uncertainty obscuring more-precise determinations of reduction potentials are the solvation energies of the anions. Of particular interest is the reduction potential of EC relative to PC, and relative to 1.0 V, the onset potential for Li intercalation into graphite. Experimentally, we attempted to measure the reduction potential on glassy carbon by cyclic voltammetry in purified THF electrolyte to which mM quantities of EC or PC were added. The result for EC is shown in Fig. 4. The calculated reduction potential for EC in THF was 1.11 V (vs. Li/Li^+), in reasonable agreement with a reduction peak potential near 1.2 V. More-refined calculations are in progress, as well as further experiments to measure reduction potentials of other solvents of interest. The present results support the hypothesis that the SEI layer on graphite/carbon electrodes in EC-based solvents forms at potentials positive of 1 V by preferential EC reduction.

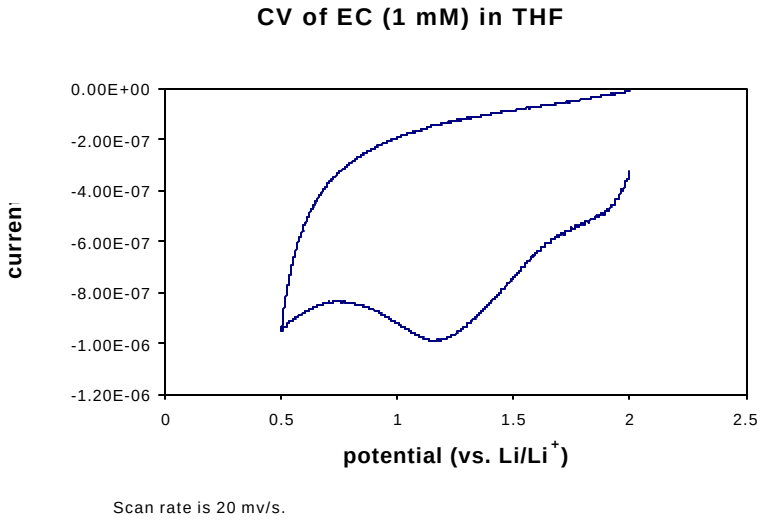

Figure 4. Electrochemical reduction of ethylene carbonate (EC) on glassy carbon by cyclic voltammetry. 1 mM EC in THF with 1 M $LiClO_4$ supporting electrolyte.

Electrode Surface Layers

Frank R. McLarnon
Lawrence Berkeley National Laboratory, 90-1142, Berkeley CA 94720
(510) 486-4636, fax: (510) 486-4260; e-mail: frmclarnon@lbl.gov

Objectives

- Apply advanced *in situ* and *ex situ* characterization techniques to characterize the structure, composition, formation and growth of surface layers on carbonaceous anodes.
- Investigate surface treatment of current collectors for improved adhesion, conductivity and lifetime.

Approach

- Use ellipsometry, Raman spectroscopy, scanning probe microscopy and other methods to characterize electrode surface layers.

Accomplishments

- Found that the thickness of the surface layer formed on carbon electrodes is weakly dependent on the type of carbon material.

Future Directions

- Use optical, spectroscopic and microscopic techniques to characterize changes in surface layers on carbon electrodes in non-aqueous electrolytes at elevated temperatures.

We have characterized SEIs on five types of carbonaceous materials: (i) HOPG (Advanced Ceramics Corp.), (ii) natural graphite powder (Hydro-Quebec), (iii) pyrolyzed carbon film on silicon wafers (produced in the Microfabrication Facility at the University of California at Berkeley), (iv) electron-beam evaporated carbon film on glass (Tufts University), and (v) electron-beam evaporated carbon film on a glass-based substrate (International Crystal Manufacturing Co.). All as-received carbon surfaces were specular, except for the natural graphite powder which we pressed at ~50 kpsi to form a smooth disk. We used spectroscopic ellipsometry to measure the optical constants of these carbons, which exhibited non-dispersive refractive indices ranging from 2.5 to 3.5 and extinction coefficients above 1.5.

The carbon films deposited on the glass-based substrate exhibited broad overlapping Raman peaks from 900 cm^{-1} to 1700 cm^{-1}, indicative of highly disordered carbon. The other carbons showed two distinct Raman peaks at 1600 cm^{-1} and 1350 cm^{-1}, corresponding to the G and D bands, respectively. We will further analyze these Raman spectra to identify changes in the carbon microstructures that accompany charge-discharge cycling.

We carried out *in situ* spectroscopic ellipsometry of carbon surfaces in a 3-electrode cell, which was designed for use with the existing LBNL ellipsometer. Viton O-rings or gaskets were used at all cell ports to ensure proper sealing. Our method to deconvolute ellipsometric spectra takes into account electrode surface roughness, which varied from carbon to carbon.

Transient ellipsometric spectra were recorded as the carbon electrode was repeatedly cycled from its open-circuit potential (~3.0 V vs Li) to 0 V and then back to ~3.0 V at 1-5 mV/s. Most of our experiments were carried out with 1M $LiPF_6$-EC-DMC (1:1 EC:DMC volume ratio, EM Industrial Inc., Selectipur LP30) with a nominal water content <30 ppm. In some experiments with HOPG and the carbon films, 1M $LiClO_4$-EC-DMC was also used. The expected irreversible electrode capacity loss during the first few charge-discharge cycles was accompanied by significant irreversible changes of the ellipsometric parameters for all carbon electrodes. Figure 5 shows the recorded transient ellipsometric spectra for a typical carbon film during the first three potential cycles between 2.0 and 0 V at 1 mV/s. Analyses of these experimental data demonstrated that the changes of the ellipsometric

parameters in first few cycles could be attributed to SEI layer formation on the carbon surface. We found SEI formation to be nearly independent of factors such as type of carbon material and electrolyte identity. Typical SEI layers were 40-60 nm thick with refractive indices 1.4-1.5, suggesting an optical compactness similar to those of common polymers. In some of our experiments, especially with $LiClO_4$-EC-DMC electrolyte, the electrode surface layers showed near-zero extinction coefficients, which indicates a small SEI electronic conductivity.

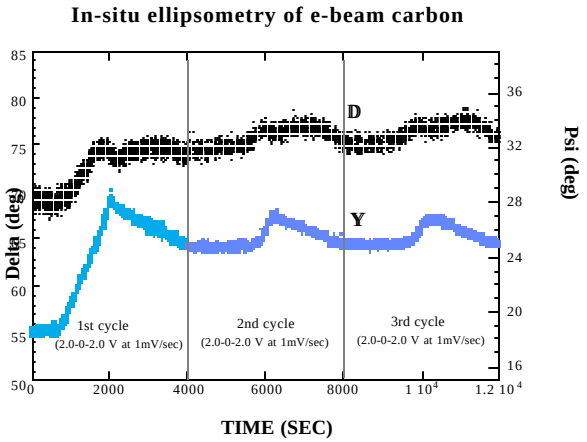

Figure 5. Transient ellipsometric spectra for a carbon film during the first three potential cycles between 2.0 and 0 V at 1 mV/s.

In collaboration with the research group of Prof. J. Evans, we combined the complementary electrochemical quartz crystal microbalance (EQCM) and spectroscopic ellipsometry techniques to characterize electron-beam deposited carbon films. For EQCM studies, a 100-nm thick carbon film was deposited onto one side of smooth AT-cut quartz substrate with two transition layers (500-nm Cu and 10-nm Cr), and a 1-μm thick Au layer was coated onto the other side of the quartz substrate. A homemade EQCM instrument and potentiostat [H. Yang and J. Kwak, *J. Phys. Chem., B*, **101**, 774 (1997)] was used for frequency measurements; its theoretical mass sensitivity was 12 ng/Hz cm^2. For ellipsometric measurements, the 100-nm thick carbon films were deposited onto a glass substrate with similar transition layers, and a somewhat larger working electrode area was used in order to match the ellipsometer geometry. The combined EQCM and ellipsometry results strongly suggest that the SEI layer was formed mainly during the first potential cycle. Because the EC in the electrolyte can be reduced relatively easily, it is commonly accepted that the SEI layer on carbon electrodes contains mostly alkyl carbonates. Based on this assumption and using a single homogeneous SEI layer model, we derived the thickness and optical properties of the SEI on a typical e-beam carbon electrode; more-detailed analyses are underway. This collaborative research allows us not only to confirm the presence of the SEI layers formed on carbon electrodes but also to determine their densities and optical properties.

Development of Novel Electrolytes

Kraig A. Wheeler
Delaware State University, Department of Chemistry, Dover DE 19901
(302) 739-4934, fax: (302) 739-3979; e-mail: kwheeler@dsc.edu

Objectives

- Develop electrochemically stable arylsulfone and sulfone cross-linked polyethylene glycol (PEG) electrolytes.
- Characterize and investigate electrochemical and physical properties of these electrolyte materials.

Approach

- Prepare sulfone cross-linked PEG and arylsulfone materials.
- Assess material structure and purity by standard spectroscopic techniques and solubility of Li salts.

- Evaluate the electrochemical performance of sulfone materials in Li-ion cell applications.

Accomplishments

- Prepared and characterized a divinylsulfone cross-linked PEG-400 and six arylsulfones.
- Observed effective Li-ion dissolution by arylsulfones with $LiN(CF_3SO_2)_2$.

Future Directions

- Prepare sulfone-based PEG polymers *via* methylvinylsulfone precursors to assess structure-function relationships of polymeric materials.
- Complete electrochemical characterization of sulfone materials.

The objective of this project is to develop sulfone-based electrolytes for Li-ion cells. The research effort centers on synthesis and characterization (spectroscopic and electrochemical) of electrolyte materials to determine the structural principles responsible for electrochemical stability.

The synthesis of arylsulfones with formula aryl-SO_2-R (where R = CH_3, CF_3, CH_3CH_2, and benzyl) were carried by (i) treatment of an arylthiol with NaOH to give sodium arylthiolate, (ii) direct alkylation of the anion to form an alkylarylsulfide, and (iii) subsequent oxidation via *m*-chloroperbenzoic acid or H_2O_2. Confirmation of the chemical structures of these arylsulfones was obtained by spectroscopic or XRD analysis. Several methods to remove trace impurities were employed; the most notable by successive recrystallizations in CH_2Cl_2/ligroine solvent systems.

PEG sulfone polymers were successfully prepared by employing a combination of anionic and radical initiation conditions. Condensation of PEG and 3-chloro-2-(chloromethyl)propene via the Williamson ether synthesis resulted in polyether precursors. It was observed that extended reaction times, elevated temperatures, or radical initiation processes resulted in the unwanted cross-linking of the polyethers. The development of alternative methods using *in situ* reaction conditions provided highly viscous materials with minimal cross-linking. The radical-initiated reaction of divinylsulfone and these olefinic polyethers formed controlled cross-linked molecular architectures lacking olefinic functionality (Scheme 2). These synthetic methods produce self-standing polymer films with excellent mechanical properties. The introduction of cross-linking groups to the backbone of PEO polymers improved the amorphous content and electrochemical stability of the compounds.

To understand the effect of structural parameters of arylsulfone-based electrolytes on electrochemical performance, we evaluated the electrolytes in Li-ion cells. This effort had limited success due to the unexpected insolubility of $LiPF_6$, $LiSO_3CF_3$, and $LiClO_4$ in the arylsulfones. A search for compatible Li salts revealed $LiN(SO_2CF_3)_2$ as a suitable selection. The infinite solubility of $LiN(SO_2CF_3)_2$ in sulfones is due to the structural similarities of both chemical classes. The electrochemical behavior of arylsulfones/ $LiN(SO_2CF_3)_2$ in Li-cells showed favorable responses and did not undergo electrolytic degradation at 4.5 V.

PRESENTATION

J.-J. Lee, T. Bae, D.A. Scherson, B. Miller and K.A. Wheeler, "Nitrogen-Incorporated Tetrahedral Amorphous Carbon Electrodes in Ambient Temperature Chloroaluminate Melts," *196th Meeting of the Electrochemical Society*, Honolulu, HI, October 17-22, 1999.

Scheme 2

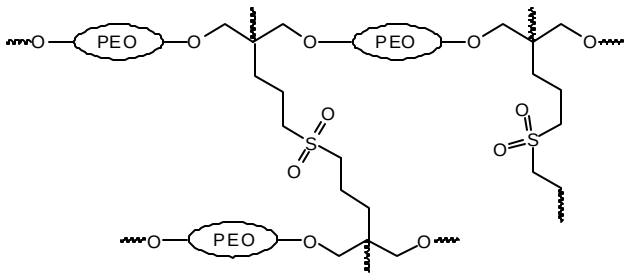

Carbon Electrochemistry

Kim Kinoshita
Lawrence Berkeley National Laboratory, 90-1142, Berkeley CA 94720
(510) 486-7389; fax: (510) 486-4260; e-mail: k_kinoshita@lbl.gov

Objective

- Identify the critical parameters that control the reversible intercalation of Li in carbonaceous materials and determine their maximum capacity for Li intercalation.

Approach

- Couple electrochemical studies with physical measurements to correlate the relationship between the physicochemical properties of carbonaceous materials and their ability to intercalate Li.
- Apply thermal analysis and microscopy techniques to characterize the structure of carbon materials for Li-ion batteries.

Accomplishments

- Observed a strong correlation between the irreversible capacity loss (formation of SEI layer) and the relative fraction of edge sites associated with graphitized carbons.
- *In situ* ellipsometry/electrochemistry studies on graphite indicated that SEI formation was strongly influenced by the type of Li salt (conducted in collaboration with HydroQuebec and Frank McLarnon's group at LBNL).

Future Directions

- Continue collaboration with Superior Graphite and HydroQuebec to identify a low-cost carbon with improved rate capability in Li-ion batteries.
- Continue *in situ* ellipsometry studies of lithiated carbons, and determine the relationship between the type of carbon and the properties of the surface layer formed during the first charge cycle.

The objective of this project is to identify the critical parameters that control the reversible intercalation of Li in carbonaceous materials. This project involves investigations of the role of physicochemical properties of carbonaceous materials on their ability to reversibly intercalate Li. This latter effort is coordinated with the research conducted at HydroQuebec to develop improved carbons for Li-ion batteries.

The oxidation of natural graphite particles with a prismatic (flake-like) structure was investigated by thermal gravimetric analysis (TGA) and differential thermal analysis (DTA). The objective of this study is to examine the relationship between the relative fraction of edge sites and the oxidation behavior of

graphite, and use this information to gain some insight on the role of edge sites on the irreversible capacity loss (ICL) on carbon electrodes in Li-ion cells. The approximate prismatic structure of the natural graphite provided a model geometry from which the relative fraction of edge and basal-plane sites was determined. The three thermal parameters, ignition temperature (T_i), temperature maximum (T_m) in the DTA curves, and the temperature at which 15% carbon weight loss is attained (T_{15}), were determined for a series of natural graphite samples (average particle size, 2-40 μm) using simultaneous TGA/DTA. The results shown in Fig. 6 support the observation that the fraction of edge sites has a strong influence on the thermal parameters (T_i, T_m and T_{15}) for the oxidation of graphite. The relative fraction of edge sites decreases, and correspondingly, the fraction of basal plane sites increases with an increase in the average particle size of the flake graphite. Because the reactivity of carbon in the basal plane is less than that of carbon in the edge sites, the oxidation parameters increase with an increase in particle size.

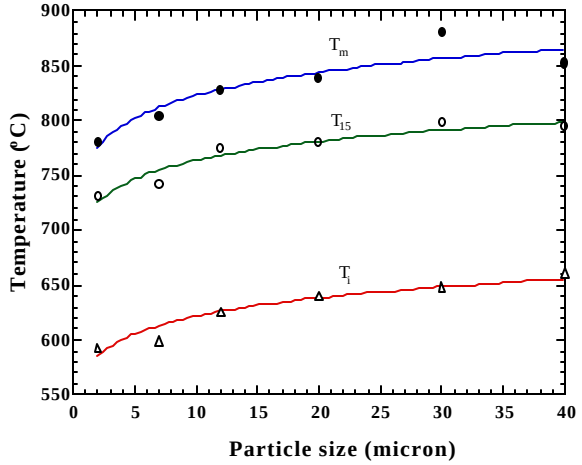

Figure 6. Change in thermal parameters with particle size of flake graphite.

The collaboration with Superior Graphite (SGC) continued with the focus to evaluate alternative graphitized carbons for the negative electrodes in Li-ion cells. SGC now has several commercially available natural graphites for Li-ion batteries. We have examined their oxidation behavior by TGA/DTA to help characterize their properties (Table 1). Their thermal parameters are compared to those of graphitized carbons obtained by heat treatment to 2800°C. It is apparent that the thermal parameters of the natural graphites are higher than those of the artificial graphites. The data show that the ignition temperature, T_i, is much higher for the natural graphites. This result suggests that these natural graphites have a higher fraction of edge sites than the graphitized carbons. The natural graphites and mesocarbon microbead (MCMB) 25-10 have comparable values of T_m and T_{15}, suggesting that they have some common crystallographic structure. The future plans are to collaborate with SGC to identify the appropriate precursor to produce a low-cost graphitized carbon with properties similar to those of MCMB.

PUBLICATIONS

T.D. Tran, D.J. Derwin, P. Zaleski, X. Song and K. Kinoshita, "Lithium Intercalation Studies of Petroleum Cokes of Different Morphologies," *J. Power Sources*, **81-82**, 296 (1999).

W. Jiang, T. Tran, X. Song and K. Kinoshita, "Analysis of the Irreversible Capacity Loss on Carbons for Li-Ion Batteries," in *Proceedings of the 34th Intersociety Energy Conversion Engineering Conference*, Society of Automotive Engineers, Warrendale, PA (1999) p. 57; paper no. 1999-01-2464; meeting held on August 1-5, 1999, Vancouver, Canada.

G. Nazri, B. Yebka, M. Nazri, D. Curtis, K. Kinoshita and D. Derwin, "Safety and Reactivity of Carbonaceous Anode in Lithium-Ion Batteries," in *Solid-State Ionics V*, Vol. 548, G. Nazri, C. Julien and A. Rougier, eds., Materials Research Society, Warrendale, PA (1999) p. 27.

T.D. Tran, X. Song and K. Kinoshita, "Investigation of Lithiated Carbons by Transmission Electron Microscopy and X-Ray Diffraction Analysis," in *Solid-State Ionics V*, Vol. 548, G. Nazri, C. Julien and A. Rougier, eds., Materials Research Society, Warrendale, PA (1999) p. 37.

K. Kinoshita, "Advanced Anode Materials for Li-Ion Batteries," in *New Trends in Electrochemical Technology: Energy Storage Systems for Electronics*, T. Osaka and M Datta, eds., Gordon and Breach Science Publishers, Reading, UK (1999), p. 193-251.

Table 1. Thermal parameters for natural graphite and graphitized carbons.

Sample	Processing	Particle size (μm)	BET Area (m^2/g)	T_i (°C)	T_m (°C)	T_{15} (°C)
LBG-73	natural graphite	43	2.8	657	850	783
LBG-25	natural graphite	10.73	5.28	645	834	770
Fluid coke	heat treated 2800°C	25	5.1	486	722	661
Needle coke	heat treated 2800°C	21	6	581	826	768
MCMB 25-10	heat treated 2800°C	10	-	559	844	772

Corrosion of Current Collectors

James W. Evans (Lawrence Berkeley National Laboratory)
University of California, 585 Evans Hall, MC 1760, Berkeley CA 94720
(510) 642-3807, fax: (510) 642-9164; e-mail: evans@socrates.berkeley.edu

Objectives

- Examine corrosion of current collectors in Li batteries.
- Develop corrosion-resistant collectors and/or corrosion inhibition approaches.
- Develop the EQCM as a tool for investigating reactions in Li batteries.

Approach

- Use EQCM technique to develop understanding of the corrosion behavior of current collectors and corrosivity of various electrolytes, along with other reactions limiting the performance/lifetime of Li cells.
- Measure rates and identify corrosion processes of current collectors in Li batteries under different charge conditions and systems by scanning electron microscopy (SEM).

Accomplishments

- Identified two major factors that are critical to the corrosion of Al current collectors, i.e., chemical and mechanical factors, by applying the EQCM technique to the mechanically damaged Al in various electrolytes.
- Observed pitting corrosion on a scratched Al electrode in electrolytes such as $LiN(CF_3SO_2)_2$/PC using SEM.

Future Directions

- Examine the corrosion of Al or other candidate materials only as needed (e.g., to examine corrosion behavior of novel electrolytes).
- Use the EQCM to examine the SEI layer at the carbon/electrolyte interface to determine SEI composition and stability. The research is a collaboration with the group of Frank McLarnon to examine the SEI layer by both ellipsometry and EQCM.
- Use the EQCM for a quantitative characterization of reversible and irreversible reactions according to the charge/discharge cycle number.

This program focuses on the characterization of corrosion of Al, which is commonly used as a current collector for the positive electrode in rechargeable Li batteries. Two kinds of Al electrodes were tested for the program (thin-film Al on the quartz crystal and carbon-coated Al provided by GM). Aluminum current collectors can be used because of the normally slow corrosion (rather than any thermodynamic inertness of Al), however a corrosion problem occurs when the passivating film on Al breaks down. Because the EQCM can simultaneously measure, with high sensitivity, the mass change of the Al electrode and the charge transfer associated with Al corrosion, this technique is our major experimental tool for the study of the mechanism of corrosion and protective film formation.

Mechanical factor. The Al_2O_3 film can be damaged during manufacturing or overcharging. Furthermore, repassivation via formation of Al_2O_3 is not facile in aprotic electrolytes. Therefore, it is important to investigate, using an Al electrode with the Al_2O_3 damaged or removed, whether another passivation process occurs and how severe the Al corrosion is. For this purpose, Al electrodes were used after polishing or scratching in a glove box.

The Al was polished with several different media: alumina particles, diamond particles, and a polishing cloth containing silicon carbide particles. Scratching was done with tweezers and was usually sufficiently extensive to disrupt the whole of the electrode surface. The cyclic voltammetry (CV) data of variously treated Al in $LiN(CF_3SO_2)_2$/PC showed that the corrosion current is much larger with electrodes that were scratched or polished with a silicon carbide cloth than with the other media. Figure 7 shows an Al surface before (7a) and after one cycle (7b). In this instance the sample was scratched only once so that an individual scratch, running from top to bottom of the micrographs can be discerned. Corrosion pits are evident in 7b and are clearly associated with the scratch. It follows from these micrographs and CV data, that corrosion occurs in the area where the passivating film is removed. The alumina and diamond particles are less effective in extensively disrupting the Al surface and rendering the metal susceptible to oxidation.

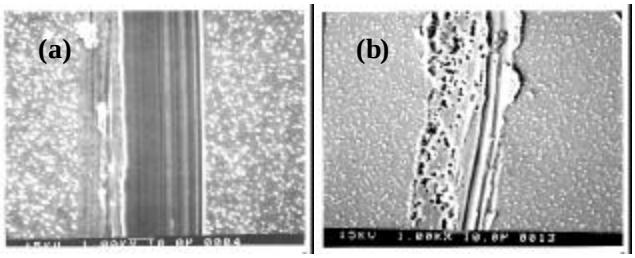

Figure 7. SEM images of a line of scratch made by tweezers on Al surface (a) before, and (b) after the cyclic voltammetry between 2 and 4.5 V in 1M $LiN(CF_3SO_2)_2$/PC.

Chemical factor. Electrolytes tested for this study are: propylene carbonate (PC) containing $LiN(CF_3SO_2)_2$, $LiC(CF_3SO_2)_3$, $LiCF_3SO_3$, $LiPF_6$, $LiBF_4$ or $LiClO_4$, singly or in a limited number of combinations, and poly(ethylene glycol) dimethyl ether (PEGDME) solution containing $LiN(CF_3SO_2)_2$.

Figure 8a shows a cyclic voltammogram for a polished Al electrode in 1M $LiN(CF_3SO_2)_2$/PC. The oxidation current is attributed mainly to Al corrosion, not to oxidation of $N(CF_3SO_2)_2^-$ or PC. Figure 8b shows a simultaneously acquired mass change diagram. The mass increases with potential scanning and then decreases. If Al is oxidized to soluble Al^{3+}, the mass should decrease with scanning. This result indicates that Al is oxidized to Al^{3+} and at the same time Al^{3+} forms a complex such as $Al[N(CF_3S)_2)_2]_3$ formed with $N(CF_3SO_2)_2^-$ anion on the Al surface. In Fig. 8a, the current is very small at <3.5 V during the cathodic scan, and the mass decreases. This suggests that an electroless desorption process takes place. Thus, the mass of the Al electrode decreases. This corrosion behavior also appears in PC solutions containing $LiC(CF_3SO_2)_3$ or $LiCF_3SO_3$.

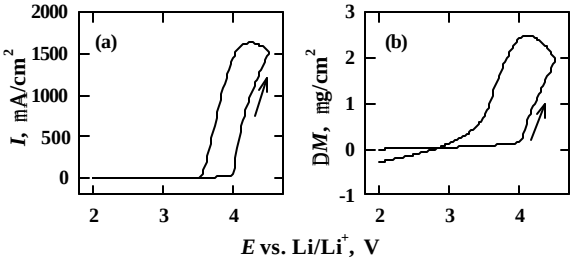

Figure 8. (a) cyclic voltammogram and (b) simultaneously acquired mass change diagram for an Al electrode polished with a SiC cloth in 1 M $LiN(CF_3SO_2)_2$/PC.

Two possible mechanisms to explain the corrosion behavior of Al in $LiN(CF_3SO_2)_2$/PC are suggested. One is that the $Al[N(CF_3S)_2)_2]_3$

complex desorbs slowly from the Al surface after it forms on the electrode. The other is that the $Al[N(CF_3S)_2)_2]_3$ complex is oxidized and then desorbs slowly. In both cases, electroless desorption occurs.

Figures 9a and 9b show a cyclic voltammogram and a simultaneously acquired mass change diagram, respectively, in $LiPF_6$/PC. The current is substantial during the first anodic scan, but it is small during the first cathodic scan and throughout the second scan. The mass shows a large increase during the first anodic scan, and only a small increase during the first cathodic scan and the second scan. The result shows that Al corrosion does not occur in this solution even though Al_2O_3 was removed from the electrode surface. Moreover, the mass increase means that the passivating film is formed during the first anodic scan. This corrosion behavior also occurs in $LiBF_4$/PC and in $LiN(CF_3SO_2)_2$/PEGDME.

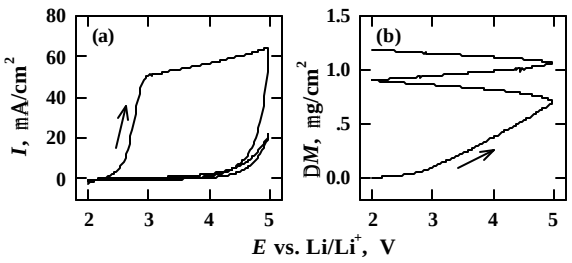

Figure 9. (a) cyclic voltammogram and (b) simultaneously acquired mass change diagram for an Al electrode polished with a SiC cloth during the first two cyclic scans in 1 M $LiPF_6$/PC.

Assuming that the mass change of Al_2O_3 is caused only by faradaic processes, the mass and charge are represented by Faraday's law where we could find the ratio of the apparent molar mass of species causing mass change to the number of electrons taking part in the process. This ratio is near 20 for the systems that show the monotonic mass increase such as $LiPF_6$/PC. Therefore, if we exclude the possibility of a composite passivating film, the main component of the film can be considered as AlF_3.

Based on the fact that Al corrosion is hindered by a passivating film in $LiPF_6$/PC and $LiBF_4$/PC, an attempt was made to prevent corrosion by addition of $LiPF_6$ or $LiBF_4$ to $LiN(CF_3SO_2)_2$/PC, and these additions were found to be helpful in limiting corrosion.

Corrosion of carbon-coated aluminum provided by GM. The corrosion behavior in $LiPF_6$/EC+DMC was investigated for three kinds of electrodes: untreated Al foil, Al foil polished with a silicon carbide cloth in a glove box, and carbon-coated Al foil. Their cyclic voltammetry data show that the electrochemical behavior of the carbon-coated Al is totally different from the other Al foils. The open circuit potential of coated Al is about 3.6 V vs. Li/Li^+, much higher than that of bare Al, and much larger current flows during the first two cycles. Contrary to the case of polished Al, for which anodic film forms during the first cycle and reduced current is observed during the second cycle, the carbon-coated Al appears to show no such corrosion-limiting characteristic of the underlying Al.

PUBLICATION

Y. Chen, T.M. Devine J.W. Evans, O. Monteiro and I.G. Brown, "Examination of the Corrosion Behavior of Aluminum Current Collectors in Lithium/Polymer Batteries," *J. Electrochem. Soc.*, **146**, 1310 (1999).

PRESENTATION

H. Yang, K. Kwon, T.M. Devine, and J.W. Evans, "EQCM Study on Aluminum Corrosion in Lithium Batteries", *196th Meeting of the Electrochemical Society*, Honolulu, HI, October 1999

HIGH-PERFORMANCE NON-FLAMMABLE ELECTROLYTES

The safe use of high-power Li-ion batteries requires a better understanding of the abuse tolerance of the cell components at higher operating temperatures, and the stability limits of the electrolyte. A major technical challenge is to develop an electrolyte that is non-flammable, and at the same time, has physicochemical properties that produce acceptable electrochemical performance in Li-ion batteries. Studies were initiated in FY 1999 to develop non-flammable electrolytes (NFEs) for Li-ion batteries.

Non-Flammable Electrolytes

Kim Kinoshita
Lawrence Berkeley National Laboratory, 90-1142, Berkeley CA 94720
(510) 486-7389; fax: (510) 486-4260; e-mail: k_kinoshita@lbl.gov

Objective

- Develop NFEs that have flash points >100°C, high ionic conductivity (>10^{-3} S/cm at 20°C), wide electrochemical voltage window (0-5 V), compatibility with other cell components, environmentally friendly and which can pass abuse tolerance testing in Li-ion batteries.
- Determine the catalytic influence of electrode active materials on the thermal stability of NFEs at elevated temperatures.

Approach

- Utilize gas chromatography to determine the thermal stability of the baseline electrolyte [1 M $LiPF_6$ in a mixture of 1:1 (mol ratio) EC/DMC] and NFEs at elevated temperatures.
- Apply chromatographic and spectroscopic techniques to investigate the catalytic interactions between the electrolyte and electrode components.

Accomplishments

- Carried out gas chromatography (GC) and nuclear magnetic resonance (NMR) studies which suggested that polyether carbonates are formed during thermal decomposition of the baseline electrolyte at 85°C.

Future Directions

- Complete chemical analysis of the decomposition products from the baseline electrolyte.
- Initiate chemical analysis of the decomposition products from the flame-retardant additives and NFEs provided by subcontractors.

Experiments were conducted to determine the thermal stability of the baseline electrolyte [1M $LiPF_6$ in 1:1 (mol ratio) EC/DMC] electrolyte for Li-ion batteries. The electrolyte was heated to 85°C and samples were removed periodically for analysis by GC. Gas evolution (which may be CO_2) was observed in electrolytes heated at 85°C for several days and the production of a brown-black material was also observed. Extraction of the material in water/methylene chloride and GC analysis of the organic phase produced no change in the GC trace; therefore, removal of water-soluble compounds from the reaction mixture does not change the chromatogram.

The GC trace from the electrolyte mixture shows two clearly separate solvent peaks for DMC (5-min retention time) and EC (about 14.1-min retention time). The GC trace shows that a sample of electrolyte heated to 85°C contains the solvent peaks along with a large new peak at 13.8-min retention time and several others of lower intensity. The peak intensity for EC decreases as a function

of storage time, indicative of the gradually decomposition of EC at 85°C. On the other hand, the GC signal intensity for DMC remains essentially constant, indicating that DMC is stable during storage at 85°C. The identity of the major new compound is unknown at this time, but its relative intensity increases with storage at 85°C.

The decomposition mechanism may occur through the ring opening of EC via complexation with a Lewis acid. The Lewis acid, PF_5, may be generated by a disproportionation reaction of the electrolyte salt

$$PF_6^- <-> PF_5 + F^- \quad (1)$$

When pyridine is added to the electrolyte (20 mg/2mL), it remains clear even after heating at 85°C for 11 days. Thus, the overall decomposition reaction is inhibited by the addition of organic bases (such as pyridine), which increase the stability of the salt by inhibiting the disproportionation reaction. A ring-opened product from EC may be etheric in structure; mass spectroscopy of the peak confirmed this possibility as such moieties are observed. The solvent heated alone produces this product in a very small quantity, adding any salt increases the reactivity of the EC; however mixtures with 1 M lithium trifluoromethane sulfonate (LiTf) or lithium trifluromethane sulfonimide (LiTFSI) are much more stable than those with $LiPF_6$.

A sample of trifluoroethylene carbonate ($CF_3CH_2OCOOCH_2CF_3$) (ETC) was obtained from Sandia National Laboratories (SNL) and used as an additive to the baseline electrolyte. It appears that no appreciable difference in the decomposition rate of the baseline electrolyte is observed when 10 wt% ETC is added. However, the gas chromatogram from the sample containing ETC shows peaks that may be indicative of 17 new compounds, whereas the $LiPF_6$ electrolyte has GC peaks that may be associated with four new compounds after heating to 85°C. Clearly the ETC is involved in decomposition or reaction with the electrolyte.

Thermogravimetric analyses (TGA) were initiated to study the stability of $LiPF_6$. The weight loss of solid $LiPF_6$ at 70°C under flowing nitrogen was measured with a microbalance (Model SDT 2960, TA Instruments). The results indicate that $LiPF_6$ undergoes significant weight loss in a matter of hours (weight loss of 60% in 200 min). The electrolyte salt, $LiPF_6$, exists in an equilibrium that is dependent on the PF_5 pressure in the products:

$$LiPF_{6\,(s)} <-> LiF_{(s)} + PF_{5\,(g)} \quad (2)$$

Addition of a solvent with minimal vapor pressure hindered the escape of PF_5 in the TGA experiment. This was verified by using a solution of polyether carbonate, $(CH_2CH_2O)_3COO)_n$ (PE_3), as an involatile solvent in the TGA experiment. After 200 min at 70°C, the weight loss was only 20%. The colligative properties of the solution decrease the rate of PF_5 loss, and the solvent/PF_5 reactivity slows its loss rate at 70°C. The solvent increases the reverse-rate of the process (2) or reacts with the gas to produce new products.

A Shlenk technique was developed to follow the reaction of PF_5 gas and electrolytes at room temperature. The preliminary experiments to demonstrate the viability of the method involved reactions of solid $LiPF_6$ and EC/DEC/$LiPF_6$. The reactions produced a brown solution within a day. The appearance of the solution after this reaction is identical to that obtained by heating electrolytes EC/DMC/$LiPF_6$ and PE_3/$LiPF_6$.

Proton NMR studies of the thermal reaction products from EC/DMC/$LiPF_6$ show the presence of peaks at 3.73, 3.74, 4.31 and 4.49 ppm (from TMS). Singlets at 3.73 and 4.31 are due to DMC and EC, respectively, and the other peaks match well with the proton NMR spectrum for polyether carbonates $(CH_2CH_2O)_mCOO)_n$ reported in the literature ["The polymerization of ethylene carbonate" L. Vogdanis & W. Heitz *Macromol. Chem., Rapid Commun*. **1986**, *7*, 543]. These results suggest that PF_5 is responsible for the polymerization reactions in the electrolyte.

Development of Nonflammable Electrolytes

J. Prakash
Illinois Institute of Technology, Department of Chemical and Environmental Engineering,
10 W 33rd Street, Chicago, IL 60616
(312) 567-3639, fax: (312) 567-8874; e-mail: prakash@iit.edu

Objectives

- Develop nonflammable electrolytes with high flash point (>100°C), high ionic conductivity (10^{-3} S/cm), and wider voltage window (0-5 V vs. Li) in an effort to provide better thermal stability and fire safety.

Approach

- Modify existing electrolytes by using novel flame-retardant (FR) additives that are compatible with active electrode materials and the environment.
- Use chemical, electrochemical, and thermal techniques to investigate the stability and performance of electrolytes modified with FR additives.

Accomplishments

- Filed a provisional U.S. patent (#60/152,071) on "Nonflammable electrolytes for batteries".
- Transferred FR to Argonne National Laboratory (ANL) for further evaluation in PNGV Li-ion cells.

Future Directions

- Investigate hexa-methoxy-triaza-phosphozene (HMTAP) in sealed large (18650) cells in collaboration with ANL and Polystor Co.
- Investigate the utilization mechanism of FR in Li-ion cells.
- Initiate investigations of the synergistic effect of FR and thermally stable salts (triflate and imide) in Li-ion cells.

Experiments were conducted to evaluate the thermal and electrochemical behavior of the baseline electrolyte (EC-DMC/$LiPF_6$), and to identify FR additive(s) that provide improved thermal and flame properties such as phosphorous oxide (P_2O_5). Addition of P_2O_5 in the electrodes did not produce any significant improvement in the thermal behavior of a Li-ion cell. Subsequently, we synthesized and characterized HMTAP, ($N_3P_3[OCH_2CH_3]_6$, as a FR for Li-ion cells. CV was used to investigate the electrochemical stabilities of the baseline electrolyte and the electrolyte containing FR in the voltage window of 0-5 V vs. Li. The CVs were obtained on a Pt disk electrode in a voltage range of 0-2.0 V and on a glassy carbon disk electrode between 2.0 and 5.0 V. Comparable electrochemical stabilities were observed for both the baseline electrolyte and FR-containing electrolyte, suggesting that the FR was electrochemically stable between 0 to 5.0 V vs. Li.

The electrochemical performances of cells fabricated with and without FR were evaluated in 2016 coin cells at various charge and discharge rates. The charge and discharge capacities of a Li/$LiNi_{0.8}Co_{0.2}O_2$ cell containing 1.5 wt% FR were noticeably higher than that of a comparable cell without FR. However, the reason for this capacity increase is not clear at this stage. Further experiments to quantify this difference are currently underway.

The self-heat rate profile of the electrolyte with and without FR was evaluated using an Accelerating Rate Calorimeter (ARC). These results are shown in Fig. 10. It is evident that the maximum self-heat rate of the electrolyte without FR is 0.68°C/min, which occurs at T=177.6°C. This is attributed to the reaction of Li with the electrolyte. As the reaction proceeds, Li is consumed, and thus the exothermic peaks decrease as the temperature increases above 177.6°C. On

the other hand, the maximum self-heat rate of the electrolyte containing FR is only 0.1957°C/min at T=170.2°C. The peaks were suppressed in comparison with those for the electrolyte without FR, which may be attributed to the passivation layer that is formed on the surface of the Li metal by the flame-retardant additive. Results of these thermal investigations strongly suggest that the addition of the FR to the electrolyte significantly reduces the self-heat rate, which in turn, helps to improve the non-flammability of the electrolyte. Methods to investigate the flame characteristics of the FR additives in Li-ion cells are currently being designed.

The results of the present investigations show that HMTAP is a viable FR for Li-ion cells. This FR performed very well in small coin cells in short-term cycling. However, there are several important issues related to the use of this material in Li-ion cells that must be investigated in detail. These are related to the performance of the FR in scaled-up Li-ion cells, investigation of internal pressure due to the FR, the effect of FR on long-term cycling, and the mechanism responsible for the capacity increase. In addition, the reaction mechanism by which the FR works also must be investigated. These include the formation of a less-permeable and protective coating on the electrode surface, reducing the oxygen concentration in the flame, and heat dissipation by an endothermic change in the retardant such as by fusion or sublimation. It may or may not be necessary for the flame retardant to decompose with the liberation of halogens at somewhat lower temperatures than the decomposition temperatures of the substrate. The understanding of the mechanism will greatly help in synthesizing better and inexpensive materials as FR additives, and in selecting ways to incorporate these additives in cells.

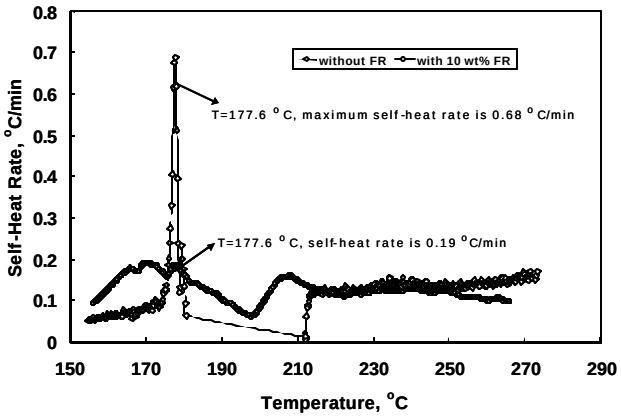

Figure 10. Thermal behavior of 1 M $LiPF_6$ with EC-DMC containing 0.0 and 10.0 wt% of the HMTAP flame-retardant additive using ARC.

Non-Flammable Electrolytes

K.M. Abraham
Covalent Associates, Inc., 10 State Street, Woburn, MA 01801
(781) 938-1140; fax: (781) 938-1364; e-mail: abraham@covalent.tiac.net

Objective

- Develop NFEs for Li-ion batteries which meet the goals for high power and thermal abuse tolerance for transportation applications.

Approach

- Investigate fluorinated esters as electrolyte solvents for Li-ion batteries.
- Prepare and characterize electrolytes in 2,2,2-trifluoroethyl acetate (TFEA) and ethyl trifluoroacetate (ETFA), solvents chosen to determine how the positions of the fluorine atoms relative to the carbonyl group in the ester affect their performance as electrolyte solvents.

Accomplishments

- Evaluated TFEA and ETFA as electrolyte solvents for Li-ion batteries.

- Prepared highly conductive electrolytes in TFEA with $LiPF_6$, $LiN(SO_2C_2F_5)_2$ and $LiC(SO_2CF_3)_3$.
- Identified TFEA/EC(1:1)-LiX solutions where LiX is $LiPF_6$ or $LiC(SO_2CF_3)_3$, as electrolytes suitable for reversibly intercalating Li into graphite and compatible with high-voltage cathodes.

Future Directions

- Construct Li-ion cells with the new electrolytes and evaluate their cycling and safety behavior.
- Compare and contrast the electrochemical and safety characteristics of the electrolytes in fluorinated ethyl acetates versus their chlorinated analogs.

The objective of the program is to develop NFEs for Li-ion batteries that meet the requirements for high power and thermal abuse tolerance in transportation applications. Our approach is to use halogenated esters as solvents for Li-ion battery electrolytes. Electrolytes were prepared and characterized in TFEA and ETFA and in the mixed solvents formulated from these esters and EC.

Physical Properties of Solvents and Electrolytes. Both TFEA and ETFA were isolated as colorless liquids with the former having a boiling point of 78-80°C and the latter 60-62°C. They were isolated with >99% purity and a water content of <20 ppm. Electrolytes were prepared in both TFEA and ETFA with $LiPF_6$, $LiN(SO_2C_2F_5)_2$ [LiBeti] or $LiC(SO_2CF_3)_3$ [Li methide], and the two solvents showed marked differences in their ability to dissolve these salts. Solutions with about 1 M Li salt could be prepared in TFEA with all three salts, but poor Li salt solubility was observed in ETFA.

Conductivities of 3.3, 2.3 and 1.8 mS/cm were measured at room temperature for 1M solutions of $LiPF_6$, $LiC(SO_2CF_3)_3$ and $LiN(SO_2C_2F_5)_3$, respectively. It was possible to increase the conductivities with EC as a cosolvent. For $LiPF_6$, $LiC(SO_2CF_3)_3$ and $LiN(SO_2C_2F_5)_3$ solutions in a 1:1 (by volume) TFEA:EC mixed solvent, conductivities of 7.5, 4.7 and 5.1 mS/cm, respectively, were measured at 20°C.

Preliminary IR and ^{13}C NMR spectral data for $LiPF_6$ solutions in ETFA and TFEA suggested that the solubility differences of the Li salts in these solvents is attributable to their ability to solvate Li^+ ions. The ^{13}C NMR spectrum revealed a downfield chemical shift in the carbonyl carbon of TFEA from 170.34 ppm to 172.63 ppm when 1 M $LiPF_6$ was added, indicating strong interactions between Li^+ and C=O. On the other hand, for ETFA, $LiPF_6$ addition produced little change in the ^{13}C NMR chemical shift, suggesting poor chemical interactions between Li^+ and C=O. It appears that when the highly electronegative CF_3 is closer to the carbonyl group, the oxygen lone-pair electrons are pulled toward CF_3 making the oxygen poorly solvating. This view is substantiated by IR-spectral data that showed C=O absorption peaks due to both Li^+-complexed and uncomplexed species in TFEA-$LiPF_6$. Conversely, no separate peaks attributable to a Li^+-complexed specie was observed in ETFA-$LiPF_6$.

Electrochemical Stability. Electrochemical stabilities of TFEA electrolyte solutions were determined from slow-sweep (1 mV/s) CV on a Pt electrode. The potential scan from 3.0 to 0.0 V vs. Li^+/Li in TFEA/1M $LiPF_6$ showed a reduction peak at ~2.5V, which completely disappeared in a second scan. It appears that the initial reduction of the electrolyte results in the formation of a SEI, which prevents further reduction of the electrolyte as it is impermeable to the solvent. This electrolyte showed good oxidative stability as the oxidation current remained below 5 $\mu A/cm^2$ when the potential was scanned from 0.0 to 5.0V vs. Li^+/Li. There were no significant differences in the CV responses of the solutions prepared with the different salts. The use of EC as a cosolvent, however, increased the reduction stability of the electrolytes, as evidenced by the significant decrease in the cathodic current at 2.5 V. Therefore, it appears that an EC:TFEA mixed solvent is a better choice for Li-ion cells.

Li/Graphite Cells. Lithium intercalation/ deintercalation capacities of graphite were determined in EC/TFEA-LiX electrolytes. A

typical result with the EC/TFEA(1:1)-1M $LiPF_6$ solution is displayed in Fig. 11. The reversible capacity of ~360 mA/g is very close to the theoretical value of 372 mAh/g for graphite.

$Li/LiCoO_2$ Cells. $Li/LiCoO_2$ cells were also cycled using EC/TFEA(1:1)-1M LiX electrolytes (Fig. 12). These results demonstrate the suitability of TFEA-based electrolytes for Li-ion battery application in conjunction with high-voltage cathodes.

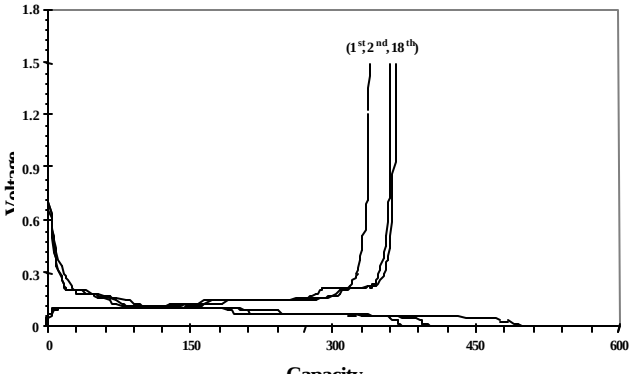

Figure 11. Typical charge/discharge cycles for a Li/graphite cell using the EC/TFEA (1:1)-$LiPF_6$ (1M) solution. $I_d = I_c$ - 0.1 mA/cm^2

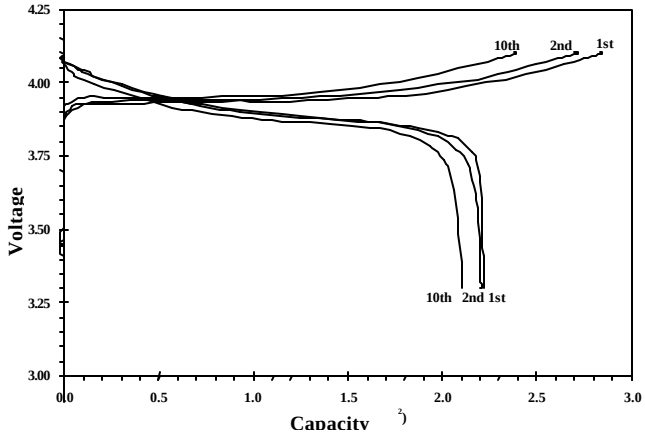

Figure 12. Charge/discharge cycles for a $Li/LiCoO_2$ cell using the 1:1 EC/TFEA- $LiC(SO_2CF_3)_3$ (1M) electrolyte. $I_d = I_c = 0.25$ mA/cm^2

NON-CARBONACEOUS ANODE MATERIALS

Every Li-ion battery on the market today uses some form of carbon as its anode material. These batteries suffer from safety, cycle life, and storage-life problems. It is for these reasons that non-carbonaceous anodes are being developed as possible alternatives to carbon. Investigations are underway to identify low-cost metal alloys with potentially acceptable capacity, rate, cyclability and calendar life.

Non-Carbonaceous Anode Materials

Michael M. Thackeray
Argonne National Laboratory, Chemical Technology Division, Argonne IL 60439
(630)-252-9183; fax: (630)-252-4176; e-mail: thackeray@cmt.anl.gov

Objective

- Develop and characterize high-capacity non-carbonaceous anode materials that operate a few hundred millivolts above the potential of metallic Li.

Approach

- Investigate selected intermetallic structures that operate as insertion electrodes for Li with relatively little volume expansion compared to conventional "alloy" electrodes.
- Focus on NiAs and zinc-blende-type structures, and characterize their structural and electrochemical properties for Li-ion insertion.

Accomplishments

- Identified Cu_6Sn_5 (NiAs-type structure) and InSb (Zn-blende-type structure) as possible insertion electrodes for Li.
- Recognized Zn-blende framework recognized to have three-dimensional interstitial space for Li; upon lithiation Cu_6Sn_5 structure transforms to lithiated Zn-blende ("Li_2CuSn"-type) structure at ~400 mV above Li potential.

Future Directions

- Undertake detailed structural and electrochemical characterization of Cu_6Sn_5 and InSb electrodes.
- Continue to explore NiAs-type and Zn-blende-type structures with optimized electrode and electrochemical properties.

The objective of this task is to develop and characterize non-carbonaceous anode materials for high-energy rechargeable Li batteries for EVs and HEVs. A specific objective of the research effort is to identify materials that are inherently safer than carbon-based electrodes without compromising capacity, rate capability and cycle life (particularly when subjected to overcharge conditions at elevated temperature). The search for new, inexpensive materials has focused on intermetallic materials that have potentials a few hundred millivolts above Li and with capacities >300 mAh/g, or 1000 mAh/ml.

Our research demonstrated that certain binary intermetallic systems, such as those in the Cu-Sn and In-As systems, can accommodate Li topotactically within their structures. In particular, it was demonstrated by *in situ* XRD that Li is inserted into η-Cu_6Sn_5 which has a structure that is closely related to the NiAs-type; it also has some structural features displayed by the Ni_2In-type structure. During Li insertion, one half of the Sn atoms migrate into interstitial sites of the NiAs-type structure such that on full lithiation a Li_2CuSn-type structure is formed; the remaining $Cu_6Sn_{2.5}$ thus acts as a stable host framework for Li. The insertion reaction is accompanied by a volume expansion of 59%, which is significantly less than that for the full lithiation of Sn to $Li_{4.4}Sn$ (358%). The reaction is reversible provided that the upper and lower voltage limits are strictly controlled. This system yields a reversible capacity of ~200 mAh/g, which translates to a volumetric capacity of ~1660 mAh/ml, based on the density of Cu_6Sn_5 (8.3 g/ml), or 1060 mAh/g based on the density of Li_2CuSn (5.3 g/ml). The practical volumetric capacity of Cu_6Sn_5 is thus significantly greater than the theoretical capacity of graphite (~800 mAh/ml). Lithiation beyond "Li_2CuSn" destroys the $Cu_6Sn_{2.5}$ framework because an irreversible displacement reaction occurs during which Cu and $Li_{4.4}Sn$ are formed.

To confirm the validity of these results stoichiometric Li_2CuSn was prepared from which Li was extracted chemically with an excess of $NOBF_4$ in acetonitrile at room temperature. An XRD analysis confirmed that the product had a structure that resembled Cu_6Sn_5.

Of particular significance was the observation that the CuSn framework of the Li_2CuSn structure has a Zn-blende-type arrangement of atoms. This feature has immediate implications for designing alternative negative electrode materials for Li batteries. Therefore, the research was extended to include intermetallic compounds having the Zn-blende framework. For the initial studies, InSb was selected as an example of an intermetallic compound with a Zn-blende-type structure. InSb is

a small band-gap semiconductor that has relatively large atoms, which provide an attractive three-dimensional interstitial space for Li atoms. The voltage profile of a typical Li/InSb cell is shown in Fig. 13a from which it is apparent that most of the initial electrochemical reaction occurs with a steadily decreasing voltage between 0.80 and 0.60 V. In subsequent cycles, the discharge and charge processes occur in a series of reproducible steps between 1.2 and 0.5 V, as shown in an enlarged representation of the 3rd discharge and charge cycle (Fig. 13b). The exact reason for the marked change in the voltage profile of the initial discharge reaction to subsequent cycles is presently unknown. It is believed that the change in profile may be associated with structural changes to the InSb framework during the initial "break-in" cycle.

The electrochemical discharge in Fig. 13b is divided into three distinct steps, D(1), D(2), and D(3); the three steps correspond closely to the cumulative reaction of InSb with 1.0, 2.0, and 2.5 Li atoms, respectively. The reaction is reversible. On charge, step C(2) occurs in a two-stage process [C(2a) and C(2b)], each stage corresponding to the removal of ~0.5 Li atoms. A possible mechanism is proposed in which Li is initially inserted into the InSb structure to a nominal composition Li_2InSb; thereafter, it appears that In is extruded from the structure, possibly as Li_xIn. More *in situ* XRD, X-ray absorption near-edge spectroscopy (XANES) and extended X-ray absorption fine structure (EXAFS) studies are in progress to determine the structural changes that occur during the initial lithiation reaction and the differences between that reaction and subsequent charge and discharge reactions.

PUBLICATIONS

K.D. Kepler, J.T. Vaughey and M.M. Thackeray, "$Li_xCu_6Sn_5$ ($0<x<13$): An Intermetallic Insertion Electrode for Rechargeable Lithium Batteries," *Electrochemical and Solid State Letters*, **2**, 307 (1999).

M.M. Thackeray, J.T. Vaughey, A.J. Kahaian, K. D. Kepler and R. Benedek, "Intermetallic Insertion Electrodes Derived from NiAs-, Ni_2In- and Li_2CuSn-type Structures for Li-Ion Batteries," *Electrochem. Comm.*, **1**, 111 (1999).

K.D. Kepler, J.T. Vaughey and M.M. Thackeray, "Copper-Tin Anodes for Rechargeable Lithium Batteries: An Example of the Matrix Effect in an Intermetallic System," *J. Power Sources*, **81-82**, 383 (1999).

J.T. Vaughey, K.D. Kepler, R. Benedek and M.M. Thackeray, "NiAs- vs. Zinc-Blende-type Intermetallic Insertion Electrodes for Lithium Batteries," *Electrochem. Comm.*, **1**, 517 (1999).

J.T. Vaughey, J. O'Hara and M.M. Thackeray, "Intermetallic Insertion Electrodes with a Zinc-Blende-Type Structure for Li Batteries: A Study of Li_xInSb (0#x#3)," *Electrochemical and Solid State Lett.*, **3(1)** 13 (2000).

PRESENTATIONS

A.J. Kahaian J.T. Vaughey, K.D. Kepler, C. Chen, A.N. Jansen and M.M. Thackeray, "Synthesis and Characterization of Alternative Anode Materials for Li-ion Batteries," *3rd Int. Symposium on New Materials for Fuel Cell and Modern Battery Systems*, Montreal, Canada, July 6-10, 1999.

J.T. Vaughey, K.D. Kepler, M. Scott, C.S. Johnson, T. Sarankonski, A. Kahaian, S. Hackney and M.M. Thackeray, "Intermetallic Insertion Anodes for Lithium Batteries," *196th Electrochemical Society Meeting*, Hawaii, HI, October 17-22, 1999.

M.M. Thackeray, J.T. Vaughey, C.S. Johnson and K.D. Kepler, "Intermetallic Insertion Electrodes for Lithium Batteries," *13th IBA Meeting*, Marrakesh, Morocco, November 7-11, (1999).

C.S. Johnson, M.M. Thackeray, J.T. Vaughey, K.D. Kepler, A.J. Kahaian and K. Amine, "Intermetallic Insertion Electrodes for Lithium Batteries," *40th Japan Battery Symposium*, Kyoto, Japan, November 14-16, (1999).

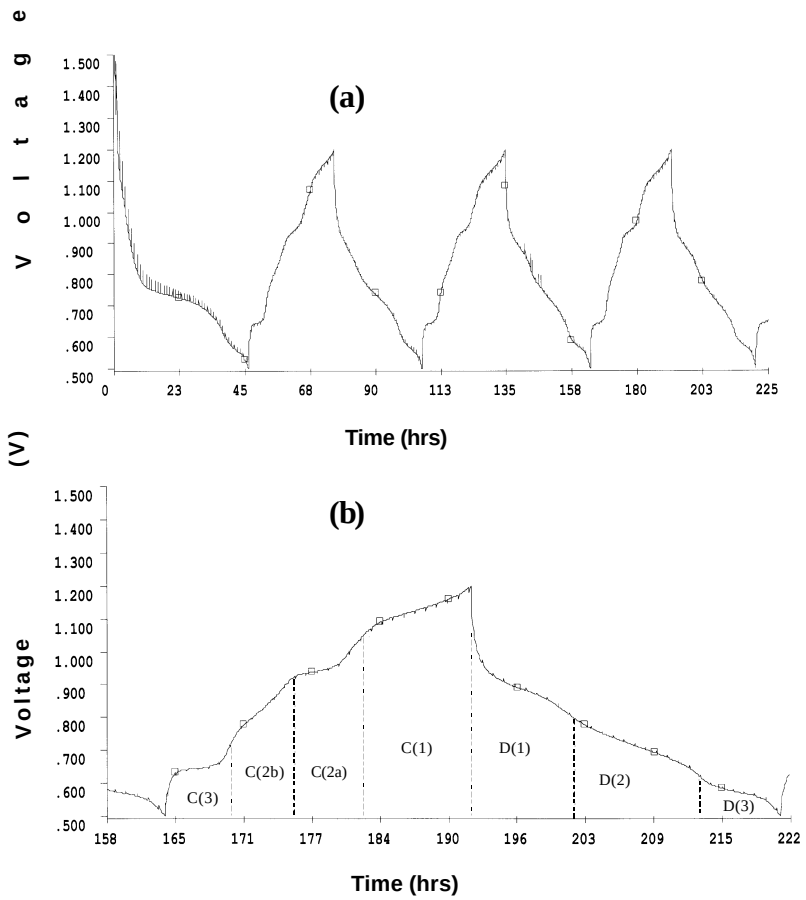

Figure 13. Electrochemical characteristics of a Li/InSb cell: (a) the voltage profile (first 3 cycles) between 1.2 and 0.5 V, and (b) an enlarged representation of the 3rd charge and discharge cycles.

Non-Carbon Anodes

M. Stanley Whittingham
State University of New York at Binghamton, Chemistry and Materials Research Center, Binghamton, NY 13902-6000
(607) 777-4623, fax: (607) 777-4623; e-mail: stanwhit@binghamton.edu

Objective

- Find a low-cost, low-weight and safer anode material for rechargeable Li batteries to replace carbonaceous compounds.

Approach

- Synthesize manganese and vanadium oxides and evaluate as anodes.
- Explore opportunities for enhancing the electrochemical behavior of simple metal alloys such as Al.

Accomplishments

- Synthesized a series of manganese oxides and determined their capacity at low potentials; observed little recycling capacity in pure manganese oxides.
- Synthesized the LiAl alloy electrochemically and chemically.

Future Directions

- Evaluate vanadium oxides and manganese vanadium oxides.
- Investigate Al-based materials, $LiAlM_y$, to improve the cyclability of simple alloy systems.

The goal of this project is to identify low-cost, low-weight materials that are safer than carbonaceous materials for negative electrodes. Aluminum is the ideal anode material, being low cost, readily available and forming a simple alloy with Li, LiAl. This reaction occurs at about 0.3 V from pure Li with an essentially flat voltage plateau as shown in Fig. 14. However, the material expands by 57% upon Li incorporation, causing powdering. This combined with the brittleness of LiAl causes contact problems during cycling, resulting in relatively poor cycling behavior. Even so, it was the first anode used in rechargeable Li batteries, being coupled with TiS_2 (Exxon-1978).

Although carbonaceous materials are being successfully used in Li-ion cells, there are safety issues. This project is taking two approaches: use of oxides giving essentially a simple symmetric cell:

$$Li_{1+y}MnO_2|electrolyte|Li_{1-y}MnO_2$$

or use of simple Al-based metal alloys: $LiAlM_y|electrolyte|Li_{1-y}MnO_2$.

We have studied several manganese oxides including the spinel and layered phases. In each case, the material reduced to Li_2O and Mn, based on the Li utilization. However, little capacity was retained after recharge to 1 V vs. Li. Effort is thus being switched to mixed manganese vanadium oxides and to vanadium oxides. In the process of this work, a new low-temperature synthesis route to the synthesis of $LiMnO_4$ was found. We can now prepare both the spinels and layered phases of Li_xMnO_2 at temperatures below 200°C.

The LiAl alloy was prepared by several routes including: in cells: Li |electrolyte| Al Al |electrolyte| $LiCoO_2$ as well as by direct reaction between Li and Al immersed in a Li-containing electrolyte. These materials are being evaluated in cells.

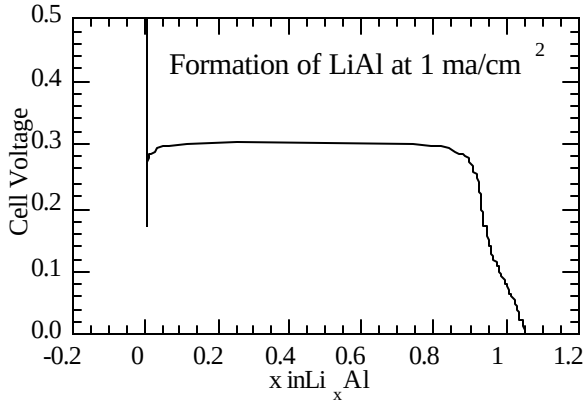

Figure 14. Incorporation of Li into Al at 1 mA/cm^2.

NOVEL CATHODE MATERIALS

$LiCoO_2$ used in commercial Li-ion cells for consumer electronic devices is too expensive for large-scale applications. Thus alternative cathode materials, which combine high reversibility and current-drain capabilities, are desired. The focus of this task is to develop Mn-based oxides because of their low cost, low toxicity and familiarity to the battery industry. Research is directed at understanding the reasons for the capacity fade and developing methods to stabilize this material

New Cathode Materials Based on Layered Structures

M. Stanley Whittingham
State University of New York at Binghamton, Chemistry and Materials Research Center, Binghamton, NY 13902-6000
(607) 777-4623, fax: (607) 777-4623; e-mail: stanwhit@binghamton.edu

Objective

- Find lower-cost and higher-capacity oxide cathodes for rechargeable Li batteries to replace $LiCoO_2$.

Approach

- Synthesize manganese oxides with a crystallographic structure that permits facile intercalation of Li^+ ions, and does not revert to the spinel structure.
- Characterize the metal oxide structures by XRD analysis and evaluate materials in electrochemical cells.

Accomplishments

- Hydrothermally formed Co-, Fe- and Ni-substituted manganese oxides, which exhibited enhanced conductivity and electrochemical behavior; found cycling rate to be a critical factor in stability of the layered phase.
- Recognized vanadium-pillared manganese oxides as possible cathode materials.

Future Directions

- Continue synthesis and electrochemical studies of stabilized manganese oxides, with emphasis on those with layered structures.
- Investigate impact of multiple phases and additives such as bismuth.

The goal of this project is to identify layered manganese oxides with properties superior to $LiCoO_2$. Layered $LiMnO_2$, which has the potential of cycling 1 Li per Mn ion, is unstable relative to the spinel $LiMn_2O_4$ on cycling. This ease of phase change is enhanced by both structures having a cubic close packed (ccp) oxygen lattice, so that simple manganese migration is all that is required for structural transformation. If this packing arrangement is disrupted, then perhaps a layered MnO_2 structure can be stabilized over the entire Li range $0 \leq x \leq 1$ in Li_xMnO_2, just as in Li_xTiS_2. We have been exploring several ways to stabilize the layered structure including: (1) inserting pillars between the MnO_2 sheets (e.g., K) and immobile, electrochemically active pillars such as VO_y, and (2) structure modification by doping with ions such as Co, Ni and Fe. Our research showed that K^+ ions disrupt the ccp arrangement of the oxygen ions and give better retention of cycling capacity than pure Li_xMnO_2.

We have made a series of substituted layer manganates of formula $A_xMn_{1-y}M_yO_2$ (A= K, Na, or Li and M = Ni, Fe or Co and $y \leq 1$), at both high temperatures and under hydrothermal conditions. The M elements stabilize different arrangements of the oxygen atoms. For example, Ni disrupts the ccp structure and Co stabilizes the layer structure to much lower alkali contents, thus $Na_{0.44}Co_{0.05}Mn_{0.95}O_2$ is layered rather than the tunnel structure of $Na_{0.44}MnO_2$.

Pure trivalent manganese compounds have a high resistivity, typically 10^5 to 10^7 ohm-cm at room temperature, just like MnOOH in dry cells. In contrast, even small amounts of doping of manganese sites in $K_yCo_{0.1}Mn_{0.9}O_2$ decreases the resistivity by two orders of magnitude (Fig. 15). Neither alkali ion nor preparation method makes any difference.

Figure 16 shows the cycling results for a 1% Co-substituted lithium manganese dioxide formed by hydrothermal synthesis. It is single phase, and electron microprobe analysis showed that the Co was incorporated into the structure. The discharge and charge behavior is much better than for pure Li_xMnO_2, but overcharge was observed for each cycle. The capacity retention is also much higher than for the undoped material. The voltage profile indicates that the layered structure is maintained over these cycles. Evaluation of a range of lithium manganese oxides doped with Co prepared by hydrothermal synthesis is now underway.

Cycling of the K-Mn oxide materials at higher current densities (1 mA/cm^2) showed very different behavior to that at 0.1 mA/cm^2 (Fig. 17). At the higher rate the voltage profile is typical of that of spinel even though the potassium ions cannot be incorporated into spinel-like lattices. Studies are now underway on lithium manganese oxides to see if this rate effect is also present.

The V pillaring of manganese oxide sheets shows that in many cases we form Mn pillars between vanadium oxide sheets. Three phases have been formed and structurally characterized, and electrochemical evaluation is underway. The g-MnV_2O_5 phase cycles one Li reversibly but with large polarization. The pipe structure is uninteresting electrochemically, but the delta phase has an initial discharge capacity exceeding 220 mAh/g. We appear to have successfully synthesized a vanadyl manganese dioxide, $(VO)_yMnO_2$, and its capacity upon cycling is shown in Fig. 18. This material is presently being characterized.

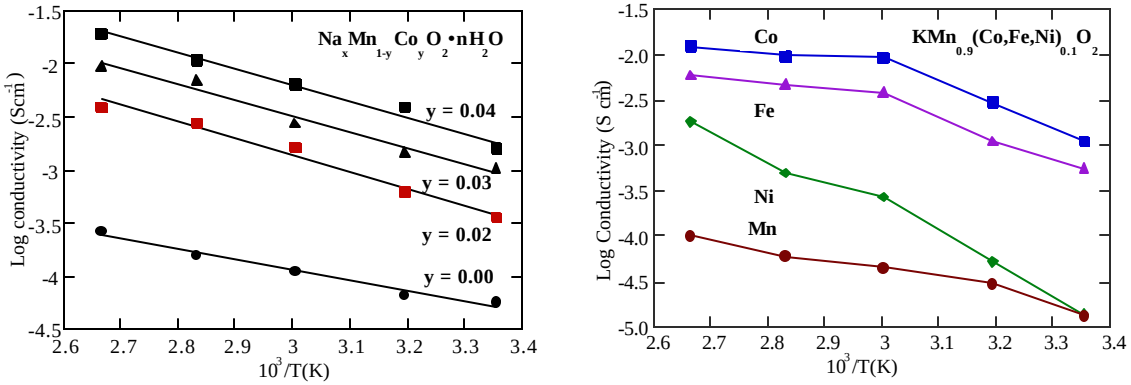

Figure 15. Conductivity of (top) hydrothermal $Na_xMn_{1-y}Co_yO_2$ and (bottom) high temperature $KMn_{0.9}(Co,Fe,Ni)_{0.1}O_2$ materials.

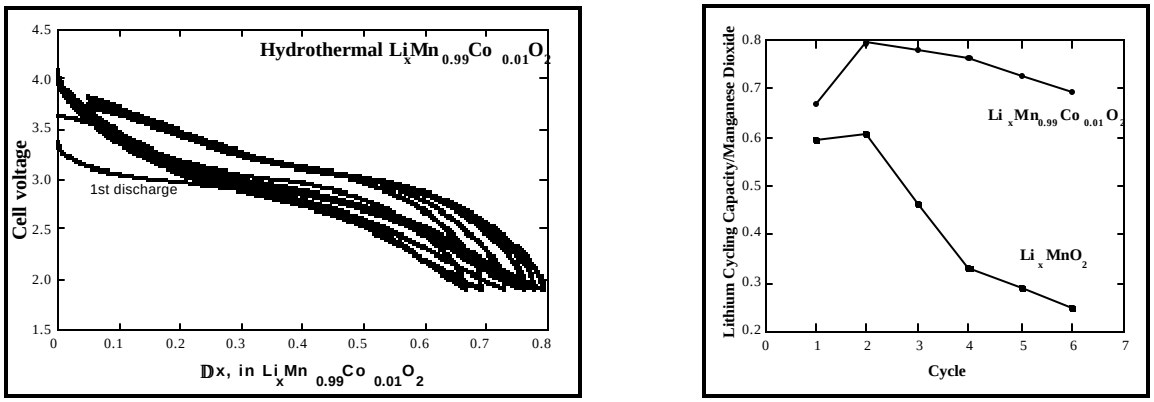

Figure 16. (Top) Cycling of hydrothermal $Li_xMn_{1-y}Co_yO_2$ for y=0.01 and (bottom) capacity on cycling compared with undoped Li_xMnO_2.

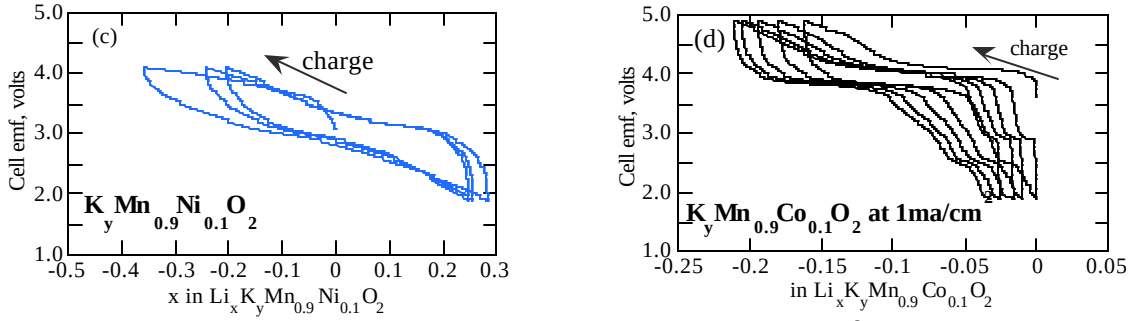

Figure 17. Effect of rate on cycling of manganese dioxides (top) 0.1 mA/cm^2, and (bottom) 1.0 mA/cm^2.

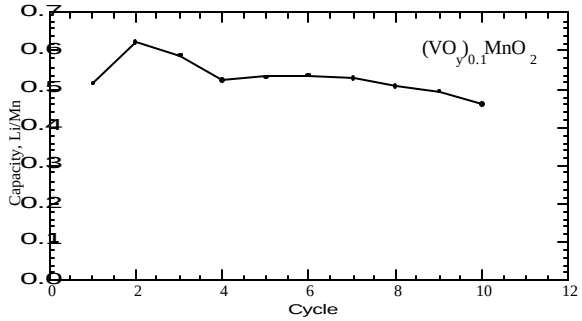

Figure 18. Capacity on cycling of $(VO_y)_{0.1}MnO_2$.

PUBLICATIONS

P. Sharma, G. Moore, F. Zhang, P.Y. Zavalij and M.S. Whittingham, "The Conductivity of Cobalt Doped Manganese Oxides," *Electrochem Solid-State Lett*, **2**, 494 (1999).

F. Zhang, P.Y. Zavalij and M.S. Whittingham, "Hydrothermal Synthesis and Electrochemistry of a Manganese Vanadium Oxide, g-MnV_2O_5," *Electrochem Commun*, **1**, 564 (1999).

F. Zhang, P.Y. Zavalij and M.S. Whittingham, "Synthesis and Characterization of a Pipe Structure Manganese Vanadium Oxide by Hydrothermal Reaction," *J Mater Chem*, **9**, 3137 (1999).

F. Zhang and M.S. Whittingham, "Hydrothermal Synthesis and Electrochemistry of a d-type Manganese Vanadium Oxide," *Electrochem Commun*, **2**, 69 (2000).

M.S. Whittingham, P. Zavalij, F. Zhang, P. Sharma and G. Moore, "Solid State Ionics of Manganese and Vanadium Oxides," *Electrochem Soc Proc*, **99-13**, 1 (1999).

P.K. Sharma, G.J. Moore and M.S. Whittingham, "The Hydrothermal Synthesis of K_zMnO_2 in the Presence of Citric Acid," *Mater Res Soc Proc*, **548**, 125 (1999).

Novel Cathode Materials

Michael M. Thackeray
Argonne National Laboratory, Chemical Technology Division, Argonne IL 60439
(630)-252-9183; fax: (630)-252-4176; e-mail: thackeray@cmt.anl.gov

Objective

- Find lower-cost and higher capacity cathodes than $LiCoO_2$ for rechargeable Li EV batteries.

Approach

- Perform a comprehensive study of pure and doped manganese oxide cathodes with structures (tunnel, layered three-dimensional framework and amorphous) that lead to higher capacities, higher power densities and longer life than $LiCoO_2$.
- Investigate alternative oxides, notably those of vanadium.

Accomplishment

- Synthesized a layered $Li_{2-x}MnO_{3-x/2}$ compound that showed different electrochemical properties and greater resistance to transformation to spinel than Li_2MnO_3 obtained ed by ion-exchange from $NaMnO_2$.

Future Directions

- Investigate alternative routes to synthesize $Li_{2-x}MnO_{3-x/2}$ using other synthesis procedures and precursor materials.
- Perform synthesis, electrochemical and structural characterization of composite Li_xMnO_2 electrodes.

The specific goal of this project is to identify new or modified transition metal oxide cathodes for Li EV batteries, particularly manganese oxides, with superior electrochemical properties and structural stability to $LiCoO_2$. A major focus is to stabilize the manganese oxide structures against conversion to the spinel phase.

Two approaches were adopted to obtain stabilized manganese oxide electrodes. The first approach is to synthesize a layered lithium manganese oxide structure by leaching Li_2O from the rock salt phase Li_2MnO_3. The second approach is to develop composite Li-Mn-O electrodes containing a spinel component that show enhanced cycle life over both the 4 V and 3 V plateaus in a Li cell. During 1999, the emphasis of the work was predominantly on investigating the layered structure derived from Li_2MnO_3.

Data have shown that a layered structure of nominal formula $Li_{2-x}MnO_{3-x/2}$ ($x \approx 1.8$-1.9) can be synthesized by leaching Li_2O from Li_2MnO_3 but only when the Li_2MnO_3 precursor is synthesized at moderate temperature, such as 400°C. If synthesized at higher temperature, the Li_2MnO_3 product is relatively stable to acid-treatment, thereby making it difficult to remove Li_2O from the structure. Delithiation of Li_2MnO_3 causes a shear of the cubic-close-packed oxygen array such that the Mn atoms remain octahedrally coordinated, whereas the remaining Li^+ ions (and possibly some H^+ from the acid treatment) are located in trigonal prismatic sites (Fig. 19). Relithiation of the layered $Li_{2-x}MnO_{3-x/2}$ product regenerates the cubic-close-packed array. Because Li_2O is initially removed (chemically) from the structure, electrochemical relithiation does not regenerate the Li_2MnO_3 structure, but rather one which appears to be more closely related to the layered $LiMnO_2$ structure that can be synthesized by Li-ion exchange from $NaMnO_2$. Preliminary data showed that layered $Li_{2-x}MnO_{3-x/2}$ may be more resistant to the electrochemical conversion to spinel than the layered $LiMnO_2$ prepared by ion-exchange. However, it has been difficult to synthesize layered $Li_{2-x}MnO_{3-x/2}$ by the acid-treatment route reproducibly and in high quantity. Because the products are not highly crystalline (Fig. 20) and are of small particle size, it has been difficult to obtain accurate information about their structures by XRD analysis or transmission electron microscopy (TEM). The layered $Li_{2-x}MnO_{3-x/2}$ product formed by this technique is unstable to heating in air at 275°C, as reflected by the collapse in the XRD peaks of the heat-treated sample (Fig. 20). Because of the promising electrochemical behavior of $Li_{2-x}MnO_{3-x/2}$, further experiments have been initiated to investigate alternative routes to synthesize this layered MnO_2 phase with a greater degree of crystallinity.

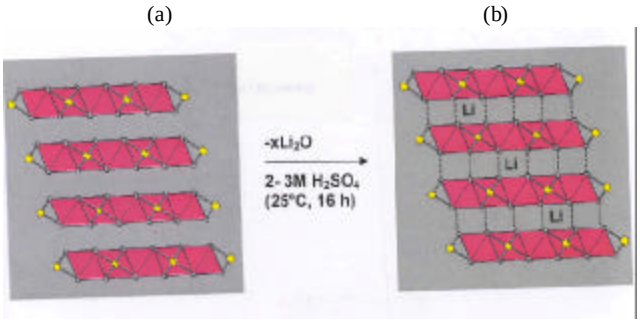

Figure 19. The structure of Li_2MnO_3

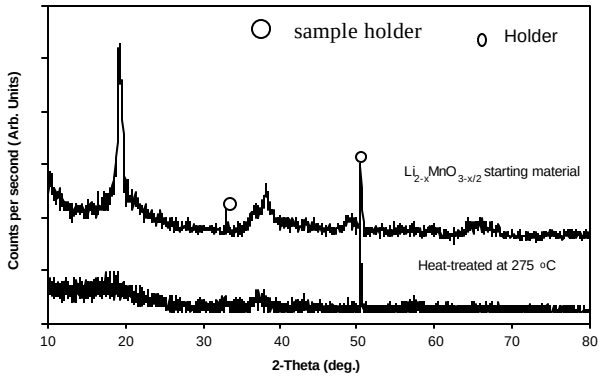

Figure 20. The XRD patterns of a parent $Li_{2-x}MnO_{3-x/2}$ sample (top) and a sample heated to 275°C (bottom).

PRESENTATION

C.S. Johnson, "Structure and Insertion Chemistry of New Composite Electrodes for Lithium Batteries," *The Society for Advanced Battery Technology*, Osaka National Research Institute, Osaka, Japan, November 17, 1999.

Novel Cathode Structures

Lutgard C. De Jonghe
Lawrence Berkeley National Laboratory, 62-203, Berkeley CA 94720
(510) 486-6138, fax: (510) 486-4881; e-mail: lcdejonghe@lbl.gov

Objective

- Develop low-cost manganese oxide electrodes for rechargeable Li/polymer and/or Li-ion cells with reversible capacities of at least 150 mAh/g and the ability to discharge 1000 times to 80% utilization or better at C/3 rate or higher.

Approach

- Select and synthesize manganese oxides with tunnel structures showing good reversibility to Li^+-ion intercalation, which are inherently robust, abuse-tolerant, and do not undergo deleterious phase changes.
- Characterize materials chemically and electrochemically.
- Discharge and cycle promising manganese oxides in Li/polymer and Li/liquid electrolyte cells.

Accomplishments

- Improved reversible capacity from 70-85 mAh/g to 95-120 mAh/g in polymer and liquid electrolyte cells at C/3 to 1.5C rates.
- Cycled Li/$P(EO)_8$LiTFSI/$Li_xTi_{0.33}Mn_{0.67}O_2$ cell 220 times at C/2 rate to 95% initial capacity or better.
- Cycled Li/$P(EO)_8$LiTFSI/Li_xMnO_2 cell at 1.5C rate more than 50 times with no discernible capacity fading.

Future Directions

- Use glycine-nitrate combustion, sol-gel and other solution synthesis techniques to produce high-surface-area materials with good rate capability and improved capacity.
- Dope tunnel MnO_2 structure with electroactive metals (e.g., V, Cu, Ni) to increase reversible capacity and improve electronic conductivity.
- Investigate alternatives to the tunnel $Na_{0.44}MnO_2$ structure for cathode materials.

We have identified a remarkably stable manganese oxide phase with an unusual double-tunnel structure ($Na_{0.44}MnO_2$). The theoretical capacity is estimated to be at least 200 mAh/g. It undergoes ion-exchange and reductive intercalation processes readily and reversibly, and does not convert to the spinel phase below about 400°C. Over-charge/over-discharge studies have also indicated that this structure is highly resistant to damage from abuse.

$Li_xNa_yMnO_2$ exhibits a sloping discharge profile with an average potential of ~3.1 V vs. Li. The reversible capacity decreases as the Li/Na ratio increases, suggesting that Na ions prop open the tunnels, making more Li ion sites available. However, *in situ* exchange occurs for Na-containing compounds, resulting in an apparent fade upon cycling. Fully exchanged materials made from conventionally prepared $Na_{0.44}MnO_2$ cycle without losses, but utilization is low (70-85 mAh/g, depending on the cell configuration, voltage limits, and discharge rate). Substitution of Mn by larger ions such as Ti should result in increased unit cell size and higher capacity, without complications from *in situ* exchange.

A series of Ti-doped compounds, $Li_xTi_yMn_{1-y}O_2$ (y=0.11, 0.22, 0.33, 0.44 and 0.55) with the $Na_{0.44}MnO_2$ structure was prepared. The unit cell size progressively increases with higher doping levels. Stepped potential experiments indicate that

the reversible capacity increases up to y = 0.22 (to about 120 mAh/g in a polymer-electrolyte cell), but decreases thereafter, suggesting that Ti is not electroactive in this structure. The excellent cycling behavior is retained in the Ti-doped materials with higher capacity (Fig. 21). For example, polymer-electrolyte cells with $Li_xTi_{0.33}Mn_{0.67}O_2$ cathodes lose <0.02% of their capacity per cycle on average, even at 85°C, and are projected to meet the USABC goal of 1000 cycles to 80% depth of discharge or better.

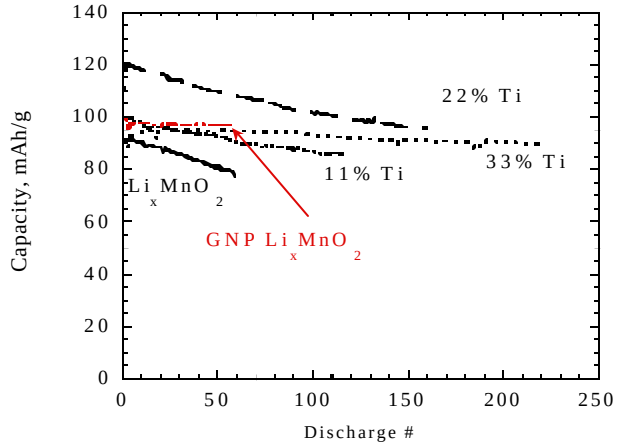

Figure 21. Discharge capacity upon cycling for $Li/P(EO)_8LiTFSI/Li_xTi_yMn_{1-y}O_2$ cells at 85°C; Li_xMnO_2 at 0.2 mA/cm^2 (C/1.5 rate), GNP Li_xMnO_2 at 0.5 mA/cm^2 (1.5C rate), and $Li_xTi_{0.33}Mn_{0.67}O_2$ (33% Ti) at 0.1 mA/cm^2 (C/3 rate) (3.6-2.5V), $Li_xTi_{0.22}Mn_{0.78}O_2$ (22% Ti) at 0.1 mA/cm^2 (3.6- 2.4V), and $Li_xTi_{0.11}Mn_{0.89}O_2$ (11% Ti) at 0.1 mA/cm^2 (3.6-2.25V).

Li_xMnO_2 made by glycine-nitrate combustion produced $Na_{0.44}MnO_2$ powder with an average particle size <1 µm. The utilization is increased to nearly 100 mAh/g in a Li/polymer cell, and there is no fading during cycling at 1.5C rate over 50 cycles (Fig. 21, GNP Li_xMnO_2). Thus, kinetic limitations were partly responsible for the poorer performance seen previously. Higher capacity should likewise be exhibited for Ti-doped powders with higher surface area. We have now prepared $Li_xTi_{0.22}Mn_{0.78}O_2$ from high-surface-area precursors made by a sol-gel technique and plan to test them in Li cells.

Similar improvements are seen in liquid-electrolyte cells when the average particle size of Li_xMnO_2 is reduced. Figure 22 compares discharges in a liquid-electrolyte cell at ~C rate for Li_xMnO_2 used as is (cell E4) and an attritor-milled sample (cell A8). Figure 23 shows that the increased capacity obtained for cell A8 is retained upon cycling.

Better utilization should be obtained in materials doped with electroactive metals (e.g., Cu, Ni, V) or at low levels with inactive ions larger than Ti (e.g., Zr). Tunnel compounds containing 11% Cu or Zr were synthesized successfully, but attempts to dope with Co and Fe resulted in layered phases. A goal of 150 mAh/g or higher reversible capacity has been set using these approaches.

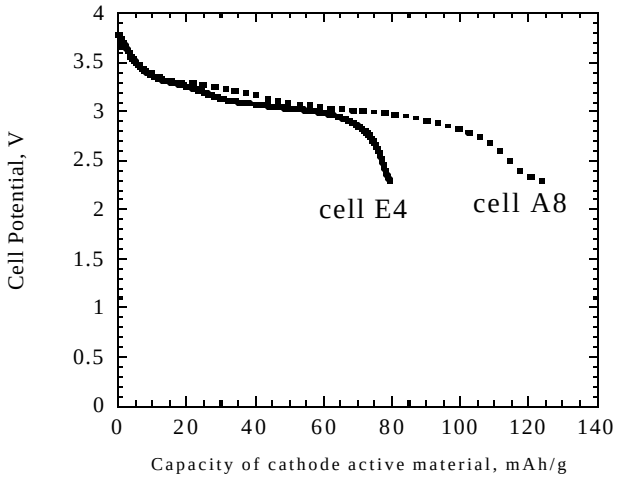

Figure 22. Discharges at 0.53 mA/cm^2 (~C rate) of two Li_xMnO_2/EC-DMC, 1M $LiPF_6$/Li cells at room temperature. The Li_xMnO_2 sample used in cell A8 was attritor-milled for four hours.

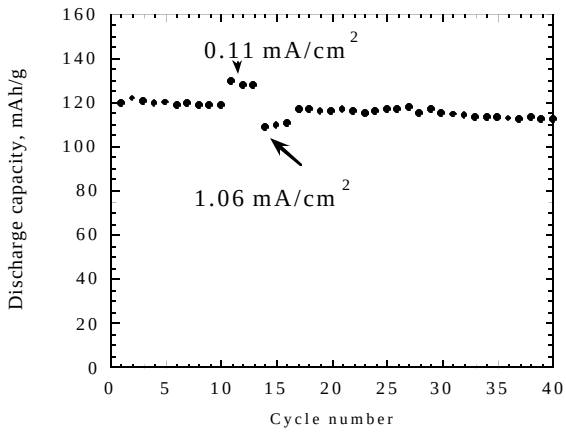

Figure 23. Cycling data for cell A8, discharged between 4.0 and 2.3V at 0.53 mA/cm^2 (~C rate), except where otherwise noted. Forty cycles at different rates, voltage limits are not shown.

PUBLICATION

M.M. Doeff, P. Georen, J. Qiao, J. Kerr and LC. De Jonghe, "Transport Properties of a High

Molecular Weight Poly(propylene oxide)-$LiCF_3SO_3$ System", *J. Electrochem. Soc.*, **146**, 2024 (1999).

PRESENTATIONS

M.M. Doeff, T.J. Richardson and L.C. De Jonghe, "Cathodes Derived from $Na_{0.44}MnO_2$ for Rechargeable Lithium and Lithium Ion Batteries", *The Second Hawaii Battery Conference (HBC 99)*, Waikoloa, Hawaii, p. 340.

M.M. Doeff, T.J. Richardson, K.T. Hwang and A. Anapolsky, "Factors Influencing the Discharge Characteristics of $Na_{0.44}MnO_2$-based Positive Electrode Materials for Rechargeable Lithium Batteries", Paper B2-0184, *196th Meeting of the Electrochemical Society*, Honolulu, HI, October, 1999. LBNL-44565.

New Cathode Materials: Aerogels

Elton J. Cairns
Lawrence Berkeley National Laboratory, 70-108B, Berkeley CA 94720
(510) 486-5028, fax: (510) 486-7303; e-mail: ejcairns@lbl.gov

Objectives

- Identify new electrode structures and compositions, which will eliminate or minimize fundamental mechanisms of Li/MnO_2 cell capacity loss.

Approach

- Synthesize and characterize new sol-gel based lithium metal oxide materials.

Accomplishments

- Prepared novel lithium metal oxide "hexagel" materials with specific capacities up to 138 mAh/g.
- Reduced initial capacity fade rates from 8% per cycle to 3% per cycle through improvements in cathode fabrication.

Future Directions

- Improve the performance of aerogel materials by using a new sol-gel method which can retain sufficient Li in the final gel.

Elemental analyses of our aerogel cathode material showed that almost no Li was present, and that the Mn:O ratio was 1:1.75. The lack of Li could be the cause of the less-than-expected specific capacity and severe capacity fading. A "hexagel" was made by evaporation of hexane from the sol-gel instead of supercritical removal of carbon dioxide. The resulting hexagel material exhibited a specific capacity of 138 mAh/g, however it showed the same severe capacity fade rate as the original aerogel material. Both aerogel and hexagel were derived from the same batch of sol-gel.

Another method involving metal nitrates and citric acid was used to prepare sol-gels of cobalt/manganese oxides. This material was characterized by TGA to determine the optimum drying temperature before use in cells. Electrochemical tests showed that this type of material is not suitable for electrodes. Although stable, the discharge capacity was only about 10 mAh/g and was probably a result of double-layer charging rather than Li intercalation.

We modified our original sol-gel method to produce gels with a higher Li content. Our new method uses lithium fumarate directly, rather than our original method in which lithium permanganate

and fumaric acid were mixed to initiate sol-gel formation. Also, other transition metals will be incorporated by making the corresponding metal fumarate solution. Samples using the new method have been produced and electrochemical tests are underway.

ADVANCED SOLID POLYMER ELECTROLYTES

The long-term energy density goals of USABC can be met by use of Li-metal batteries, but this will require "dry" polymers or gels containing ether-like functions. Both modeling studies and synthesis of novel solid polymer electrolytes (SPEs) are needed to meet the requirements for high conductivity, high transference number and interfacial chemical stability. The effort in this task focuses on understanding polymer performance characteristics by studies of the transport properties of the electrolyte as a function of polymer structure, polymer structural changes as a function of temperature, and interactions at the electrode/polymer interface during charge and discharge. A multi-pronged approach involving chemical synthesis, advanced diagnostic tools, and coordinated modeling studies is being used.

Advanced Solid Polymer Electrolytes

John B. Kerr
Lawrence Berkeley National Laboratory, 62-203, Berkeley CA 94720
(510) 486-6279; fax: (510) 486-4995; e-mail: jbkerr@lbl.gov

Objectives

- Determine the upper limits of conductivity of binary salt and single-ion "dry" polymer electrolytes by polymer synthesis, theoretical calculations, and transport measurements.
- Determine the influence of polymer architectures and salt structures on the mechanical strength and processability of the polymer electrolyte membranes.
- Design, construct, characterize and demonstrate SEIs that lead to extended cycle life and reduced cost required for commercial introduction of EV batteries.

Approach

- Prepare comb-branch (CB) polymer electrolytes with mechanical strength and optimum ion transport for rechargeable Li batteries.
- Measure transport properties (conductivity, diffusion coefficients and transference numbers) by electrochemical methods and electrophoretic NMR.
- Use the experimental results in electrochemical system modeling (Newman) and molecular modeling (Ratner) to predict the behavior of Li batteries.

Accomplishments

- Developed methods for *in situ* curing or cross-linking of polymer membranes that have excellent mechanical strength, good electrode adhesion, acceptable ion-transport properties and minimal reactivity towards Li.
- Developed method of grafting anions on to CB polymers to provide single-ion conductors.
- Determined transport properties of linear polymer, oxymethylene-linked polyethylene glycol 400 (PEMO), with lithium trifluoromethanesulfonate (LiTf) and lithium bis(trifluoromethanesulfonyl)imide (LiTFSI) at 40, 60 and 85^{o}C.

Future Directions

- Complete transport measurements of CB network polymers and determine the effect of cross-linking, backbone and side-chain structure on these properties.
- Prepare CB polymers with pendant, crown ether units and determine their physicochemical properties.

Synthesis. Acceptable mechanical properties were obtained with cross-linked CB polymers (Fig. 24). PEPE2-5 is the polyepoxide ether pre-polymer (MW in the range of 50,000), and it displays viscous liquid behavior. PEPE2-5X and PEPE2-10X are cross-linked materials (5 and 10% density, respectively) that show properties of an elastic rubber. The elastic modulus increases with salt concentration. A side-chain with an allyl group was used. The reagents used for the cross-linking reaction form products that are volatile and easily removed by vacuum to ensure that the membrane is not reactive to Li. These membranes were cycled with Li metal for >200 cycles and show no obvious degradation of performance compared with the non cross-linked materials.

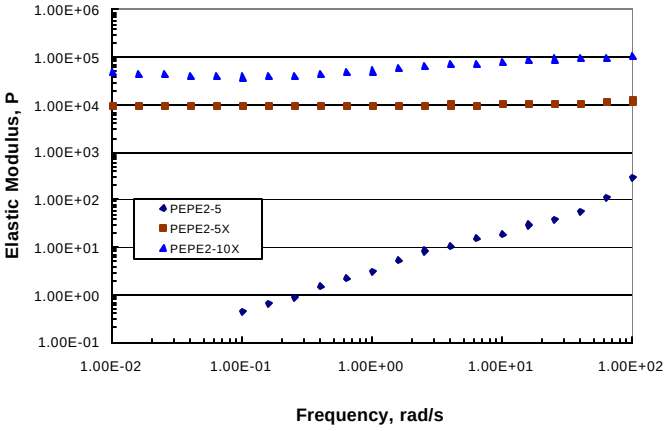

Figure 24. Elastic modulus of polyepoxide ether electrolytes (no salt) at 25°C as a function of frequency. Measurements were performed on a Rheometrics RMS-800 rheometer.

A similar synthesis was used to prepare a single-ion conductor material. A trifluoromethane-sulfonyl anion group was grafted onto the allyl side chain of a CB polymer. This membrane was cycled in a symmetrical Li/Li cell, and the results are shown in Fig. 25, together with the behavior of a binary salt. The SIC-80 showed no concentration polarization, but it had a high voltage, which is attributed to ohmic and interfacial resistance from reactions with Li. The cycle capacity is 8 coulombs/cycle. The lack of concentration polarization of SIC-80 is dramatic in contrast to the PVBE-LiTFSI binary salt electrolyte.

Transport Property Measurements. Transport properties were measured for PEMO-LiTf and PEMO-LiTFSI as a function of salt concentration and temperature. Figure 26 shows the transference numbers for PEMO-LiTFSI. Similar trends are evident for salt diffusion coefficients as a function of concentration and temperature. The transference number and diffusion coefficients are lower with LiTf, which also shows evidence of inhomogeneity that may be responsible for the negative transference numbers. The transport properties were used to calculate the polarization behavior and limiting currents. The limiting current for LiTf easily exceeded 0.2 mA/cm^2 in a Li/Li symmetrical cell at 40°C; the limiting current with LiTFSI was much higher. It was observed that dendrites formed rapidly with LiTf under these conditions while LiTFSI cycled for many cycles before failure.

PUBLICATION

M.M. Doeff, P. Georén, J. Qiao, J. Kerr and L.C. De Jonghe, "Transport Properties of a High Molecular Weight Poly(propylene oxide)-$LiCF_3SO_3$ System", *J. Electrochem. Soc.*, **146**, 2024 (1999).

PRESENTATIONS

J.B. Kerr, J. Hou, S. Wang, S. Sloop, O. Buriez and Y.B. Han, "Reactivity of Polymer Electrolytes in Rechargeable Lithium Batteries," ACS National Meeting, Anaheim, CA, March 1999.

J.B. Kerr, M.M. Doeff, J. Hou, S. Wang, S. Sloop and Y.B. Han, "Effect of Structure on Ion Transport in Polymer Electrolytes", *ACS National Meeting*, Anaheim, CA, March 1999.

J.B. Kerr, "Polymer Electrolytes In Rechargeable Lithium Batteries: 'Alice In Wonderland' or The Solution to the Electric Vehicle Battery Problem?," Invited Speaker, *Golden Gate Polymer Forum Spring Symposium*, Mountain View, CA. June 7, 1999.

O. Buriez, Y.B. Han, J. Hou, J.B. Kerr, J. Qiao, S.E. Sloop, M. Tian and S. Wang, "Performance Limitations of Polymer Electrolytes Based on Ethylene Oxide Polymers," *DOE Workshop on Lithium-Polymer Batteries*, Towson, MD, July, 1999.

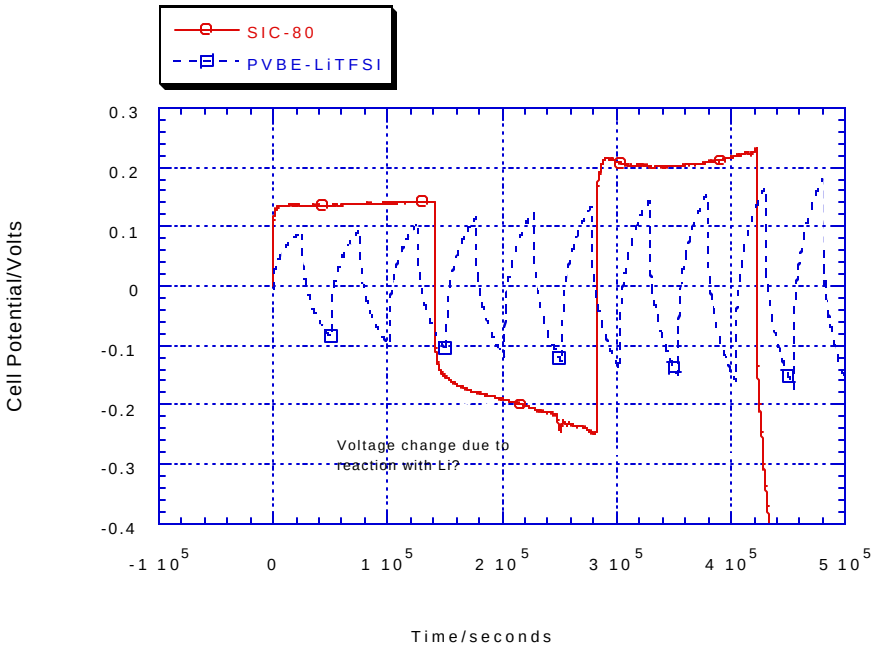

Figure 25. Cycling behavior of Li/Li symmetrical cells at 85°C. Both cells are cycled galvanostatically at 0.05mA/cm^2. SIC-80 is a polyelectrolyte with a glass transition temperature of -51°C and a conductivity of 10^{-5} S/cm at 85°C. The PVBE polymer is a cross-linked polyvinylbenzyl ether with a side chain length of 12 EO units.

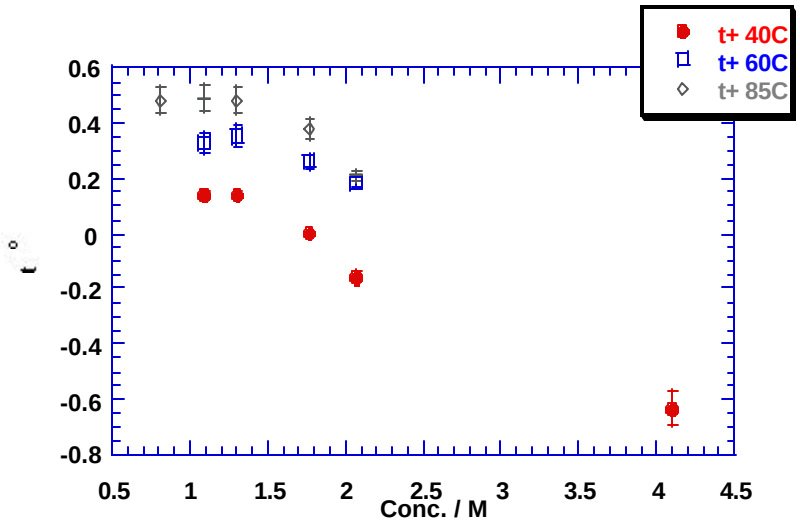

Figure 26. The Cationic Transference number vs[LiTFSI]

Lithium-Polymer Electrolyte Interface

Philip N. Ross, Jr.
Lawrence Berkeley National Laboratory, 2-100, Berkeley CA 94720
(510) 486-6226, fax: (510) 486-5530; e-mail: pnross@lbl.gov

Objectives

- Determine the Li/poly(ethylene) oxide (PEO) interfacial reactions products using the interaction of oligoethers on metallic Li as a simulated Li/PEO SEI layer.
- Investigate Li/PEO SEI layer stability as a function of temperature and electrolyte composition.

Approach

- Apply a combination of UHV surface analytical methods and *in situ* infrared vibrational spectroscopy.

Accomplishments

- Completed a study of Li/oligoether interfacial reactions products by PES in UHV for the homologous series of glymes, $CH_3(OCH_2CH_2)_nOCH_3$, n=1,2 etc. Large n values correspond to polyethylene glycol dimethyl ether (PEGDME). Spontaneous polymerization is a proposed reaction for monoglyme/diglyme, but the character of the polymer is unclear.
- Completed a full *ab initio* computational study of the electrochemical reduction of ethereal solvents for Li batteries.

Future Directions

- Analyze *in situ* Fourier transform infrared (FTIR) spectra of the SEI layer on Li electrodeposited under ideal conditions in oligoether electrolytes, $CH_3(OCH_2CH_2)_nOCH_3$, n=1,2 etc.
- Extrapolate the results from oligoethers to the Li/PEO interface.

The reaction of clean, metallic Li with monoglyme and/or diglyme molecular multilayers was observed using photoemission spectroscopy in UHV. These linear alkyl ethers are relatively reactive with metallic Li, producing $LiOCH_3$ and ethylene. However, in addition there appear to be reactions in which the chemical state of C and O atoms remains essentially unchanged from the parent molecule, but in a molecular state bound to the surface. Polymerization is a likely parallel reaction, as we observed previously in identical experiments with THF and dioxolane. Further studies with another spectroscopy, e.g., FTIR, will be needed to confirm this pathway.

Electronic structure calculations were performed on a number of carbonate and ethereal solvent molecules and their radical anions. These results were then used to calculate the standard potentials (E°) for electrochemical reduction of the solvent molecules at an inert electrode, e.g., such as glassy carbon or graphite, from classical Born-Haber type thermochemical cycles. These calculations showed that E° for reduction of the carbonates PC, EC and DEC are ca. + 1.0 V $\pm$ 0.3 V (vs. Li/Li^+) whereas for the ethers THF, DME (monoglyme) and 1,3 dioxolane the reduction potentials are all negative of 0 V (vs. Li/Li^+). Thus, reduction of oligoethers at Li electrodes is due to the chemical interaction of the solvent molecule with the Li surface, i.e., the formation of specific Li-solvent bonds. Electronic structure calculations of oligoethers adsorbed on a Li(110) surface are underway. These calculations will help identify possible reaction intermediates and provide theoretical infrared (IR) spectra of adsorbates and intermediates to assist in the analysis of FTIR data.

Samples of polyethers, e.g., poly-THF, poly-dioxolane, are being obtained from various sources and will be used to generate FTIR reference spectra.

G. Zhuang and P. Ross, "Contrasting Film Formation Reactions of Ethereal and Carbonate Solvents on Metallic Lithium", *DOE Workshop on Advanced Lithium Solid State Batteries*, Towson, MD, July 13-15, 1999; to be published in *J. Power Sources*

PRESENTATION

Composite Polymer Electrolytes

Saad A. Khan, Peter S. Fedkiw and Gregory L. Baker*[+]
North Carolina State University, Department of Chemical Engineering, P.O. Box 7905, Raleigh NC 27695-7905;
[+] *Michigan State University, Department of Chemistry, East Lansing, MI 48824-1322*
**(919) 515-4519; fax: (919) 515-3465; e-mail: khan@eos.ncsu.edu*

Objectives

- Develop solid composite polymer electrolytes (CPEs) utilizing synthesized fumed silica with tailored surface chemistries
- Investigate the electrochemical and rheological characteristics of these novel composite polymer electrolytes.

Approach

- Utilize a combination of electrochemical and rheological techniques, and chemical synthesis, to study the effects of silica surface chemistry on the electrochemical and mechanical properties of CPEs.

Accomplishment

- Determined that presence of fumed silica in CPEs improves cycle life and interfacial stability in Li/CPE/Li cells.

Future Directions

- Characterize CPEs in Li/Li_xCoO_3 Cells.
- Investigate the interfacial stability of CPEs containing fumed silica.
- Evaluate crosslinking protocols and processing methods to develop low-cost, efficient polymer electrolytes with tailored mechanical properties.

The objective of this research is to develop a new range of CPEs for rechargeable Li and Li-ion batteries. In particular, our goal is to develop highly conductive electrolytes that exhibit good mechanical properties, and at the same time show good compatibility with typical electrode materials. The unique feature of our approach is the use of surface-functionalized fumed silica fillers to control the mechanical properties of the electrolytes. A low-molecular-weight liquid PEO is used as the matrix polymer, thereby ensuring high conductivities, and the fumed silica serves to provide mechanical support.

The CPEs containing fumed silica showed excellent interfacial stability to Li metal. The effect of surface groups attached to fumed silica was explored by cycling a Li/CPE/Li button cell at 1 mA/cm^2 (Fig. 27). The polymer electrolyte was PEG-DME with lithium imide salt (Li:O=1:20). Various types of functionalized fumed silica were added: OH-terminated (A200), oligomer ethylene oxide-terminated (FS-EG3), and octyl- terminated (R805). In the absence of silica-filler (refer to the 0% FS curve in Fig. 27), the interfacial resistance rapidly increases and after 327 cycles reached its safety limit. Addition of any type and amount of silica improves the interfacial stability. CPEs with

A200 showed the greatest and most prolonged improvement in interfacial stability.

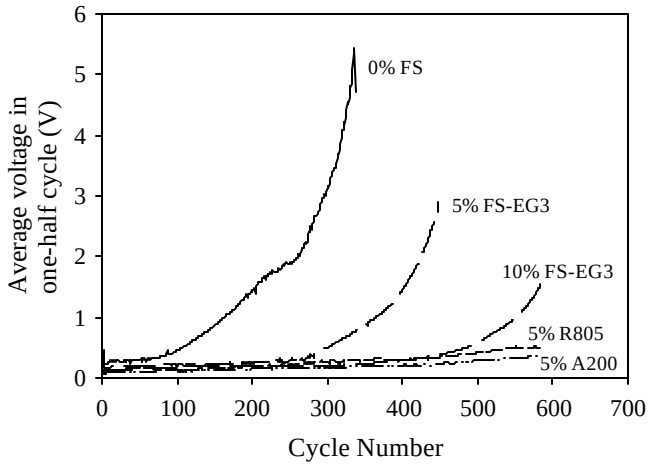

Figure 27. Effect of fumed silica surface groups on interfacial stability at 1 mA/cm^2. Samples are PEG-DME, Li imide (Li:O=1:20), and fumed silica: OH terminated (A200), oligomer ethylene oxide terminated (FS-EG3), and octyl terminated (R805). Samples are assembled as at Li/CPE/Li button-cell with moisture content < 40 ppm.

Figure 28 illustrates the effect of filler content on interfacial stability via measurement of the interfacial resistance before and after cell cycling. AC impedance spectroscopy was used to measure the impedance of the interface in Li/CPE/Li button cells. These cells were then subjected to cycling at 1 mA/cm^2, and then the interfacial resistance was measured. As shown in Fig. 28, even 5% silica results in a significant decrease in interfacial resistance. A larger amount of silica continues to improve the interfacial stability but with less drastic effect. From these results and those of Fig. 27, we propose that fumed silica is acting as a scavenger for impurities, with a likely impurity being water. The A200 silica has the greatest number of available silanol groups and shows the most improvement in interfacial stability. The FS-EG3 has the least number of available silanol groups and shows the least improvement in interface impedance with cell cycling. Furthermore, the more silica present the better in interfacial stability. We are continuing to study the mechanism of how the fumed silica stabilizes the interface by deliberately varying water content and fumed silica content and subsequently measuring the impedance of the interface.

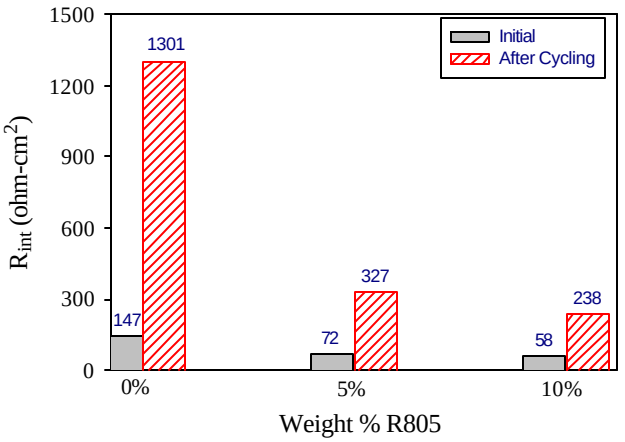

Figure 28. Effect of fumed silica content on interfacial resistance before and after cell cycling. Samples are PEG-DME, Li imide (Li:O=1:20), and R805 fumed silica in a Li/CPE/Li button-cell. Interfacial resistance measured before and after cycling via AC impedance spectroscopy; 584 cycles were applied to the 5 and 10% R805 samples, but only 327 cycles were applied to the 0% sample due to the equipment limitations (impedance of cell became too large).

PUBLICATION

S.A. Khan, P.S. Fedkiw, S.R. Raghavan, J. Fang, G.L. Baker and J. Hou, "Composite Polymer Electrolytes Using Crosslinked Fumed Silica Fillers," ***U.S. Patent 5,965,299*** (issued 10/12/99).

PRESENTATIONS

J. Hou and G.L. Baker, "Photopolymerization of Methacrylate-Functionalized Fumed Silicas and Alkyl Methacrylates in Low MW PEO-$LiClO_4$ Matrices", *217th National Meeting of the American Chemical Society*, Anaheim, CA. March 1999.

S.R. Raghavan and S.A. Khan, "Colloidal Silica Gels as Novel Polymer Electrolytes: Correlating Rheology with Colloidal Interactions", Invited Speaker, *Engineering Foundation Conference on Rheology in the Mining and Energy Industries*, Honolulu, HI; March 1999.

H.J. Walls, P.S. Fedkiw, S.A. Khan and T.A. Zawodzinski, "Ionic Transport in Ethylene Oxide-Based Inorganic/Organic Composite Electrolytes," *Electrochemical Society Joint*

International Meeting, Honolulu, HI, October 1999.

J.A. Yerian, P.S. Fedkiw and S.A. Khan, "Cross-linked Composite Polymer Electrolytes for Lithium and Lithium-ion Batteries," *Electrochemical Society Joint International Meeting*, Honolulu, HI, October 1999.

Modeling of Lithium/Polymer Electrolytes

Mark A. Ratner
Northwestern University, Department of Chemistry, Evanston IL 60208-3133
(847) 491-5371, fax: (847) 491-7713; e-mail: ratner@mercury.chem.nwu.edu

Objectives

- Develop a predictive capability based on electronic structure calculations and formal site models to optimize polyelectrolyte-based soft electrolytes for Li batteries.
- Identify the roles of concentration, anion basicity, free volume, polymer compliance and dynamic coupling on the Li^+-ion conductivity in polyelectrolyte soft separators.
- Identify optimized composite structures that utilize inorganic fillers in the polymeric hosts to obtain high cation transference number and ion mobility.

Approach

- Use theoretical models, both of electronic structure type and of dynamic transport type, to understand and predict the effects of specific variation of variables (temperature, density, salt choice, filler size, plasticizer, thermal history) on conductivity of polymer-based electrolytes.

Accomplishments

- Completed the first calculations on true polyelectrolyte structures, using a dynamic disorder model with bound anions.
- Completed *ab initio* calculations on a series of polyelectrolyte anionic centers, quantitatively comparing different basicities to show structural correlation between local electronic structure and numbers of available Li carriers.
- Interpreted the conductivity of hard polycarbonate-based polymer/salt complex in terms of the connected limit of dynamic percolation theory, which suggests transport by a largely uncoupled mechanism.

Future Directions

- Extend polyelectrolyte calculations to develop a phase diagram, computing conductivity as a function of the number of functionalized side chain branches.
- Compare dynamic disorder models for hard and soft polyelectrolytes to identify a possible optimal decoupling behavior for polyelectrolyte structures.

The theoretical molecular-level modeling activity focuses on (a) mechanistic study (using *ab initio* techniques, Monte Carlo studies and molecular dynamics) of ion transport in polymer/salt complex electrolytes and in polyelectrolytes exhibiting high Li^+-ion conductivity; and (b) mechanisms for substantial enhancement of conductivity in alternative electrolytes.

We completed milestone targets on electronic structure studies of varying local basicity in lithium polyelectrolyte systems. In particular, a series of studies of aluminate and aluminosilicate systems was completed that focused on the ability of Si to

reduce the local basicity, and therefore increase the number of mobile Li^+ ions and their conductivity. This is the optimization necessary to develop polyelectrolytes, which exhibit unit transference number for Li^+ ions.

Our study shows two important results: first, in agreement with experimental results from the Shriver group, we observed increased Li^+-ion mobility by substituting aluminate with aluminosilicate. Second, natural-bond orbital analysis has allowed us to analyze the reasons for this: it is not the $p\pi$-$d\pi$ interaction, but rather the actual dipole/charge interaction that is modulated by the substitution of Si for C in the beta position. This is an important design issue because if reduced basicity occurs, polyelectrolyte hosts could be effective in optimizing electrolyte materials for Li-ion batteries.

Collaboration with Shriver's group, and discussions with Kerr's group at LBNL (plus some reports on the current literature and the results of a Ph.D. examination in Sweden) strongly suggest that in polyelectrolyte systems (that is, bound counter-ion charge to Li) local mobility of the mobile counter ion could result in substantive increase in the conductivity of Li^+-ions. Effectively, this means that decoupling defined by the Angell decoupling index is allowed, and still provides high Li^+-ion conductivity, if the local relaxation motions are fast enough. A series of Monte Carlo modeling calculations was completed in which Li^+-ion hopping is indeed modulated by the counterion motion, but the counterion motion is restricted by harmonic binding. As the harmonic force constant changes from a very large number (characteristic of hard polyelectrolytes) to a very small number (characteristic of polymer/salt complex electrolytes), substantial modifications in the conductivities were observed. By loosening the local binding geometries, polyelectrolytes of substantially increased conduction are predicted.

The original results were obtained for two dimensions, which are being extended to three dimensions. In addition, enhanced transport by co-ions are being evaluated. The results of these simulations, combined with the insight that the dynamic percolation model offers into possible "hard" polymer electrolyte systems, suggest promising new directions for optimized polyelectrolytes. If facile local relaxation and approximate decoupling are combined, it might be possible to produce polyelectrolytes with the conductivity goal of 10^{-3}S/cm.

Studies involving dynamic hopping models and formal biphasic hopping models showed quite clearly that the dynamic hopping model can be extended to polyelectrolyte structures, and can be used to optimize polyelectrolytes. This work is being extended to understand the tunnel-like, helical structures obtained by Bruce (*Nature*, 1998), and how these materials become conductive upon slight disordering. The aim will be to analyze the experimental and theoretical behavior of hard polyelectrolytes, with local high mobilities.

An investigation of decoupling between viscosity and transport is the most challenging aspect of this research. The results obtained with hard materials and polyelectrolytes will be combined to produce materials with attractive physical properties (probably composites), high conductivities, low polarization and good interfacial stability. Activities have begun in collaboration with Professor Nitzan in Tel Aviv. We are also collaborating with John Kerr to identify new comb aluminosilicates and triflates to optimize the weak basicity of local sites and facilitate ion transport due to rapid relaxation.

PUBLICATIONS

Y.C. Lee, L.A. Curtiss and M.A. Ratner, "Computational Studies of Polyelectrolytes Containing Zeolitic Fragments," *J. Phys. Chem. B* **103**, 6445-6449 (1999).

M.A. Ratner, "Ionic Charge Transport in Molecular Materials: Polymer Electrolytes", D.A. Jelski, T.F. George, eds., *Computational Studies of New Materials*, 174-209 (1999).

Y-C. Lee, L.A. Curtiss, M.A. Ratner and D.F. Shriver, "Computational Studies of Polyelectrolytes Containing Zeolitic Fragments," *J. Phys. Chem. B* **103**, 6445 (1999).

Highly Conductive Polyelectrolyte-Containing Rigid Polymers

Duward F. Shriver and Seymon Vaynman***
**Chemistry Department, Northwestern University, Evanston, IL 60208*
***Department of Materials Science and Engineering, Northwestern University, Evanston, IL 60208*
(847) 491-5655; fax: (847) 491-7713; e-mail: shriver@chem.nwu.edu/svaynman@nwu.edu

Objectives

- Synthesize a new class of rigid polymer electrolytes.
- Test rigid polymer electrolytes in rechargeable Li and Li-ion batteries.

Approach

- Synthesize new polymer electrolytes that contain a rigid polymer rather than the flexible low-T_g polymers used in conventional polymer electrolytes.
- Fabricate and evaluate polymer electrolytes in electrochemical cells.
- Correlate the chemical structure and reactivity of polymer electrolytes with performance in electrochemical cells.

Accomplishments

- Synthesized the rigid polymer electrolyte, poly(1,3-dioxolan-2-one-4,5-diyl oxalate) (PVICOX), with ionic conductivity of the polymer-lithium triflate (1:1) complex of $\approx 10^{-4}$ Scm^{-1} at room temperature.
- Conducted tests of symmetrical Li/polymer/Li and cathode/polymer/cathode cells, which indicated the formation of resistive interface(s) in the cells.

Future Directions

- Modify the electrolyte to reduce its reaction with anode and cathode components.
- Test the modified electrolyte in Li and Li-ion batteries.

Two rigid polymer systems were prepared, poly(vinylene carbonate) (PVIC) and PVICOX, which display both favorable conductivity and mechanical properties. These systems are easily synthesized, and they contained a high density of coordinating sites, which is necessary to dissolve salts. In addition, the high density of polar groups should reduce the activation energy for ion hopping from one polar site to the next. Of the two polymers, PVICOX is more irregular, and we hypothesize that this property will frustrate close packing, and thereby increase static free volume and conductivity.

Cells that contained the rigid polymer electrolyte, PVICOX-lithium triflate (1:1) complex were assembled and tested. With a cathode of 55% $LiMn_2O_4$ (Kerr-McGee), 35% polymer electrolyte and 10% carbon (Superior Graphite),

the resistance of the cell was extremely high (on the order of megaohms), and the capacity of the cell was negligible. When PVICOX-lithium triflate was replaced by polybis(methoxyethoxyethoxide) phosphazene (MEEP)-lithium triflate (4:1) in the cathode, the resistance was much lower, and the cell could be cycled. The resistance was lower because MEEP is a gel-like material that allowed a more intimate contact between cathode components. However, the discharge current could not exceed 15 mA/cm^2. Figure 29 shows the continuous discharge of the cell that was charged/discharged at 815 mA/cm^2. The cell capacity increases from the first to the second cycle, then it falls dramatically due to an increase in the electrical resistance. This behavior indicates that the polymer electrolyte reacts either with Li or lithium manganese oxide during cycling.

The electrical impedance studies of the interfaces between PVICOX and Li, and PVICOX and cathode material (55% $LiMn_2O_4$, 35% polymer electrolyte and 10% carbon) showed that PVICOX reacts with both Li and lithium manganese oxide (Fig. 30). The electrical resistance of the cell doubled upon reaction of lithium manganese oxide and PVICOX. Similarly, the resistance increased by one order of magnitude when Li reacted with PVICOX.

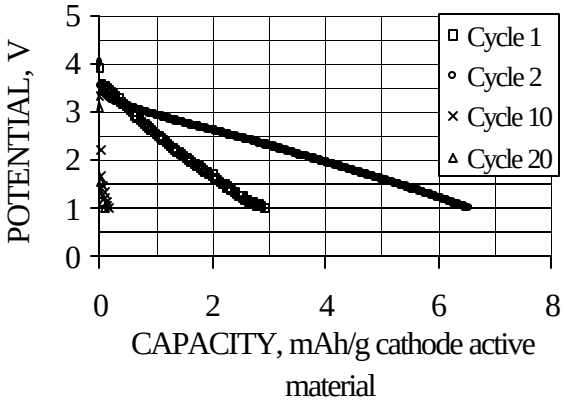

Figure 29. Discharge of Li/(PVICOX)/ $LiMn_2O_4$;C; MEEP-lithium triflate cell at 25°C. Discharge current 8 mA/cm^2.

Sulfone or sulfoxide functionalized organic molecules have some of the highest dipole moments and dielectric constants known and display very good cation complexing properties. Therefore, it was expected that polymers containing sulfur-oxygen bonds should readily dissolve significant amounts of Li salts and provide fast ion transport.

Furthermore, due to the strongly electron-withdrawing character of these groups, their polymers should have very good anodic stability. Based on these expectations, we propose the synthesis and testing of sulfone and sulfoxide functionalized polymers. The synthetic method will follow a path similar to that of the PVICOX synthesis, but instead of using vinylene carbonate as the starting material we will use the sulfones or sulfoxides. Various synthesis routes are being considered.

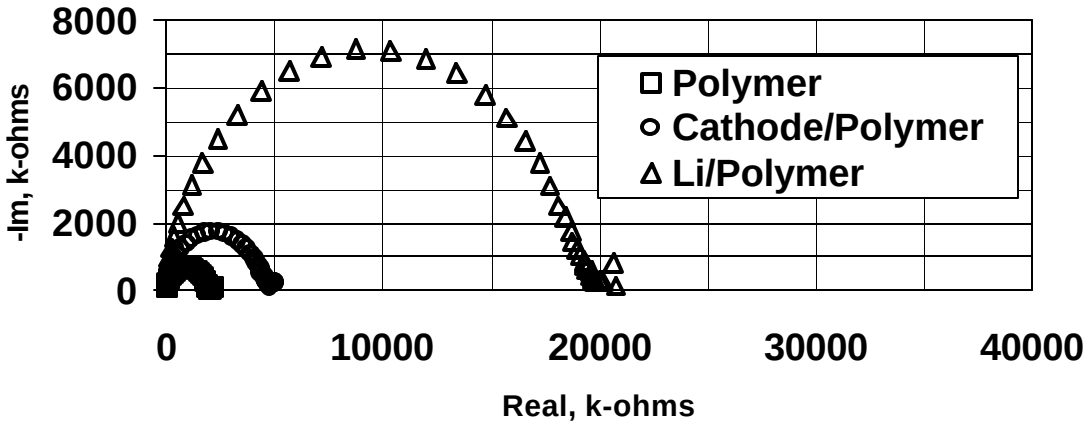

Figure 30. The electrical impedance of bulk electrolyte, cathode/electrolyte and Li/electrolyte systems.

Advanced Solid Polymer Electrolytes

Thomas Zawodzinski
Los Alamos National Laboratory, Electronic and Electrochemical Materials and Device Research Group, MST-11, MS D429, Los Alamos NM 87545
(505) 667-0925; fax: (505) 665-4292; email: zawod@esa.lanl.gov

Objective

- Provide detailed physicochemical characterization of polymer-based electrolytes for Li batteries.

Approach

- Develop electrophoretic NMR (ENMR) methods to study transport in polymer electrolytes.
- Use transport and spectroscopic measurements to characterize the properties of polymer electrolytes.

Accomplishments

- Implemented ^{19}F ENMR and demonstrated greatly improved sensitivity and response to measure anion and cation transference numbers.

Future Directions

- Study effects of additives and 'mixed salt' systems on polymer electrolytes.
- Use 'flow' tracking capability to measure relaxation of concentration gradient in polarized systems.
- Study transport and related phenomena in composite electrodes and electrolyte stability at positive-electrode interfaces.

We have developed a method to assess the Li^+-ion transference numbers of various electrolytes. Specifically, ENMR was investigated to separate the transference of various species in a complex electrolyte. Increased response is achievable from ENMR measurements using ^{19}F rather than ^{7}Li because:

- the anion transference number is typically larger than the cation transference number;
- the phase shift from a given molecular motion is amplified by the number of ^{19}F atoms per molecule;
- ^{19}F typically has longer relaxation times than ^{7}Li, allowing the use of longer diffusion/ migration times (Δ).

An estimate of the impact of these factors led us to expect (conservatively) at least an order of magnitude increase in the measurement capability.

ENMR studies of polymer electrolytes are challenging because of their relatively poor conductivity (low currents achievable) and poor signal-to-noise obtained with thin-film samples. The recent acquisition of a ^{19}F transmitter enabled us to overcome this problem. Figures 31 and 32 show examples of the ENMR phase shifts. Note that the phase shifts are roughly five times as large for ^{19}F as for ^{7}Li. The ^{19}F phase shift is opposite to that of ^{7}Li, which is reasonable because the anions migrate in the opposite direction to the cations. In addition, the scatter about the line is much less with ^{19}F, reflecting the higher signal-to-noise (yielding more accurate determination of phase shift).

The results obtained for anion and cation transference numbers in LiX/PEGdm electrolytes (as developed by Khan and Fedkiw) are summarized in Table 2. The transference numbers sum to 1 (within experimental error) with several different anions in the salt. This is a critical check of the method, and illustrates the accuracy of the ^{19}F measurement to determine transference numbers.

The ^{19}F NMR method was used to determine the transference number of Li in a polymer electrolyte (PPO/LiTFSI) obtained from LBNL. A transference number of about 0.5 was obtained at 85°C. This value is in agreement with that determined at LBNL by the method of Newman and co-workers.

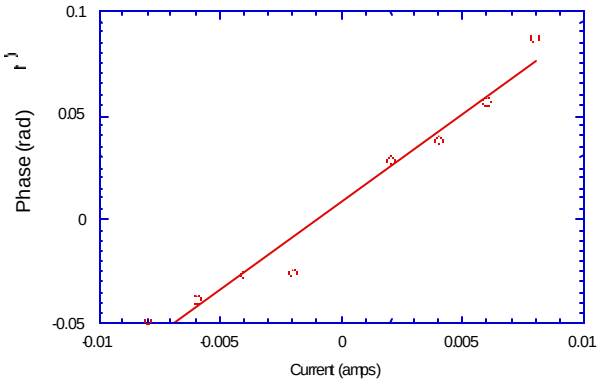

Figure 31. Phase shift of ^{7}Li signal vs. applied current for a sample of 0.292 M Li methide in PEGdm and 5% R805 fumed silica. The slope is proportional to the Li transference number.

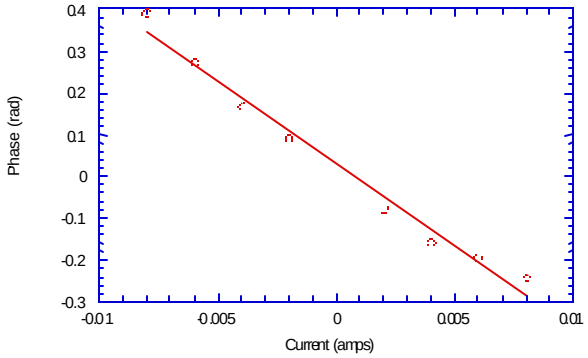

Figure 32. Phase shift of ^{19}F signal vs. applied current for a sample of 0.292 M Li methide in PEGdm and 5% R805 fumed silica. The slope is proportional to the anion transference number. The negative slope is a result of the fact that the anions migrate in the opposite direction (-Z) of the cations.

Table 2. Anion and cation transference numbers in LiX/PEGdm electrolytes.

TLi	Tf	Sum	$\sigma_{(S/cm)}$	Conditions
0.19	0.78	0.97		~0.5 M Li triflate
0.31	0.64	0.95	1.52 E-03	~0.5 M Li imide
0.43	0.59	1.01	8.57 E-04	~0.3 M Li methide

ADVANCED DIAGNOSTIC METHODS

Improved diagnostic techniques are needed to identify the fundamental causes of performance degradation and life limitations in rechargeable Li batteries. The principal analytical techniques that are being used include x-ray spectroscopy, spectroscopic ellipsometry, Raman spectroscopy, scanning probe microscopy, and other complementary techniques for the *in situ* characterization of electrode surface chemistry and electrode surface processes.

Diagnostics: Electrode Surface Layers

Frank R. McLarnon
Lawrence Berkeley National Laboratory, 90-1142, Berkeley CA 94720
(510) 486-4636; fax: (510) 486-4260; e-mail: frmclarnon@lbl.gov

Objectives

- Apply advanced *in situ* and *ex situ* techniques to characterize the structure, composition, formation and growth of surface layers, SEIs, on electrodes used in rechargeable Li batteries.
- Identify surface layer properties that improve Li battery cycle-life performance, specific energy and specific power.

Approach

- Use ellipsometry, Raman spectroscopy, scanning probe microscopy, and other methods to characterize electrode surface layers.

Accomplishments

- Detected significant changes in manganese oxide surface chemistry, which accompany exposure to nonaqueous electrolytes.
- Initiated studies to characterize the effect of temperature on manganese oxide electrode surface chemistries in nonaqueous electrolytes.

Future Directions

- Use optical, spectroscopic and microscopic techniques to characterize changes in surface layers on Li, carbon and metal oxide electrodes in non-aqueous electrolytes at elevated temperatures.

$LiMn_2O_4$ Cathode Studies: A spin-coating technique to prepare thin films of lithium manganese oxide was refined. Solutions of manganese acetate and lithium nitrate were cast onto a spinning Pt substrate, dried the precipitate at room temperature, and then heat-treated it at 260°C for 2 h followed by 1 h at temperatures up to 750°C to produce films 300-500 nm thick.

The film structure and composition were determined using XRD and Raman spectroscopy. The cubic cell lattice parameters and vibration modes revealed a spinel-type structure, however the film stoichiometry depended strongly on heat-treatment temperature. The film composition varied from $LiMn_4O_9$ to $LiMn_2O_4$ for films produced at 260°C to 750°C. This composition variation was accompanied by narrowing of the X-ray peaks and Raman bands, suggesting that better crystallinity was achieved for films heat treated at higher temperatures.

The surface morphology and surface conductivity of the freshly deposited film were resolved by current-sensing atomic force microscopy (CSAFM). AFM images revealed a densely packed polycrystalline morphology with uniformly distributed crack-free grains of size 100-200 nm. CSAFM images showed a strongly non-uniform distribution of surface electronic conductivity, with tip-to-film current varying from 0 to 10 nA for a 1 V tip-to-film bias voltage.

The electrochemical performance of our thin-film lithium manganese oxide electrode was examined during cycling in 1 M $LiPF_6$-EC-DMC (1:1 EC:DMC by volume) electrolyte at ambient temperature. Stoichiometric $LiMn_2O_4$ electrodes were electrochemically active and displayed significant capacity in the 4 V region. Figure 33 shows a representative CV recorded at 1 mV/s for a thin-film $LiMn_2O_4$ electrode. Two cathodic and two corresponding anodic peaks appeared during each cycle, and their positions and magnitudes varied little during successive cycles. The electrode capacity declined by only 4% after 43 cycles, i.e., its stability was comparable to that for $LiMn_2O_4$ electrodes prepared from commercially available powders.

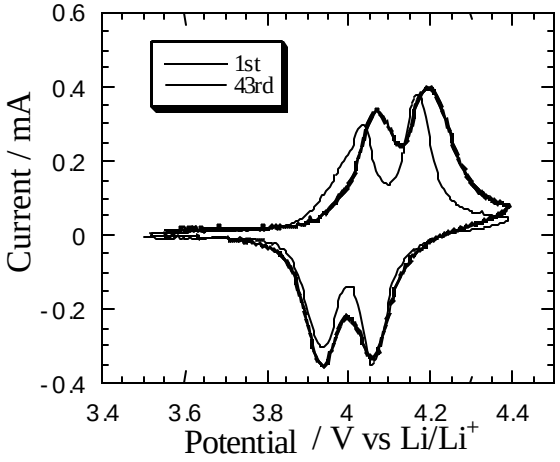

Figure 33. Cyclic voltammograms of a thin-film $LiMn_2O_4$ electrode in 1 M $LiPF_6$-EC-DMC electrolyte, recorded at 1 mV/s.

We examined the effect of exposing our thin-film electrodes to 1.0 M $LiPF_6$-EC-DMC electrolyte at ambient temperature. The diffraction patterns of the $LiMn_2O_4$ and $Li_2Mn_4O_9$ electrodes after 4-days exposure showed relative line positions which were nearly identical to those of the original materials, however the lines were shifted to slightly higher angles and the peak intensity ratios changed noticeably. The Raman spectrum of the electrolyte-exposed film (Fig. 34B) changed into one nearly identical to that of λ-MnO_2. These results indicate

that prolonged exposure of thin-film $LiMn_2O_4$ and $Li_2Mn_4O_9$ electrodes to nonaqueous electrolyte leads to the formation of a manganese dioxide structure derived from the original cubic spinel, but with most of the Li removed from the tetrahedral sites. Examination of topographic AFM images recorded after exposure to the electrolyte revealed no significant change in the electrode morphology. The initial globular structure was well preserved with no evidence of deposits, corrosion or mechanical breakdown. All of our data are consistent with the extraction of Li from the $LiMn_2O_4$ and $Li_2Mn_4O_9$ particles without significant disruption of their structure or morphology. It is difficult to determine at this stage if the entire film was converted into λ-MnO_2. The calculated lattice constant is slightly higher than that reported in the literature for a pure λ-MnO_2 phase, suggesting that the conversion was incomplete. In contrast, the Raman spectra show the signature of a basically pure λ-MnO_2 phase, however the Raman sensing depth is limited to that of light penetration, which is ~30 nm in our case.

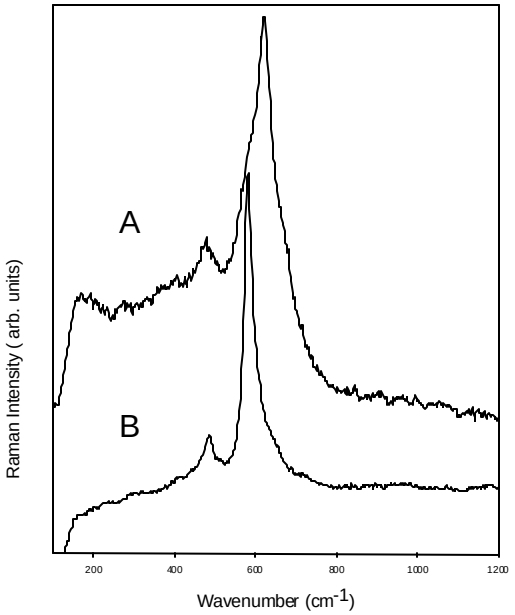

Figure 34. Raman spectra of a $LiMn_2O_4$ electrode before (A) and after (B) exposure to 1.0 M $LiPF_6$-EC-DMC electrolyte for 4 days.

Electrode Surface Layers. We used spectroscopic ellipsometry and CSAFM to characterize interfacial processes and film formation on thin-film lithium manganese oxide electrode surfaces in both pure DMC and 1.0 M $LiPF_6$-EC-DMC electrolyte at ambient temperature. Optical constants and electrode surface conductivity were compared to those of an electrolyte-exposed electrode. A clear signature of interfacial processes was provided by CSAFM images of a $Li_2Mn_4O_9$ electrode after exposure to electrolyte: the conductivity dropped significantly over most of the electrode surface, which may be attributed to passive film formation. Because no vibrational bands characteristic of an organic layer surrounding the oxide particles or bands specific for LiOH or Li_2CO_3, were observed, we surmise that the thin passive layer consists mainly of Li_2O which is insoluble in EC-DMC solvent. However, we observed a substantial decrease in the $LiMn_2O_4$ electrode surface conductivity upon exposure to pure DMC, i.e., in the absence of Li salt. Attempts to analyze the composition of the SEI layer by Raman spectroscopy revealed only spectra characteristic of the oxide. Our failure to detect vibrational spectra of a SEI layer may be a result of its small thickness and small Raman scattering cross-section.

The electrode ellipsometric parameters changed markedly upon exposure to the electrolyte. Both Δ and Ψ shifted to higher angles and showed significantly different spectral characteristics. Calculated optical constants of the electrolyte-exposed film suggest a contribution from an insulating medium present at the film surface, but more analysis is required.

Surface-enhanced Raman spectroscopy (SERS) is employed to provide a detailed picture of the cathode interfacial chemistry. We used an AC sputter-coater to deposit small amounts of Ag microparticles on thin-film $LiMn_2O_4$ electrode surfaces. In a series of experiments we determined how the deposition parameters influence the Ag particle morphology, and consequently the Raman signal enhancement. Preliminary SERS experiments with DMC-exposed and 1.0 $LiPF_6$-EC-DMC electrolyte-exposed $LiMn_2O_4$ electrodes revealed a series of surface-specific bands at 234, 918, 924, 999, 1283, 1353, 1577, 2127 and 2166 cm^{-1}. A detailed band assignment will be conducted in forthcoming studies.

PUBLICATION

R. Kostecki, F. Kong, Y. Matsuo and F. McLarnon, "Interfacial Studies of a Thin-Film $Li_2Mn_4O_9$ Electrode," *Electrochimica Acta*, **45**, 225-33 (1999).

Battery Materials: Structure and Characterization

James McBreen
Brookhaven National Laboratory, DAS-Bldg. 480, P.O. Box 5000, Upton NY 11973-5000
(516) 344-4513, fax: (516) 344-4071; e-mail: jmcbreen@bnl.gov

Objective

- Elucidate the molecular aspects of battery materials and processes by *in situ* high-resolution XRD and X-ray absorption (XAS).

Approach

- Apply *in situ* XRD and XAS to study low-cost $Li_xMn_2O_4$ based cathodes and metal alloy anodes.

Accomplishments

- Completed *in situ* XRD studies on $Li_xMn_2O_4$ with various stoichiometries.
- Used *in situ* XRD to study the charge/discharge processes in a Li-Cu-Sn alloy anode material prepared at ANL.
- Achieved high-resolution *in situ* XRD with fast data acquisition by using a beam line with high energy and a position-sensitive detector.
- Devised methods for *in situ* XRD on $Li_xMn_2O_4$ at low temperatures.

Future Direction

- Synthesize and characterize doped lithium manganese oxides.
- Evaluate manganese oxide materials in new electrolytes.
- Conduct *in situ* XRD studies of thermal degradation processes.

High-resolution XRD studies of $Li_xMn_2O_4$. Two powder diffraction facilities (Beam Lines X7A and X18A) at the National Synchrotron Light Source. (NSLS) were used. Beam Line X7A has a position-sensitive detector, which increases the resolution of the data and permits data acquisition at fast rates. Three well-characterized $Li_xMn_2O_4$ spinels, (x = 1.00, 1.06 and 1.10) were studied. The increased Li content resulted in several changes in the electrochemical behavior. $LiMn_2O_4$ displayed two flat voltage plateaus of equal length during charge. With increased Li the length of the second plateau decreased and both plateaus were sloping. The increased Li greatly increased the capacity stability on cycling for 50 cycles. *In situ* XRD revealed several changes in the structural behavior of the three oxides. The XRD results in Fig. 35, covering the diffraction peaks (511), (440) and (531), show the occurrence of three cubic phases during the first discharge of $Li_{1.0}Mn_2O_4$.

Materials with higher Li content, in particular $Li_{1.1}Mn_2O_4$, displayed pseudo single-phase behavior. This is illustrated in Fig. 36.

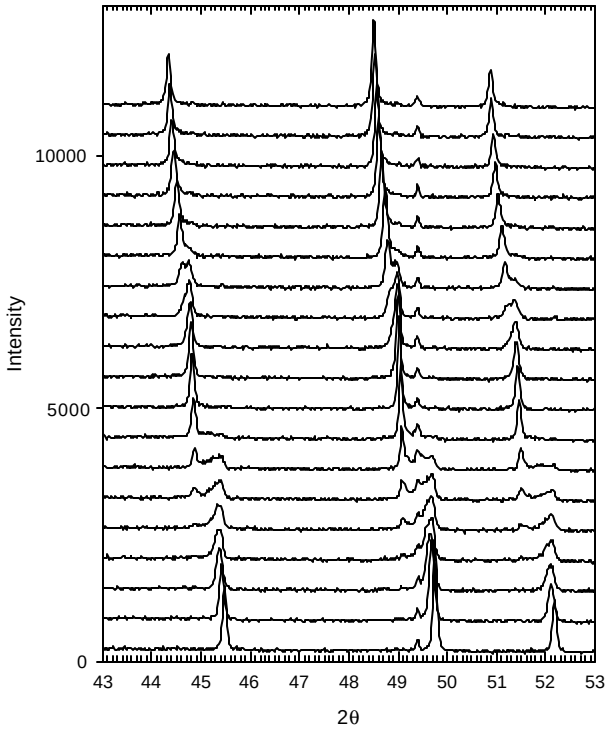

Figure 35. XRD patterns for $Li_{1.0}Mn_2O_4$ for the first discharge from 4.5 to 3.5 V at C/8 rate. The change in Li_x content during each scan,Δx=0.053. Bottom scan beginning of discharge, top scan end of discharge.

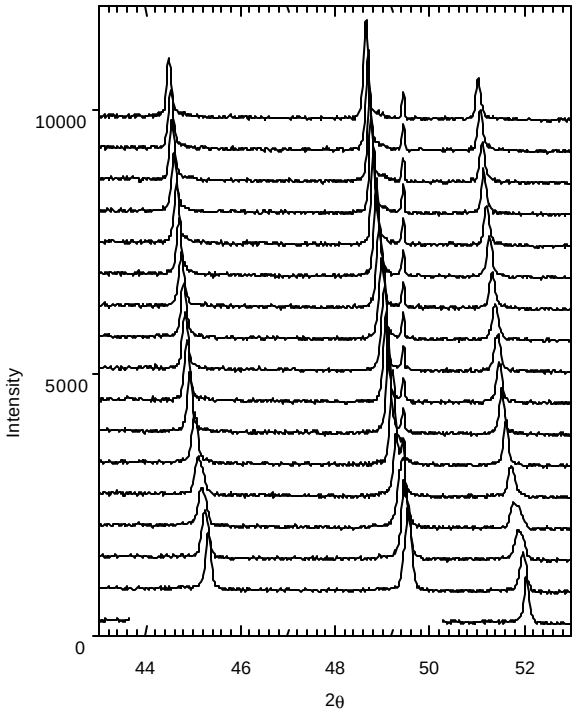

Figure 36. XRD patterns for $Li_{1.1}Mn_2O_4$ for the first discharge from 4.5 to 3.5 V at C/8 rate. The change in Li_x content during each scan, Δx=0.065. Bottom scan beginning of discharge, top scan end of discharge.

The diffraction peaks shifted during charge without the formation of new peaks. However, at some states of charge there was line broadening, indicating formation of phases that could not be resolved by XRD. The absence of well-defined phase transformations improves cycling stability. In the case of both $Li_{1.0}Mn_2O_4$ and $Li_{1.1}Mn_2O_4$, the XRD patterns during charge were similar to those during discharge. When these electrodes were discharged on the 3-V plateau, XRD peaks for the tetragonal phase were not seen until very close to the end of the 3-V plateau. Discharging to the end of the 3-V plateau caused several irreversible changes in the electrodes. Upon charge, the peaks for the tetragonal phase did not disappear until almost the end of the 3 V plateau. On the 4.1-V plateau, all materials showed clear three-phase behavior. This is illustrated in Fig. 37 for $Li_{1.1}Mn_2O_4$. In this case the cell was discharged to 1.8 V. The cell was recharged over a period of 11 h to 4.17 V and charging was continued at half the initial rate to 5.18 V.

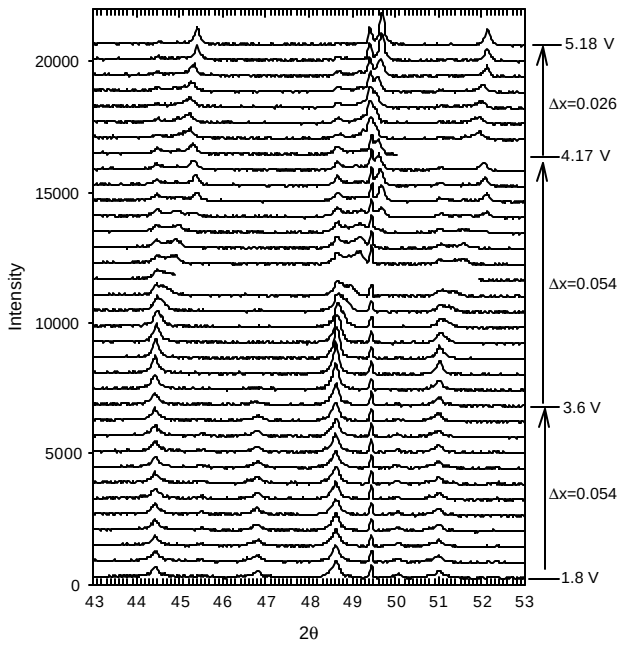

Figure. 37. XRD patterns for $Li_{1.1}Mn_2O_4$ during charge after a discharge to 1.8 V. The right ordinate indicates voltages at various stages of charge as well as the value of Δx for each scan.

The peak at 46.8°, which is ascribed to the tetragonal phase, disappears at 3.6 V. Also all materials showed residual features of the cubic

phase at 3.9 V, when charged to 4.3 V. This can be seen in the case of the (511) peak at 44.5°. In the past this has been ascribed to loss of contact of the active materials. However, by reducing the charge rate and increasing the voltage limit to 5.18 V it was possible to remove these residual features. This indicates that the irreversibility is due to structural changes caused by the deep discharges.

Effect of temperature on the phase behavior of $Li_xMn_2O_4$. $LiMn_2O_4$ undergoes a phase transformation at temperatures slightly below room temperature, with the temperature depending on the composition. The effect of these phase transformations on the stability of the electrode was investigated. XRD studies were carried out while cooling the material from ambient temperature to -20°C. By using the facilities at Beam Line X7A with a position- sensitive detector it was possible to obtain complete spectra and follow the phase change as a function of temperature. This permits us to index the reflections more precisely. Methods were devised for *in situ* XRD in cells, during charge, while maintaining the cell at low temperatures (-20 - 10°C) and controlling the temperature to within about 0.1°C

Preparation and characterization of amorphous lithium manganese oxides. Amorphous MnO_2 and $Li_{0.38}Na_{0.28}Mn_2O_4$ were prepared by methods described in the literature. These were characterized by CV, X-ray methods and cycling in cells. Heat-treated $Li_{0.38}Na_{0.28}Mn_2O_4$ consisted of layered $NaMnO_2$ and small particles of $LiMn_2O_4$ spinel. During the first charge the layered $NaMnO_2$ disappeared and did not reform on subsequent discharges. Discharge to voltages as low as 2.0 V did not result in the formation of the tetragonal phase. So far all of these high-surface-area materials can only be discharged at low rates. Also $Li_{0.38}Na_{0.28}Mn_2O_4$ is moisture sensitive.

***In situ* XRD of intermetallic anode materials:** Preliminary *in situ* XRD studies were carried out on Li-Cu-Sn alloys obtained from M. Thackeray at ANL. The X-rays at Beam Line X7A have an energy of ~17 KeV. With these penetrating X-rays it was possible to obtain excellent XRD patterns in the transmission mode when using a Cu foil current collector.

PUBLICATIONS

X.Q. Yang, X. Sun, S.J. Lee, S. Mukerjee, J. McBreen, M.L. Daroux and X.K. Xing, "*In Situ* Synchrotron X-ray Diffraction Studies of the Phase Transitions in $LiMn_2O_4$ Cathodes," *Electrochem. Sci. and Solid State Lett*., **2**, 157 (1999).

X.Q. Yang, X. Sun and J. McBreen, "New Findings on the Phase Transitions in $Li_{1-x}NiO_2$: "*In Situ* Synchrotron X-ray Diffraction Studies," *Electrochem. Commun.*, **1**, 227 (1999).

X.Q. Yang, X. Sun and J. McBreen, "New Phase and Phase Transitions Observed in $Li_{1-x}CoO_2$ During Charge: *In Situ* Synchrotron X-ray Diffraction Studies," *Electrochem. Commun*. **2**, 100 (2000).

A.N. Mansour, S. Mukerjee, X.Q. Yang and J. McBreen, "*In Situ* XAS of the Reaction of Lithium with Tin-Based Composite Oxide Glass," *J. Synchrotron Radiation*, **6**, 596 (1999).

Y. Ein-Eli, J.T. Vaughey, M.M. Thackeray, S. Mukerjee, X.Q. Yang and J**.** McBreen, "$LiNi_xCu_{0.5-x}Mn_{1.5}O_4$ Spinel Electrodes, Superior High-Potential Cathode Materials for Lithium Batteries. I. Electrochemical and Structural Studies", *J Electrochem. Soc.* **146**, 908 (1999).

A.N. Mansour, J. McBreen and C.A. Melendres, "An *In Situ* X-ray Absorption Spectroscopic Study of Charged $Li_{(1-z)}Ni_{(1+z)}O_2$ Cathode Material," *J. Electrochem. Soc*. **146**, 2799 (1999).

M. Giorgetti, S. Passerini, W.H. Smyrl, S. Mukerjee and J. McBreen, "*In Situ* X-ray Absorption Spectroscopy Characterization of V_2O_5 Xerogel Cathodes upon Lithium Intercalation", *J. Electrochem. Soc*. **146**, 2387 (1999).

PRESENTATIONS

A.N. Mansour, X.Q. Yang, X. Sun, J. McBreen, L. Croguennec and C. Delmas, "*In Situ* X-ray Absorption Spectroscopic Study of Charged $Li_{(1-z)}Ni_{(1+z)}O_2$ (z<0.02) Cathode Material," *195th Meeting of the Electrochemical Society*, Seattle, WA, May 2-6, 1999.

X.Q. Yang, X. Sun, J. McBreen, S. Mukerjee, Y. Gao, M.V. Yakovleva, X.K. Xing and M.L. Daroux, "*In Situ* X-ray Diffraction Studies of Cathode Materials in Lithium Batteries," *196th Meeting of the Electrochemical Society*, Honolulu, HI, October 17-22, 1999.

X.Q. Yang, X. Sun, J. McBreen, Y. Gao, M.V. Yakovleva, X.K. Xing, M.L. Daroux and S. Mukerjee, "*In Situ* X-Ray Diffraction Studies of a New $LiMg_{0.125}Ti_{0.125}Ni_{0.75}O_2$ Cathode Material," *195th Meeting of the Electrochemical Society*, Seattle, WA, May 2-6, 1999.

X.Q. Yang, X. Sun, J. McBreen, Y. Gao, M.V. Yakovleva, X.K. Xing, M.L. Daroux and S. Mukerjee, "Correlation between Performance and Structural Changes of $LiCoO_2$ and $LiM_yNi_{1-y}O_2$ (y=Co, Al, Mg, Ti) Studied by *In Situ* X-ray Diffraction," *3rd International Symposium of New Materials for Electrochemical Systems*, Montreal, Canada, July 4-8, 1999.

X. Sun, X.Q. Yang, J. McBreen, Y. Gao, M.Y. Yakovleva, X.K. Xing and M.L. Daroux, "Studies on Relationship Between Structure of Over-charge State and Thermal Stability for $LiNiO_2$ Based Cathode Material," *196th Meeting of the Electrochemical Society*, Honolulu, HI, October 17-22, 1999.

IMPROVED ELECTROCHEMICAL MODELS

Mathematical models with minimal assumptions are being developed to create computer programs to guide the experimental efforts. The numerical codes solve derived systems of equations to study coupled transport, kinetic, thermodynamic and mechanical problems relevant to the performance of rechargeable Li batteries. Models are being advanced to elucidate the failure mechanisms of the Li-ion and Li/polymer systems, and to understand the mechanisms for thermal runaway.

Improved Electrochemical Models

John Newman (Lawrence Berkeley National Laboratory)
University of California, Department of Chemical Engineering, 201 Gilman Hall, MC 1462, University of California, Berkeley CA 94720
(510) 642-4063, fax: (510) 642-4778; e-mail: newman@newman.cchem.berkeley.edu

Objectives

- Improve the performance of electrochemical cells used in the interconversion of electrical energy and chemical energy by identifying the controlling phenomena.
- Identify important parameters crucial in the operation of advanced secondary Li batteries.
- Determine transport and other properties for electrochemical applications.

Approach

- Develop and implement mathematical models, computer programs, and characterization experiments to describe phenomenologically batteries and their components.

Accomplishments

- Calculated and experimentally verified the entropy of $LiMnO_4$ vs. SOC.
- Refined experimental (galvanostatic polarization) and theoretical (molecular dynamics) methods for transport in concentrated electrolytes.

Future Directions

- Develop molecular dynamics method for transport in $LiMnO_4$ electrode system.
- Study dendrite formation in the degradation of Li battery systems.

The purpose of this research is to develop mathematical and experimental models of batteries, components, and related phenomena for engineering applications. By providing understanding of the relevant transport, thermodynamics, and physico-chemical mechanisms and properties, the research program seeks to enable the design and implementation of efficient electrochemical systems. In the area of system design, a multi-year quantitative evaluation of double-layer capacitors was completed. Final work included the calculation of cycle energy efficiency for finite and reversible charging times. Our experimental model of porous electrode capacitors predicts optimized efficiencies up to 99% for extremely slow discharge. However, for rates applicable to HEV applications (1 s), for instance, efficiencies fall to 70% for 4 to 2 V cycling, 0.05 S/cm solution conductivity with a 25 micron separator. Universal curves were generated for examining efficiency of capacitors for various uses.

The experimental determination of transport properties in concentrated solutions is an effort pertinent to polymer separators for proposed flexible-cell batteries. The development of the galvanostatic polarization method for transference number measurement was completed. Applicable to polymer electrolytes, the technique was improved using a model concentrated binary system. The method consists of measuring the open-circuit potential just after current interruption. A product of the magnitude and the square root of the time duration of the current before interruption are plotted versus the measured potential. A linear extrapolation of this product to zero yields the transference number. Improvements to this 5-year old method include a refined extrapolation and fitting procedure, and the identification of unreliable data by means of an error analysis.

The thermal management of batteries is an important engineering objective considered in this task. Cells with lithium manganese oxide electrodes, among other porous insertion compounds, are proposed for many applications. Thermal modeling is important in assessing and improving the operation and safety in electric devices. The two key goals are the quantitative understanding of reaction entropy and the interpretation of heat generation data in Li cells. An overall thermal model accounts for SOC and position dependence of the porous electrode local reaction rate and open-circuit potential. These considerations, developed by Newman and Rao (1995), are applied to compare theoretical heat generation predictions with experimental work. A mathematical model and computer program are developed for this purpose. The cell entropy, obtained by independent experiments, is used in the model. The entropy as a function of SOC is determined using a new method of short current cycles for obtaining accurate open-circuit potential measurements at a given temperature. Experiments are then conducted at different temperatures to evaluate the temperature derivative of the potential to yield the entropy. Preliminary measurements show a characteristic two-maxima, two-minima profile of entropy vs. SOC as found with vanadium oxides.

Another avenue for property determination involves statistical molecular simulations. Monte Carlo calculations are underway to evaluate the entropy by differentiating the open-circuit potential. Results match closely with the entropy data obtained from experiments mentioned above. Molecular dynamics simulations demonstrate

promise in determining the Stefan-Maxwell, multicomponent diffusion coefficients. The predicted coefficients for aqueous KCl and NaCl solutions agree to within 20% of experiment values. Refinements of the computer programs are underway for improved accuracy and physical representation.

PUBLICATIONS

K.P. Ta and J. Newman, "Proton Intercalation Hysteresis in Charging and Discharging Nickel Hydroxide Electrodes," *J. Electrochem. Soc.* **146**, 2769 (1999).

I.J. Ong and J. Newman, "Double-Layer Capacitance in a Dual Lithium Ion Insertion Cell," *J. Electrochem. Soc.* **146**, 4360 (1999).

R. Darling and J. Newman, "Dynamic Monte Carlo Simulations of Diffusion in Li_yMnO_4," *J. Electrochem. Soc.* **146**, 3765 (1999).

D. Dunn and J. Newman, "Predictions of Specific Energies and Specific Powers of Double-Layer Capacitors Using a Simplified Model," LBNL-43151, April 1999.

H. Hafezi and J. Newman, "Verification and Analysis of Transference Number Measurements by the Galvanostatic Polarization Method," LBNL-44731, December 1999.

PRESENTATION

K.E. Thomas and J. Newman, "Thermal Modeling of Batteries with Porous Insertion Electrodes," *196th Meeting of the Electrochemical Society*, Honolulu, HI, October 17-22, 1999. LBNL-44653.

Thermal Modeling/Thermal Management

James W. Evans (Lawrence Berkeley National Laboratory)
University of California, Department of Materials Science and Mineral Engineering, 585 Evans Hall, MC 1760, Berkeley CA 94720
(510) 642-3807, fax: (510) 642-9164; e-mail: evans@socrates.berkeley.edu

Objectives

- Investigate heat generation and heat transfer in large-scale Li batteries for EV application.
- Design thermal management systems for large-scale Li batteries.

Approach

- Measure thermal conductivities of TiS_2 and V_6O_{13} composite cathode by a guarded heat flow meter over Li/polymer batteries operating at 25 to 150°C.
- Measure the heat generation rate of Li/polymer cells, Li/PEO-lithium triflate/TiS_2, Li/PEO-lithium methide/V_2O_2, and Li/PEO-lithium imide/$Li_2Mn_2O_2$ at 70, 80 and 90°C using an electrochemical calorimeter.
- Develop a thermal model (2-D) coupled with an electrochemical model (1-D to study heat transfer phenomena and thermal management of Li/polymer batteries.

Accomplishments

- Completed measurements of important unknown thermal conductivities of electrolytes and composite cathodes used in Li/polymer batteries.
- Measured heat generation rates for various Li/ polymer cells under various discharge/charge rates.
- Developed a mathematical model coupling thermal and electrochemical phenomena and predicted electrical and thermal behavior of large batteries.

Future Directions

- Apply new coupled thermal/electrochemical model to investigate the behavior of various conceptual designs for Li batteries.
- Modify the new model so that it may be applied to Li-ion batteries.
- Measure heat generation in Li-ion batteries, starting with commercial batteries.

Thermal conductivity measurements were completed on component materials used in Li/polymer batteries. The thermal conductivities of the Li negative electrode, Cu current feeder and Al current collector are well known. However, the thermal behavior of the battery is a strong function of two unknown conductivities, i.e., Li salt/polymer electrolyte and composite positive electrode (cathode). A guarded heat flowmeter was used to measure the thermal conductivities of TiS_2 and V_6O_{13} composite cathodes. The conductivities increased with temperature up to the melting point of the electrolyte, but showed little increase thereafter. The measured effective conductivity of the composite cathode was close to that estimated from the conductivities of its components. To determine the latter, the thermal conductivities of pressed samples of TiS_2 and V_6O_{13} were measured.

An electrochemical calorimeter was used to determine the rate of heat generation during the discharge/charge of Li/polymer batteries. Three different Li/polymer cells (i.e., Li/PEO-lithium triflate/TiS_2, Li/PEO-lithium methide/V_6O_{13}, and Li/PEO-lithium imide/$Li_{1+x}Mn_2O_4$) were prepared and their discharge curves, along with heat generation rates, were measured at different galvanostatic discharge current densities, and different temperature from 70, 80 to 90°C. Figures 38 and 39 show the results for a Li/PEO-lithium imide/$Li_{1+x}Mn_2O_4$ cell discharged at 90°C. The corresponding heat generation rates for the cell in Fig. 38 are presented in Fig. 40. The solid lines of both figures are the results calculated from the mathematical model. The mathematical model was used to predict the thermal behavior of cell stacks. Figure 40 shows the trajectory of the minimum and maximum temperatures for a 10-cm by 10-cm battery stack discharged at two different currents from an initial temperature of 363K for the case where there are significant heat losses from the ends of the stack. The minimum temperature was at the ends and shows an initial drop due to low heat generation early in the discharge. The maximum temperature was at the center of the stack and showed a monotonic increase, reflecting the fact that little heat is transported from this point to the exterior.

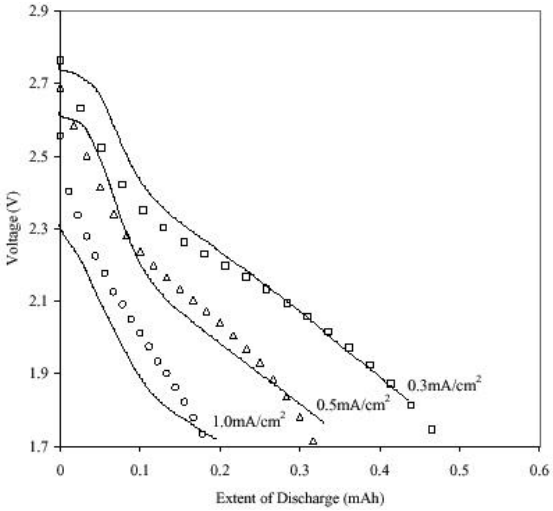

Figure 38. Temperature vs. extent of discharge with different discharge current (electrochemical-thermal model, I=1.0 mA/cm^2 and 0.5 mA/cm^2)

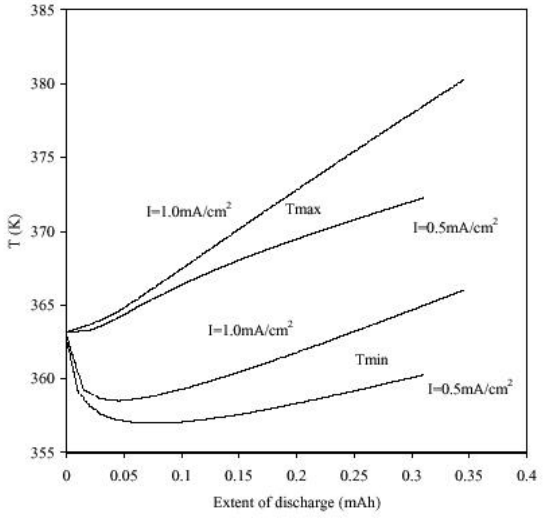

Figure 39. Comparison of heat generation rate between electrochemical modeling (solid lines) and experimental measurement (symbols) (T=363K).

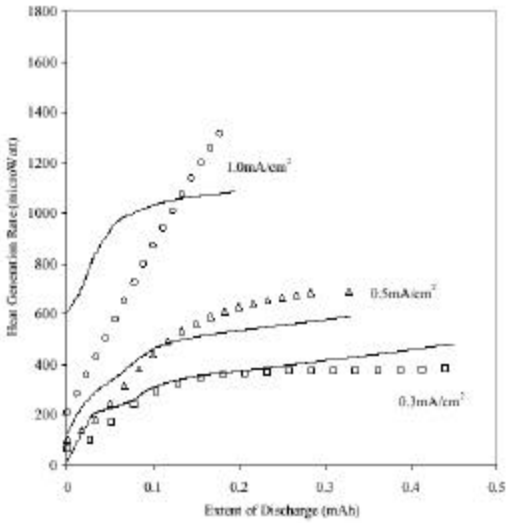

Figure 40. Temperature vs. extent of discharge with different discharge current (electrochemical-thermal mode, I=1.0mA/cm^2 and 0.5mA/cm^2).

PUBLICATION

L. Song and J.W. Evans, "Measurements of the Thermal conductivity of Lithium Polymer Battery Composite Electrodes", *J. Electrochem. Soc.* **146**, 869 (1999).

Microstructural Modeling of Highly Porous Fibrous and Particulate Electrodes

Ann Marie Sastry
The University of Michigan, Department of Mechanical Engineering and Applied Mechanics, Ann Arbor, MI 48109-2125
(313) 764-3061; fax: (313) 747-3170; e-mail: amsastry@engin.umich.edu

Objectives

Li-ion technology:

- Continue development of stochastic geometry models for key morphologies and map connectivity of Li-ion electrode materials.
- Cycle Li-ion cells to failure and identify the unique physical load mechanisms in the negative substrate materials which undergo large expansion only in the basal plane.
- Validate modeling efforts with electrochemical experiments; particularly post-mortem investigations of material properties, along with image analysis analogous to that performed in the first performance period of the Ni/MH work.
- Develop particle/fiber transport software and validate modeling efforts with electrochemical experiments.

Ni/MH technology:

- Refine damage progression simulations using experimentally determined losses in utilization to benchmark theoretical models.
- Investigate the effects of transport enhancement in operation of the cell, including the effects of finite-conductivity electrolyte and active material.

Approach

- Perform transport and mechanics simulations on stochastic geometry models for key morphologies of Li-ion electrode materials, including whiskers (~1 μm), fibers (~10 μm) and spheroidal particles (<10 μm) based on carbonaceous materials.
- Evaluate physical degradation of electrode materials with simulations using the stochastic 1D and 2D (finite element) models.

- Characterize damage progression through continued simulations, testing the validity of numerical approaches.

Accomplishments

- Identified ranges of applicability of a novel stochastic network generation technique compared with full-field finite-element solutions.
- Identified corrosion effects on material morphology by image analysis, and by mechanical and transport (electrical resistivity) testing of substrates.
- Refined damage simulations and validated experimentally the degradation hypothesis of mass transfer from particle to fiber morphology.

Future Directions

- Continue investigation of scale effects in simulation of mechanical damage and transport behavior in random networks.
- Conduct full-scale cell testing of Li-ion cells to assess to benchmark theoretical results from damage analysis.
- Develop new standards for cell testing to better assess electrode performance.

The morphology (i.e., the shapes and placement of constituent particles and fibers) and intrinsic material properties (within phases and for phase interactions) determine overall conductivity of porous electrodes. For highly porous structures, one critical factor is whether a given morphology and density of particles creates a "percolated" network, i.e., a network in which there are continuous, domain-spanning (edge-to-edge) conduction paths. If there are no, or few, such paths, conductivity is negligible across the electrode. However, for densities slightly above the percolation point, the conductivity sharply increases.

We have investigated the influence of scale effects and particle shapes on transport properties. Sample simulation results demonstrated the importance of stochastic simulations over classic, closed-form results when modeling low-density networks (as technologically required by advanced battery applications). We have identified particle shapes, which can be effectively simulated as 1-D fibers and developed a methodology for performing fully 2-D field calculations for particles of aspect ratio (L/D)<10. We have also investigated the importance of boundary conditions in such cases and the difficulties in solving the field equations around singularities, Strategic selection of boundary conditions, and adaptive remeshing, can be used to solve the commonly occurring numerical difficulties in solving the practical problem of conductivity in a mixed-particle domain. Using this approach, we have successfully modeled mixed-particle networks.

Studies were intiated on commercial Li-ion cells using optical and AFM (atomic force microscopy) of MCMB materials to generate data sets for simulations.

Mechanics modeling has progressed from simpler rigid-bond and torsion-spring models to fully 3-D finite-element studies of how particle connectivity affects bulk properties. A 3-D finite element model of two intersecting fibers was developed to model how fibers interpenetrate, especially involving corrosion processes or the effect of binder particles in "gluing" fibers together (Fig. 41). Using these approaches, we have shown equivalence between the 3-D and 2-D cases. Through the improvements and refinements in simulation techniques, we are able to solve multiphase mechanics problems for a wide range of geometries. The techniques will result in full-scale network implementations for both 3-D and 2-D systems, to determine the cases in which the less-intensive 2-D cases can be performed.

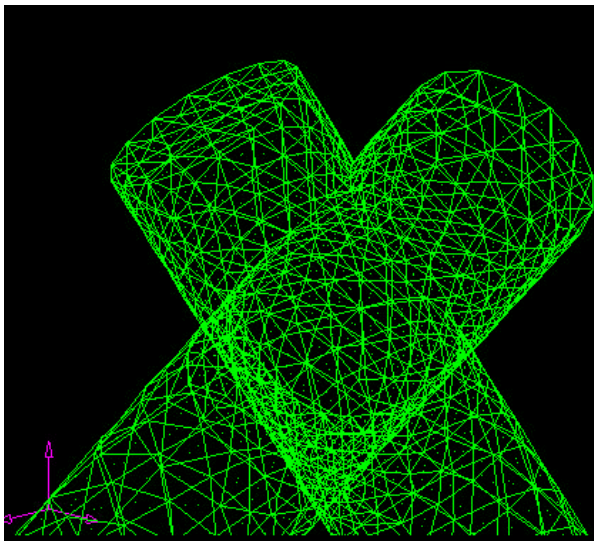

Figure 41. Two intersecting fibers, with degree of intersect 0.667.

PUBLICATIONS

C.W. Wang, X. Cheng, A. M. Sastry and S.B. Choi, "Investigation of Failure Processes in Porous Battery Substrates. I. Experimental Findings," *ASME J. Engineering Materials and Technology* **121**, 503 (1999).

X. Cheng, C.W. Wang, A.M. Sastry and S.B. Choi, "Investigation of Failure Processes in Porous Battery Substrates. II. Simulation Results and Comparisons," *ASME J. Engineering Materials and Technology* **121**, 514 (1999).

X. Cheng and A.M. Sastry, "On Transport in Stochastic, Heterogeneous Fibrous Domains," *Mechanics of Materials* **31**, 765 (1999).

PRESENTATIONS

A.M. Sastry, "On Degradation of Porous Materials in High Energy-Density Battery Systems," U.S. Congress on Applied Mechanics, Blacksburg, VA, 1999.

C.W. Wang, A.M. Sastry and X. Cheng, "Deformation and Failure of Stochastic Fibrous Networks," U.S. Congress on Applied Mechanics, Blacksburg, VA, 1999.

C.W. Wang, X. Cheng and A.M. Sastry, "Mechanics of Porous Materials for Battery Applications," *ASME-IMECE Conference*, Nashville, TN, November 1999.

C.W. Wang, L. Berhan and A.M. Sastry, "Damage Tolerance of Stochastic Fibrous Networks," *ASME-IMECE Conference*, Nashville, TN, November 1999.

A.M.Sastry, C.W. Wang and X. Cheng, "Failure Progression in Highly Porous Fibrous Networks," *U.S. Army Symposium on Solid Mechanics*, Myrtle Beach, SC, April 1999.

A.M. Sastry, C.W. Wang and X. Cheng, "Simulations of Deformation and Failure in Stochastic Fibrous Networks," *Fifth U.S. National Congress on Computational Mechanics (USNCCM99)*, University of Colorado at Boulder, CO, August 1999.

A.M. Sastry, C.W. Wang and X. Cheng, "On Scale Selection in Modeling Mechanical and Transport Property Evolution in Porous Materials," *Fifth U.S. National Congress on Computational Mechanics (USNCCM99)*, University of Colorado at Boulder, CO, August 1999.

NOVEL ELECTRODE COUPLES

The goal of this task is to develop a new electrochemistry that yields a battery of much higher specific energy, much lower cost, and minimum environmental impact compared to the current rechargeable Li-battery technologies. The low-cost sulfur cathode has already demonstrated extremely high capacities, as much as four times that provided by presently used metal oxides. The Li/polymer/S cell, with a theoretical specific energy of 2600 Wh/kg, compared to 570 Wh/kg for LiC_6/CoO_2 is under investigation.

New Couples: Lithium/Sulfur Cells

Elton J. Cairns
Lawrence Berkeley National Laboratory, 70-108B, Berkeley CA 94720
(510) 486-5028, fax: (510) 486-7303; e-mail: ejcairns@lbl.gov

Objectives

- Investigate the behavior of advanced electrode materials in high-performance rechargeable batteries, and develop means for improving their lifetime and performance.
- Improve the cycle life and utilization of the sulfur electrode in Li/polymer/S cells.

Approach

- Fabricate and characterize Li/polymer electrolyte/sulfur cells.
- Evaluate sulfur/vanadium oxide aerogel composite positive electrodes.

Accomplishments

- Fabricated cells with sulfur/vanadium oxide composite electrodes, which exhibited initial specific capacities up to 0.75 Ah/g of electrode and achieved up to 50 cycles above 0.1 Ah/g, representing factor-of-two increases in both capacity and lifetime during the last quarter.
- Conducted spectro-electrochemical experiments, which indicated that the loss of polysulfides by dissolution into the polymer electrolyte is quite small, so the primary mechanism for Li/S cell capacity fade is likely to be the segregation of Li_2S from the remainder of the sulfur electrode.

Future Directions

- Complete Li/polymer/S cell characterization studies.

Lithium/sulfur cell characterization. Spectro-electrochemical investigation of Li/polymer/S cells is being used to identify intermediate cell reaction products, assess the reversibility of cell reactions, and measure polysulfide species solubility in the polymer electrolyte. We examined several cell and chamber configurations, and ultimately chose a simple cell sandwich design in which annular Li and composite sulfur electrodes were separated by a disk-shaped polymer electrolyte. The spectrometer light beam was directed through the centers of the electrode annuli and thereby passed through the polymer electrolyte. Species that diffused into the polymer electrolyte during cell discharge could then be monitored. The cell chamber was designed for use in a glovebox with fiber optic feedthroughs to the spectrometer. Polypropylene was used to fabricate the cell chamber because other polymers tended to out-gas and damage the Li electrode.

Because no light-absorbance data for polysulfides in polymers are available in the literature, it was necessary to carry out a series of spectroscopic calibration experiments to help interpret Li/S cell spectra. These experiments also provided information on the chemical equilibria that exist between the various polysulfide species. Polysulfide solutions were prepared chemically by reacting Li_2S and sulfur in PEGDME in selected ratios to yield average compositions of Li_2S_2, Li_2S_4, Li_2S_6, Li_2S_8 and Li_2S_{10}. UV/VIS absorption spectra were then recorded at three temperatures, and peak absorbances were plotted as a function of the average polysulfide order (n in Li_2S_n) to identify each peak with a polysulfide species. Results from these preliminary experiments indicated that three polysulfide species, Li_2S_4, Li_2S_6 and Li_2S_8, were formed in the polyether solvent (which can be considered as a model for the polymer electrolyte in our Li/S cells). In addition, elemental sulfur is soluble to a limited extent in the polymer. Spectra recorded at different temperatures indicated that only one important equilibrium exists between these species:

$$Li_2S_8 \Leftrightarrow Li_2S_6 + S_8.$$

We then conducted spectroelectrochemical experiments with our annular Li/S cell. Prominent and clearly separated peaks indicated the presence of elemental sulfur and the polysulfides Li_2S_4 and Li_2S_8. The absorbances for these species increased during cell cycling for a few days, indicating that these species did not reach their solubility limit during this period and continued to form during extended cycling. However, the concentrations of Li_2S_4 and elemental sulfur were very small, at least in the electrolyte region, which was probed spectroscopically. Our results indicate that <0.01% of the sulfur initially present in the electrode was lost to the electrolyte during the course of cell cycling.

We conclude from these experiments that the polysulfide reactions are reversible, and that the loss of the intermediate polysulfide reaction products by diffusion into the electrolyte is not the primary cause of cell capacity fade. These results, together with visual inspections of cycled cells which sometimes showed substantial amounts of a white precipitate, suggest that the primary mechanism for Li/S cell capacity fade is the segregation of Li_2S from the sulfur electrode, which thereby breaks the necessary intimate contact between the cell reaction product and the electronically and ionically conducting phases.

Sulfur-vanadium oxide composite electrodes. We are evaluating novel composite positive electrodes, in which a small amount of vanadium oxide aerogel is added to the sulfur electrode, as an approach to overcome the significant capacity fading observed in Li/S cells. This is being done because vanadium oxide can provide both electronic conductivity and added capacity. In previous cells, PEGDME + LiTFSI electrolyte was added to the sulfur electrode to increase Li-ion conductivity, which was necessary because elemental sulfur is not conductive. However, the polysulfides formed during cell discharge are somewhat soluble in PEGDME, which may contribute to the high rate of capacity loss.

The vanadium oxide aerogel was synthesized by us in the laboratory of Prof. B. Dunn at UCLA. The as-prepared composite electrode contained 70 wt% sulfur, 12 wt% vanadium oxide aerogel, 10 wt% PEO, and 8 wt% carbon, i.e., an electrode composition reported by Moltech [33rd Intersociety Energy Conversion Engineering Conference, 1998]. The vanadium oxide aerogel provided nanoscale interconnecting porosity. No electrolyte was included in the composite electrode; however it is expected that electrolyte migrates from the separator phase into the composite electrode after cell assembly, and thereby provides a source of Li ions.

Two different electrolyte separators were used: PEGDME 250 in Celgard 2400; and a composite electrolyte of fumed silica, cross-linked butyl methacrylate and PEGDME 250. The Li salt used in both electrolyte separators was LiTFSI at an O:Li ratio of 30:1. Cell cycling was carried out at room temperature, and data were recorded with an Arbin battery testing system. Cells were charged and discharged at 50 $\mu A/cm^2$, with a 2 h rest period between charge and discharge. Cell A (Fig. 42) incorporated the PEGDME-LiTFSI-Celgard electrolyte separator, and Cell B (Fig. 43) incorporated the fumed silica-gel electrolyte separator. Cell A exhibited lower initial capacity (~0.425 Ah/g of electrode) but better capacity stability. Cell B exhibited very high initial capacity (~0.750 Ah/g of electrode) but poor capacity stability, falling below 0.100 Ah/g of electrode after cycle 6. These initial cell capacities are significantly higher than the 0.375 Ah/g of electrode achieved for previous cells without aerogel. Also, the cell capacity was >0.100 Ah/g of electrode for 50 cycles, which is twice the lifetime of previous cells.

Another possible mechanism of capacity fading is the chemical reaction of polysulfides with Li at the negative electrode to form isolated Li_2S, therefore we sought a means to retard polysulfide migration to the negative electrode. Dr. N. Dudney (ORNL) provided samples of lithium phosphorous oxynitride (LIPON) solid electrolyte deposited on Celgard. Because the Li-ion transport number is unity in LIPON, we expected to effectively block polysulfide migration from the positive electrode to the negative electrode. We used the same method of cell assembly as for Cell A, but we incorporated an extra layer of Celgard on which a thin film of LIPON was deposited. Unfortunately, the

capacities of these cells were very low. It appears that the LIPON lowered the conductivity of the cell so much that high overpotentials were observed at currents as low as 10 μA/cm^2, and no voltage plateaus were observed during cell charge or discharge.

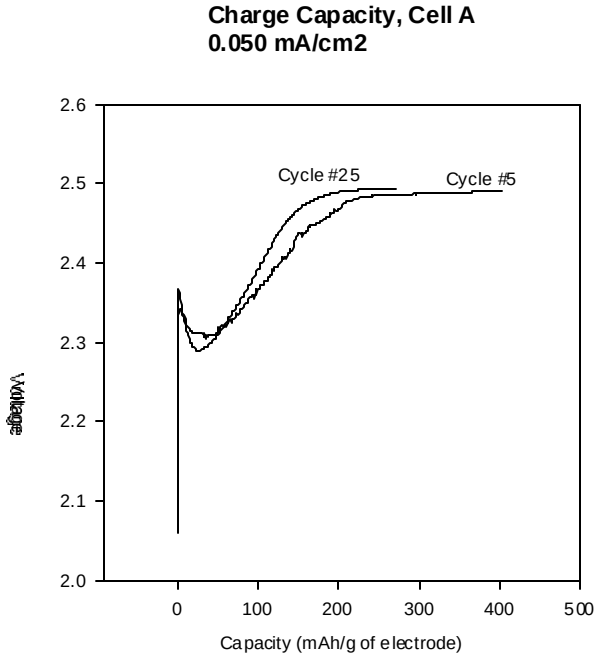

Figure 42.

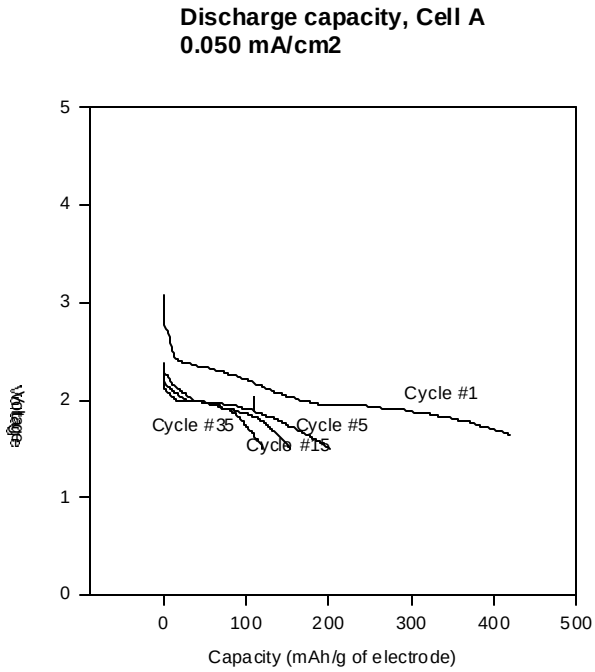

Figure 43.

ACKNOWLEDGMENTS

This work was supported by the Assistant Secretary for Energy Efficiency and Renewable Energy, Office of Advanced Automotive Technologies of the U.S. Department of Energy under Contract No. DE-AC03-76SF00098. The support from DOE and the contributions by the participants in the ETR Program are acknowledged. The assistance of Ms. Susan Lauer for coordinating the publication of this report and Mr. Garth Burns for providing the financial data are gratefully acknowledged.

LIST OF ACRONYMS

AFM	atomic force microscopy
ANL	Argonne National Laboratory
ARC	accelerating rate calorimeter
BNL	Brookhaven National Laboratory
CB	comb-branch
ccp	cubic close packed
CPE	composite polymer electrolyte
CSAFM	current-sensing atomic force microscopy
CV	cyclic voltammetry
DEC	diethyl carbonate
DMC	dimethylcarbonate
DME	dimethoxyethane
DOE	Department of Energy
DSC	differential scanning calorimetry
DTA	differential thermal analysis
EC	ethylene carbonate
ENMR	electrophoretic nuclear magnetic resonance
EQCM	electrochemical quartz crystal microbalance
ETC	trifluoroethylene carbonate
ETFA	ethyltrifluoroacetate
ETR	Exploratory Technology Research
EV	electric vehicle
EXAFS	extended X-ray absorption fine structure
FR	flame retardant
FTIR	Fourier transform infrared
GC	gas chromatography
HEV	hybrid electric vehicle
HMTAP	hexa-methoxy-triaza-phosphozene
HOPG	highly oriented pyrolytic graphite
HQ	HydroQuebec
ICL	irreversible capacity loss
IR	infrared
LBNL	Lawrence Berkeley National Laboratory
MCMB	mesocarbon microbead
MEC	methyl ethyl carbonate

MEEP	methoxyethoxyethoxide
MW	molecular weight
NFE	nonflammable electrolyte
NMR	nuclear magnetic resonance
NSLS	National Synchrotron Light Source
PC	propylene carbonate
PEG-DME	polyethylene glycol - dimethyl ether
PEMO	polyethylene-methylene oxide
PEO	poly(ethylene oxide)
PES	photoelectron spectroscopy
PNGV	Partnership for a New Generation of Vehicles
PVIC	poly(vinylene carbonate)
PVICOX	poly(1,3-dioxolan-2-one-4,5-diyl oxalate)
SEI	solid electrolyte interphase
SEM	scanning electron microscopy
SERS	surface-enhanced Raman spectroscopy
SGC	Superior Graphite Company
SNL	Sandia National Laboratories
SOC	state of charge
SPE	solid polymer electrolyte
TEM	transmission electron microscopy
TFEA	2,2,2-trifluoroethyl acetate
TGA	thermogravimetric analysis
THF	tetrahydrofuran
TMS	tetramethylsilane
UHV	ultra high vacuum
USABC	United States Advanced Battery Consortium
XANES	X-ray absorption near-edge spectroscopy
XAS	X-ray absorption spectroscopy
XRD	X-ray diffraction

ANNUAL REPORTS

1. Exploratory Technology Research Program for Electrochemical Energy Storage – Annual Report for 1997, LBNL-41950 (June 1998).
2. Exploratory Technology Research Program for Electrochemical Energy Storage – Annual Report for 1997, LBNL-41950 (June 1998).
3. Exploratory Technology Research Program for Electrochemical Energy Storage – Annual Report for 1996, LBNL-40267 (June 1997).
4. Exploratory Technology Research Program for Electrochemical Energy Storage – Annual Report for 1995, LBNL-338842 (June 1996).
5. Exploratory Technology Research Program for Electrochemical Energy Storage – Annual Report for 1994, LBL-37665 (September 1995).
6. Exploratory Technology Research Program for Electrochemical Energy Storage – Annual Report for 1993, LBL-35567 (September 1994).
7. Exploratory Technology Research Program for Electrochemical Energy Storage – Annual Report for 1992, LBL-34081 (October 1993).
8. Exploratory Technology Research Program for Electrochemical Energy Storage – Annual Report for 1991, LBL-32212 (June 1992).
9. Technology Base Research Project for Electrochemical Energy Storage – Annual Report for 1990, LBL-30846 (June 1991).
10. Technology Base Research Project for Electrochemical Energy Storage – Annual Report for 1989, LBL-29155 (May 1990).
11. Technology Base Research Project for Electrochemical Energy Storage – Annual Report for 1988, LBL-27037 (May 1989).
12. Technology Base Research Project for Electrochemical Energy Storage – Annual Report for 1987, LBL-25507 (July 1988).
13. Technology Base Research Project for Electrochemical Energy Storage – Annual Report for 1986, LBL-23495 (July 1987).
14. Technology Base Research Project for Electrochemical Energy Storage – Annual Report for 1985, LBL-21342 (July 1986).
15. Technology Base Research Project for Electrochemical Energy Storage – Annual Report for 1984, LBL-19545 (May 1985).
16. Annual Report for 1983 – Technology Base Research Project for Electrochemical Energy Storage, LBL-17742 (May 1984).
17. Technology Base Research Project for Electrochemical Energy Storage – Annual Report for 1982, LBL-15992 (May 1983).
18. Technology Base Research Project for Electrochemical Energy Storage – Report for 1981, LBL-14305 (June 1982).
19. Applied Battery and Electrochemical Research Program Report for 1981, LBL-14304 (June 1982).
20. Applied Battery and Electrochemical Research Program Report for Fiscal Year 1980, LBL-12514 (April 1981).